Chapter 1

INTRODUCTION AND BACKGROUND

1.1 Introduction

It is widely acknowledged that the k-factor plays a key role in radiowave propagation, and therefore in all radio applications such as, for example, radio coverage planning, engineering of microwave links, interference estimates, etcetera. Because of this, a knowledge of the statistical distribution of the k-factor is of paramount importance from the radio spectrum conservation point of view. As the value of the k-factor is determined by radio meteorological conditions, it is important for this to be known locally as it mainly affects local conditions, which will naturally change from place to place.

It is a popular misconception that the traditional 4/3rds value for the k-factor is sufficient for radiocommunications planning. In areas of high usage of the radio spectrum there is acute frequency congestion across all planned frequency bands. The fundamental shift from fixed to mobile radio services, as exemplified by the ubiquitous cellphone, and thus in the use of the radio spectrum, as well as the higher complexity of such communications demands in mobile services because of dynamic frequency allocations, requires more accurate values of the k-factor for coverage and interference planning.

The present research is mainly focused on extending current expertise in radio refraction studies, developed in South Africa, by reviewing and confirming values of the k-factor around the country as well as taking such work further by modelling the k-factor distribution along terrain elevation.

This first chapter serves as an introduction to describe the research reported in this thesis. It places the work in perspective from the conception of the original topic, through its early development and further research in South Africa to date. The latest results reported in this work are intended to address present requirements of the radio community, and to bring the general application of the model in communications systems design a step closer.

1.2 The k-factor's importance and motivation for the study

From experience in radio engineering practice, it became evident that it was necessary to study and develop the knowledge of the k-factor together with its properties further. This need was dictated by more demanding practical requirements for new complex radio planning of modern radio systems than has been the case until quite recently. It became apparent that the existing k-factor tables in common use would soon be inadequate for more sophisticated radio planning applications. New more refined models leading to a better understanding of the distribution of k-factor values would be urgently required.

The context of the k-factor study has not been simple, involving not only a practical study, but also empirical and theoretical studies to decide how relevant the topic was. It has been enlightening to see from the literature survey how scarce theoretical knowledge of the subject is. Apart from the fact that the concept is relatively young, and as far as can be established, first introduced by *Baker* (1927), there is no exclusive theoretical study devoted to the k-factor alone, despite the fact that it was acknowledged as a valid concept *Wait* (1960).

Initially, indeed, practical aspects prevailed in recognising the importance of the k-factor concept. Further work involving a search for a suitable function expressing the k-factor in terms of the refractivity gradient and the percentage of time for events, led to the theoretical study, further complemented by the literature survey to determine the *status quo*.

1.3 Preliminary reading provides focus for the study of the k-factor

The MSc degree of *Nel* (1989) as well as his other publications on the subject of k-factor, were essential early readings leading to the formulation of the study proposal**.**

Initially the search was confined to missing concepts, such as, for example, the formula expressing the k-factor in percentage of time for events, which was developed later. Another important concept was to investigate the possibility of determining the k-factor

values in areas between the meteorological stations used by Nel in his work. This aspect was also successfully addressed later in the study.

A growing awareness of the limited current knowledge on the subject as gleaned from the preliminary reading stimulated a further literature search. This search extended outside the most frequently quoted monographs and texts, and included a review of examples in other fields, because it was realized that only a comprehensive literature survey would define the main body of knowledge on the subject.

Clarification of the research problem came with the realisation of the need for a more refined model of the k-factor, which had to be developed in unison with the existing results. The known models of the k-factor in tropospheric propagation as promulgated by the International Telecommunication Union Radiocommunication Sector (ITU-R) had to be reviewed, and compared with data at hand.

At the beginning, the preliminary readings led to a conviction that those matters of interest being searched for would require much more effort to clarify. Therefore, the available existing data was analysed in order to determine numerically what was difficult to find in the literature. The initial results were encouraging but to prove the originality of the concepts formulated an in-depth literature survey was definitely required. The novelty of the proposed work was established from the extensive literature survey.

There still remained a requirement to establish what was known in terms of a vertical model of the troposphere in order to see how the k-factor values would vary as a function of terrain elevation. Initially an exponential model was contemplated, but later numerical analysis of some new SA Weather Service data led to other possibilities.

1.4 Identification of the research problem, questions and hypotheses

The question of modelling of the k-factor for tropospheric propagation is not a new one. However in the past it has not been an important global issue. Such models were, more often than not, confined to certain areas only. Usually the big towns were targeted first,

because of a need for a better radio planning for many radio services across the radio spectrum.

This situation changed drastically with the advent of computers and the new facilities and tools such as digital terrain maps (DTMs), which could be used with various models for communications planning, depending on the accuracy required. It became feasible to think and to work in terms of the DTM for the entire country. Therefore, all the data and models previously applied and used in isolation and in different places, could now be combined into a single entity by a means of a suitable algorithm, which would be able to accommodate all the requirements.

The main objective then became the "unified" model for the k-factor, which would be valid countrywide and for the different heights of ground elevation. When the problem was formulated, it was not known how this objective could be achieved, but the computational tools available were to be the latest ones.

Various hypotheses, except for the first one, which defines the k-factor in terms of the refractivity gradient and percentage of time for events, followed later from further work**.** At the beginning it was not known if this objective for a new model could be achieved easily as the whole theme had not been finally formulated.

Therefore, a certain risk was involved with respect to whether the project would succeed. The need for a new model prevailed and justified further research. This was at times a tedious process. However, a great deal of dedication and some luck helped to reward the efforts.

It was necessary to formulate the main research objective in terms of a new model. However, it was impossible to specify, based on the preliminary readings, how this would be achieved. Nevertheless, it was expected that various ideas and concepts would crystallise reasonably well and fairly soon after the commencement of data analysis. This went according to plan. The approach had not been over-specified in the original proposal, thus possibly anticipating what the outcomes should be. Therefore there were no unexpected comebacks and disappointments.

1.5 Methodology, research design, structure of the study

The methodology ranged from the use of theoretical analyses by means of statistical analyses, multiple regression, and a neural network algorithm, etc., to practical computational evaluations using spreadsheets and MINITAB © software. Theoretical studies of the formulas involving a calculation of the new expressions and theoretical model took relatively little time but were important from the cognitive point of view, as it impacted heavily on the overall approach and the final results.

This research was designed in such a way as to validate the existing data sources by comparing them. The initial data tables from the SABC (*Nel and Erasmus*, 1986) and CSIR (*Pauw*, 1996) were used during the early stages. However, it soon became apparent that despite the fact that the databases were attributed to almost the same observation sites, the values cited were not consistent, and therefore could not be treated as being representative.

From an evaluation of the various tables of the k-factor in use in South Africa, it soon become obvious that the main data source would be Nel's MSc work *Nel* (1989) and that these data should be evaluated independently. This was the key to a fundamentally different approach, with gratifying results. Predictions of k-factor values obtained from the SA Weather Service data processed with a different method matched Nel's results very well, with the exception of anomalous results at Alexander Bay, which should be investigated further.

The structure of the study may thus be described as being based on the literature study, evaluation of various databases (old and new), and theoretical studies pertaining to the new model. The formulation of the research problem is as important as finding a solution. It must be based on the literature review not only for determining originality, but also in terms of what contribution it has to make to the body of knowledge.

1.6 Remainder of the thesis

The literature review gives an historic account on the topic of the k-factor. This determined the profile of this work, in order to support the direction of inquiry towards the main hypotheses. Emphasis is placed on what went wrong in the past, and when, and what was considered to be a priority in research today relative to the main findings and conclusions.

Furthermore the existing data were evaluated and compared in order to check how these support the first hypothesis namely that the formula expressing the cumulative distribution of the k-factor as a percentage of time for events is a truncated normal function. This has been successful despite the differences between the SABC and CSIR sets of data. The author regards the latter as being more useful and more accurate than the first one.

A method is presented to replicate these data sets with a minimum of intervention by always keeping one original data point through which the fitted curve passes, and which approximates the set best. This is done by an Eigen-value concept, with the Eigen-function being the one, which gives the best overall fit in terms of a least mean squares approach.

It is in principle possible to extend k-factor data from the eight stations where radiosonde observations were made to other geographic locations by a means of a neural network algorithm implemented on a spreadsheet in order to visualise the effects graphically. This possibility has been explored and presented, together with a study of another possibility to do the same by means of Kriging. This is a statistical technique, which can utilise sparse data points, and which was developed locally in South Africa for application in geological models of, for example, ore body reserves (*Clark and Harper*, 2000).

The next part represents a development and analysis of the new and old models existing under the same boundary conditions, namely having a refractivity gradient of zero at the tropopause and a constant value at sea level. This has been done by means of a so-called elliptic model. This is a concept for distributing the refractivity gradient and the k-factor according to altitude and the latitude of geographical locations. The final results were

produced using a DTM and a visual form of the results is displayed. This was in fact done by use of the minimum and maximum values of the refractivity gradient, obtained from the Nel data.

The last part of the thesis contains conclusions and recommendations, and discusses potential research gaps that became evident as a result of the main purpose of inquiry. These identified gaps do not impact critically on the scope of the primary objective of this work, and therefore they were not addressed here. However, for future work these should be investigated further, firstly to assess their importance to the subject of inquiry, and then for a contribution to the overall research undertaken to date in the area of k-factor modelling.

An immediate recommendation for this work would be its application in practical radio planning and coverage design of communications systems. The difference between the use of improved models for the k-factor, as opposed to those currently in use, should in the longer term be reflected as an improvement in the efficient use of the radio spectrum.

Chapter 2

LITERATURE REVIEW

2.1 Introduction

The literature review is in fact a scholarship review. This is intended to give an account of the available body of knowledge, in order to see how other scholars have viewed and investigated various research problems relevant to the subject of inquiry in the present work.

The definitive references have been divided into three subsections, and subsequently further organised according to criteria as indicated by the titles of the subsections.

The first subsection presents the concept of the k-factor and the gradual development of its applications and importance. This is done as an historical review. The second part shows the main definitions of the k-factor with its impact on classification of the propagation modes and forms. It gives some examples of the concept of percentage of time of occurrence to express certain results as functions. The third and last part of the definitive references section contains reviews of titles directly supporting the hypotheses contemplated here. Because these are very scarce, almost inklings, they are organised by the hypotheses proposed.

The review is based on an initial selection of nearly 6000 abstracts, obtained from journal articles, scientific reports, conference papers, monographs, theses, etc. This led to 400 titles that were obtained for detailed scrutiny and investigation. From these about 65 titles were selected to be used as primary references. The titles classified as indefinite references have been organised in such a way that they indicate general applications of the k-factor in order to reflect on its state of development and importance in radio propagation.

The main aim of the review is to avoid any possible repetition or duplication of the work on the subject, which had been completed already, or to avoid taking a direction of inquiry proven to be unsuccessful for various reasons.

2.2 Definitive References of the k-factor by background, history, concept, applications

According to *Brooker and Walkinshaw* (1945) the k-factor concept was initially reported by T.Y. Baker in 1927. Its usefulness became apparent only some years later, particularly, during World War 2 when radar applications were developed. At that time it was already known from military operations that radar signals could propagate from India to the Middle East. This was when the world became aware of ducting phenomena *Durst* (1946).

It was later documented by *Sharma and Subramanian* (1983) that "*It may be mentioned here that during summer when the radio refractive index gradient is very steep in the lower atmosphere, VHF-TV transmissions have occasionally been received at Bombay from far-off stations in the Middle East*".

Kalipada Chatterjee and Mathur (1982) state "*In India early investigations relating to formation of ducts and unusually high refraction of radio waves were made from Calcutta and Bombay areas and were reported by Durst (1946)".*

These studies were based on radar observations at wavelengths of 1.5 m and 7 m. During the period January-May 1943 super-refraction observed over Calcutta during night varied from 20 to 30 occasions per month at λ=1.5 m and λ=3 m to 14 occasions per month at λ=7 m.

In the Arabian Gulf, particularly, in Bahrain serious problems in propagation were investigated by *Bashir* (1989). Difficulties experienced in regional radio planning, especially, in the VHF and UHF bands, which manifested themselves as an overreach of the TV signals through ducting modes and by fading on a 2GHz microwave link, triggered local research. The results of the measurements indicated a need for a better understanding of these effects by organising them in a new way, namely, to interpret the bigger negative values of the k-factor along vertical profiles.

In the Baltic Sea coastal region of Poland a long-term campaign of 20 years of observations led to some results formulated by *Pawlowski* (1989) regarding distributions of the radio refractive profiles up to 2 km heights above sea level. The exponential vertical

model was applied to express the values of the refractivity, the refractivity gradient and the k-factor as a percentage of time occurrence for events. The author argued that the reference atmosphere recommended by the ITU-R and the one obtained by him for this case were different, particularly as regards the extreme monthly and seasonal values. He attributed these changes to the movement of air masses, which characterise the climate.

In the Baltic Sea coastal region of Sweden observations over a period of 20 years led to results formulated by *Wickerts* (1970) regarding the radio refractive profiles up to heights of 2 km above sea level. The vertical profiles' refractivity gradients were analysed in order to determine the percentage of time of occurrence for events of ducting in layers formed over the 2-km altitude range. From measurements obtained by flying an aircraft equipped with a refractometer for 1 to 2 hours at the time, a number of vertical profiles of refractive index and temperature up to 2 km in altitude were obtained. The author claimed that the prediction methods at the time should be modified with regards to the measurement of the vertical temperature profiles within the lowest layers of the atmosphere in order to determine the altitude of ducts more accurately than before.

The follow up paper by *Pawlowski* (1995) showed how the long- term data could be processed further and a bi-exponential model applied. Long term refractivity values and their refractivity gradients for all four seasons were given. The reference atmosphere model was formulated and dispersed refractive index profiles were depicted for percentage of time of occurrence for events.

It was again noted that some discrepancies exist between values recommended by the ITU-R for the region. In conclusion the need for more investigations into the regional properties of the troposphere was identified. The importance of local data in order to determine the radio characteristics for analysis of VHF and UHF radio systems was stressed.

2.3 Definitive references organised according to the k-factor and percentage of time for events

The most serious researchers in the field of radio propagation recognised the importance of the k-factor concept *Wait* (1962), for example, wrote "*This strongly suggests that*

propagation in a linear atmosphere of radius A is equivalent to propagation over an earth of modified radius A_e with a homogeneous atmosphere".

It is, therefore, concluded *Wait* (1962), that the effective earth radius is indeed a valid concept. The same conclusion has also been reached by other authors including *Van der Pol and Bremmer* (1937,1939).

The accepted formula of the k-factor is (see for example *Hall,* 1979):

$$k = \left[1 + \left(\frac{dN}{dh}\right) / 50\pi\right]^{-1} \tag{2.1}$$

k = the k-factor,
N = refractive index in N-units, and
dN(h)/dh = the refractivity gradient,

Hall (1979) published a graph of entitled "*Effective earth radius factor k as a function of a refractive index gradient dN/dh*". Other publications, which mention this, are *Mojoli and Mengali* (1985), and *Imbeau, M. et. al.* (1993).

The first title by *Hall* (1979) gives an accepted classification of the propagation modes by indicating ranges of values for the k-factor and the refractivity gradient within which the specific modes occur.

The most extensive early work published has been by *Bean et al.* (1966). This is an atlas that covers the world and which, amongst others, gives information regarding the refractivity gradient, dN/dh. Data is presented as cumulative probability distribution functions, for ground-based 100-m thick layers, for four seasons of the year, namely, February, May, August, and November. The figures showing the function plots expressed as the percentage of time of occurrence for events for the refractivity gradients are found in Appendix C in Figures C-57 to C-78 of *Bean et al.* (1966).

These values were obtained from different stations around the world and later used to prepare plots of the annual average values. All of this was done using meteorological procedures. The work is based on the empirical model of atmospheric refractivity involving the wet-dry terms, which lead to the exponential double-term model.

Continuation of this work may be found in the report of *Samson* (1975) where he presented similar plots as before. However, these were somewhat more refined since they were based on new observations. The data leading to the new plots were processed in a novel way, allowing for final results of much higher quality. However, the report is confined to the Northern Hemisphere.

An important scientific review of the main propagation mechanisms was offered by (*Barnaby*, 1975a). Figure 8, for example, gives the cumulative probability distribution of dN/dh (or k) for low clearance paths (with layering) in dry and humid climates. This example followed the same pattern as those described before by *Samson* (1975) and *Bean et al.* (1966). However, it attributed descriptions of different phenomena to the presented curves and the refractivity ranges on the plot.

Another paper still directly supporting previous philosophy, namely that of making use of the percentage of time of occurrence for events distribution, is by *Dhein, et al.* (1993). Figures in the paper show the cumulative distributions of refractivity gradient measured by radiosonde, and by refractometer. All sites were located in different parts of Brazil. The measurements were taken over periods of time ranging from one to eight years.

The papers mentioned next, contradict the results from those references quoted above for the percentage of time occurrence for events. These indicate a reversed order of dependency for the refractivity gradients.

The first paper by *Kheirallah* (1988) showed increasing values of the refractivity gradient with an increasing amount of the percentage of time for events, in contradiction with the main concept. This represents surface refractivity and refractivity gradients for Mersa Matruh, in Egypt.

The paper by *Samir Hussain Abdul-Jauwad et al.* (1990) was a similar example, which also showed also a reversed order of dependence between the gradient and the percentage of occurrence of events.

The last paper found having a similar feature was by *Bye and Howell* (1989). This indicated that the functional dependence followed the same order as described in the previous paper. Various figures showed the trend in coastal and inland conditions. Some of the data represented combined results from 18 stations.

These papers contradict the examples indicated initially. In effect, they therefore do not support the first hypothesis in the same way that the first references do.

There is another example in a published paper illustrating the concept of expressing the cumulative distribution as percentage of time of occurrence for events, in this case path loss in dB (*Claverie* and *Dupuis,* 1997). Several figures in the paper illustrate examples using this idea. Attention is drawn to one of the figures (No.5), which mentions a k-factor value of 0.8 for which the plot is valid.

This example is important as a formula converting the refractivity gradient and the k-factor to the attenuation is still to be found for the percentage of time of occurrence for events.

2.4 References directly supporting the hypotheses in this thesis.

The first hypothesis is that the k-factor values presented for different percentage of time for events follow a truncated Gaussian probability density function of the refractivity gradient and the k-factor, see formula (2.1). This is in effect illustrated in the SABC report (*Nel,* 1986), for chosen values of percentage of time for events and for different places in Southern Africa, and also in a similar table from the CSIR (*Pauw,* 1996).

These two primary sources of data were used to investigate and search for a common, universal function representing a dependence of the percentage of time of occurrence for events on values of the refractivity gradient and the k-factor. At the time of formulating the hypothesis these were the only data sources known to the South African radio community,

and these were widely used for radio planning in the form of tables. It is stressed that the results prepared and published by the CSIR were extracted from the MSc thesis by *Nel* (1989).

These tables are substantially different from the earlier ones published in (*Nel* and *Erasmus,* 1986). They have been analysed independently and their differences compared in Chapter 3.

The second hypothesis is that the k-factor values known from observations at specific places may be extended everywhere in between these points by use of modern methods such as the neural network algorithm, or Kriging. The literature cited below provides a general guide concerning applications of these methods.

The monograph "Practical Geostatistics" by *Isobel Clark* (1979) gives a complete overview of the Kriging method in Chapter 5. She explains the concept against a wider background.

The book contains some examples that are particularly useful for practical applications of the two-dimensional cases involving maps, which can be handled in a convenient manner. However, for a greater amount of observation points it may be cumbersome to work with these on spreadsheets.

A new edition of the book appeared very recently under a similar title, "Practical Geostatistics 2000," *Clark and Harper* (2000). This is an entirely revised text, which is greatly simplified, and enriched with many new examples gathered over the last 20 years. Of particular use are the different models of variograms, which are described separately and analysed in one of the new chapters. This new book is bigger and better, and gives guidance to sources of the new software. It deserves to be studied on its own because of many useful techniques, whose implementations appear to be almost endless.

The generalised regression neural network (GRNN) is a very powerful non-linear regression technique (curve fitting function). At the Africon 1999 Conference in Cape Town at one of the workshops, Prof. J. Greene distributed a document describing the method, in principle and formally (*Greene,* 1999). It is a very popular and widely known

algorithm, which is particularly useful to work with in computer spreadsheets. The method has been fairly well known for some time. It was originally provided to the author as a private communiqué almost a quarter century ago by *Dobija,* (1978). Since then it has been widely applied.

The third hypothesis, relating to the elliptic model, is supported by many publications, which consider different aspects, for example, an important reference regarding the height of the tropopause (*Bhattacharya, et al,* 1989). This indicates that at the geographic latitudes of India the height of the tropopause is typically 16 km.

Satellite experiments quoted by *Yakovlev et al.* (1995) confirm the generally accepted heights of the tropopause at 13 and 10 km at different geographic latitudes.

The main model, however, has been derived from *Thom* (1994) where the necessary characteristics are given for the elliptic model. These include the maximum and minimum heights of tropopause above sea level as a function describing the change of the height according to latitude.

South African efforts to estimate the atmospheric refractivity and its gradient for the radio broadcasting transmitters planning purposes are reflected in a symposium paper by *Nel, et al.* (1989). Despite the fact that the *CCIR Recommendation 370-4, Report 563-2* describes insufficient climatic classification for local needs, the k-factor values and the refractivity gradient are mapped for the country.

Another paper by the same authors *Nel, et al.* (1988) deals with the establishment of a database to record the refractivity measurements, and describes the problems related to doing so. Anomalous propagation in the West Cape Coast region is described and analysed. The phenomenon is attributed to the dew-point depression, and the approach is based on the meteorological features present in the area. This climatic situation results in problems for the VHF broadcasting service. The k-factor is used to discuss the behaviour of radio propagation in the area.

Studies conducted in India provide useful indications concerning the diurnal and seasonal changes of the refractivity gradients and the k-factor values (*Sarkar et al.*, 1987).

The radio-climate over Southern India is a theme of the paper by *Narayana Rao et al.* (1985). This discusses a monthly change of the k-factor in different parts of the subcontinent. Coastal and inland areas are distinguished from each other.

There are some papers of general interest, which may be mentioned. The first of these is an older paper by *Morita* (1980), showing the Temperature Inversion Regions around the world. It suggests places in Southern Africa where radio ducts may be present.

Another paper by *Ko,* (1985) describes important features of anomalous propagation and their impact on microwave radio systems. The second part of the publication contains a classification of the three basic types of anomalous propagation depicted against the vertical profiles of the troposphere.

2.5 Indefinite references, supporting the current line of inquiry indirectly by examples

2.5.1 Terrestrial Microwave Radio-Network Applications

The paper by *Narayana Rao* and *Kesava Murphy,* (1985) discusses results obtained against the background of meteorology. Engineering of a line-of-sight microwave radio link is usually concerned with clearance of the First Fresnel Zone ellipsoid by the main obstacles along the route. This is achieved by use of "*an appropriate k-factor, which will be exceeded for 99.9% of time for events. In practice, this is not possible partly because of lack of such statistics*". The authors go on and say "*A general guideline for wet climates is normally k=1, and it is kept as low as k=1/2 for desert areas*".

A computer program uses the supplied refractivity profiles with a ray tracing technique for tracing a ray at 7GHz, changing the elevation angle from 0.1 degrees to 1.2 degrees in steps of 0.1 degrees to do this. The findings were that at about 0.8 degree the rays reach the receiving end of the link, at other elevations higher than 0.8 degree the rays propagate

above the receiver, while for the lower ones they travel below. The terrain clearances at the hilltop are compared with the microwave fadeouts. Estimated results show good agreement with the observations. The line-of-sight link was studied for the purpose of determining the radio meteorological conditions in order to improve the quality of future microwave radio links in the area. This was done by studying the fadeouts on the link in operation under particular conditions with the hilly terrain obstructing the first Fresnel zone ellipsoids, and changing values of the refractivity index as well as the k-factor, thus leading to further or lesser obstruction.

Design of terrestrial microwave links in a given climate and their performance are described by *Reddy and Reddy* (1993) against a background of the difficulties caused by associated phenomena of fading and ducting of different kinds. The authors described diurnal and seasonal changes, which were critically dependent on the extreme variability effects of the intervening medium. How the links lose their clearance for the first Fresnel zone was monitored, and the results of occurrence of different modes, indicated by the amount of percentage of time for events for each mode in the area of operation. In conclusion it was stressed that by monitoring the link's performance in the area, and simultaneously measuring the refractivity gradients over the paths, much more insight would be gained into the propagation mechanisms.

The mechanism of long distance clear-air propagation of microwaves in the troposphere is still not completely understood according to *Craig and Levy* (1987), who in their work present a further extension to the traditional approach of finding the field modes according to the refractivity profile of the troposphere. Their method is based on the choice of profile obtained from the meteorological measurements as a discrete set of values for the refractive index. A reasonable curve is fitted to these data points and then used for calculating the modes.

Intuitively, it may be expected that small perturbations of the curve would not affect the modes significantly. This is not the case, and small changes result in very different sequences of modes. Two modes are considered, namely, diffractive and ducting modes. For the piece-wise continuous refractivity profile the sequence of modes is infinite but for the holomorphic curve-fitted profile the sequence remains finite.

In conclusion, a new technique was offered for calculating the number of modes needed in the mode theory, to obtain the field strength value. As a result of the closeness of fit to the measured data points on the refractivity profile, this number is directly related to the calculation accuracy required.

Precision of the measured data decides what accuracy of prediction is achievable. Therefore the efficiency of the mode theory allows one to avoid unnecessarily high criteria for convergence.

A disagreement regarding the interpretation of the ray and mode propagation theories for an elevated duct as published earlier led to the paper by *Craig* (1985). Important assumptions were made before presentation of a new approach. These mainly concern the refractive index profile and its estimated features.

Despite the exponential atmosphere recommended by ITU-R, the author adapts a trilinear profile of refractivity with the scale height at 8km representing a singularity (discontinuity) on that profile as reference. Three essential parameters are determined, the duct height, the refractive index discontinuity across the elevated layer, and the effective earth radius. This leads to a formulation of the Maxwell equation solutions that are obtained as Airy functions for the modes. The final analysis classifies the modes according to their physical properties and concludes the discussion with the ray theory description, claiming that current interpretation justifies differences between previous and present approaches.

In a very ambitious project completed locally by the ESKOM Planning Division an unusually long UHF (410 MHz) radio link of 154.3km was envisaged, planned, built, tested and established (*Buljanovic,* 1979). A typical average line-of-sight link is about 50km long. The terrain between the two terminals Hekpoort and Thabazimbi provides favourable conditions regarding the earth profile for clearance along the route, with both towers high enough to consider space diversity system in order to minimize fading times and to make these acceptable to the transmission objectives.

The clearance of the path for the first Fresnel zone and for a k-factor of 4/3 is sufficient. However for a k-factor of 2/3 the obstructions introduce attenuation, considered as knife-edge diffraction loss, and hamper the clearance substantially. From a discussion related to the design of the system, it transpired that the main dilemma making it difficult to implement was a lack of knowledge regarding the k-factor value for the area. Therefore a monitoring period of some 200 days over the operating test link was used to observe fading types, which were analysed and classified, in order to determine the best solution. During that period three different types of fading were identified. These were slow, fast, and ducting fading, each having their own characteristics and duration of appearance. A space diversity system designed according to recommended criteria was implemented to prevent and minimise the harmful effects of fading occurrence.

In conclusion, despite insufficient height of the towers used to install the recommended spacing of antennas for the diversity system, performance of the link was found to be satisfactory. However, during severe fading the lower antenna with less clearance was also less affected, such phenomena were already reported in the literature, but no satisfactory physical explanation has yet been offered.

The paper by *Schiavone* (1981) addressed the meteorology of obstruction fading created by a substantial water-vapour pressure gradient, in turn leading to larger positive gradients of the refractive index.

Seventeen meteorological observation sites within the mainland United States were used by *Samson* (1975), *Bean et al.* (1966), and *Dougherty and Hart* (1976) to compile a geographical probability distribution of refractivity gradients, which is useful for predicting the frequency of occurrence of the positive gradients.

The model proposed in this paper comprises two parts, namely, inland and coastal components. The latter seems to be more reliable. It is a semi-empirical model, aimed at formulating invariants from the empirical parameters, which are used to model the variances of normal probability density distribution of the refractivity gradients. The total probability density function is composed of a mixture of two components of normal distributions.

The results obtained and presented by the author are not "perfect," as he put it, but generally in a good agreement with the original cumulative distributions offered by *Samson* (1975), except for four sites. The reasons for this are given and briefly discussed. Comparisons are made for all four seasons and plotted together with the original data. Inaccuracies are visible along the distribution tails. These inaccuracies are produced by more unstable climatic conditions.

The climatological model proposed for any location in the US for positive gradient occurrence distribution, fills in the gaps among the 17 locations covered by *Samson* (1975).

The contribution is significant as additional details in climatic variations with better geographical resolution than was previously possible, allows for more accurate specification of microwave antenna heights.

A preliminary paper of an empirical nature analysing fading distribution by *Schiavone* (1982) points to a need to study geographical, seasonal, diurnal conditions, which have a major effect on the characteristics of different fading phenomena.

The experiment was conducted for one year only at Palmetto, Georgia, on two 6 GHz links, with three different antenna elevations. Ray paths were analysed for a k-factor of 4/3, in other words, "normal" propagation. Along the path from Palmetto to Omaha five points were established and equipped with antennas. The data were recorded 5 times every second for the duration of fading. The sampling at all acquisition points of the meteorological data took place at every 2 minutes. The results were plotted for hourly-accumulated fading time in every hour of a 24 hours period, and constituted diurnal fading distributions. Diurnal variations to signal threshold level at every distance-point for every season were respectively plotted. Discussion of the results is done in terms of three features, namely diurnal, seasonal and geographical. The results are compared with those reported previously in the literature.

However, the author is not certain of the nature of the fast modulation in the received signals, which he attributes it to "*presumably multipath fading", or "of a more slowly varying baseline (presumably power fading)."*

Separation of the two different fading mechanisms was supposed to follow in further work, in order to test the hypothesis developed. This was that it would be possible on the grounds of meteorological interpretation, to verify the nature of the fading occurrence in a geographic area for the line-of-sight links.

Microwave link propagation over water in the Atlantic Ocean, is reported by *Goldhirsh et al.* (1992). Monitoring and research were conducted on two links in order to establish a database to tie up different types of fades with the meteorological conditions over a yearlong period. The experiment was based on two microwave links, configured in such a way that a transmitter at 4.7 GHZ, placed on the Parramore Island – Virginia, sends signals to two receivers, located on a lighthouse, at a distance of 44 km, and at lookout tower, at a distance of 39 km on Assateague Beach. These sites were separated only by 5 km.

The links were employed as indicators of real time conditions of atmospheric propagation, involving quiescent, super-refraction and ducting mechanisms to display the time-series distribution of fading. Yearly cumulative fade distributions for both the lighthouse and lookout tower links were established. The total operating times represent 88.5% and 86.7% respectively, at the "standard" or "normal" propagation conditions i.e. a k-factor of 4/3.

In summary the authors make the following comments "*it is not known whether these statistics may be applied to other over-water regions*" as "*this experiment offers a unique database of fade statistics for over-water line-of-sight geometry at 4.7GHz which is particularly suitable for the Mid-Atlantic coastal regions*".

The influence of sand and dust storms on terrestrial microwave radio networks was investigated in Iraq by *Al-Rizzo et al.* (1993), particularly with regards to the effect these have on the refractive index and attenuation. A link running through the Iraqi desert between Nasyriah-Daraji and operating at 11GHz frequency was considered as being

representative of the conditions experienced. Accordingly its performance was observed and monitored for several months.

A Fabry-Perot open cavity resonator was used to measure the dielectric properties and attenuation at 11GHz for concentrations representing three different soil samples. Analytical treatment comprised the derivation of attenuation, refractive index and loss tangent formulas. Measurements were conducted to plot the changing values of refractive index as a function of concentration, and dielectric constants of sand silt and clay. All of the data plots seem to suggest linear dependencies.

In conclusion, the measured values were compared with the calculated ones. Some of the experimental results for refractive index, loss tangent and attenuation appeared to be over estimated, but for sandy samples the experimental values were found to be higher than the calculated ones.

The authors concluded by saying: "*finally, it may be emphasised that the present state of meteorological knowledge, concerning particle sizes and their distribution is such that no conclusions can be drawn on a climatological basis*". The final remark is important for engineering of microwave links to work under such storm conditions " *The knowledge of the variations of dust concentration with height above ground is also important for estimating the precise values of the k-factor*".

An integrated approach to propagation by more than one mode at the time was presented by *Shen and Vilar* (1995). The main objective of the paper was, however, a presentation of results of monitoring the four microwave links over the English Channel. Transhorizon propagation mechanisms are discussed, namely, troposcatter, ducting and spherical diffraction against high k-factor values. The results mention the percentage of time for events for each dominant mode.

Of particular interest is the presentation of the high k-factor diffraction, which outlines the blocking mechanisms represented by the different k-factor values. A statistical study was conducted to show the cross correlation between signal levels and refractivity as the radio meteorological characteristics of the troposphere. The refractivity in turn is derived from

meteorological measurements. The seasonal distributions of diffraction and ducting as dominant modes are given. These show some complementary features.

2.5.2 Examples of the use of the k-factor in airborne radar

The operational behaviour of a radar system, which takes into account the troposphere and topography, is presented by *Abdullah et. al.* (1991). A linear refractivity profile, which leads to a shell model, is assumed.

The equations of ray tracing in the medium are based on Snell's law and lead to a second order differential equation with an analytical solution (obtained for the linear profile). The first part of the presentation contains the derivation of the analytic formula used as an algorithm with maximal computer efficiency for analytic ray tracing. The second part is concerned with the wave front reconstruction technique, which allows one to deduce values of the phase and amplitude of the radar field. The combination of these two steps leads to computation of the radar coverage diagrams, which show the lobes in the atmosphere, for a single layer for k = 4/3, or for two, or four layer cases, for different but specified k-factor values.

A computer program was used to process the results. This used the theory and model of the troposphere, and implemented this as a large number of concentric shells, each having a linear refractive index profile and constant value of the k-factor. The topography was modelled as straight segments according to the co-ordinates relating to the antenna. These segments were organised according to a numbering scheme starting from the antenna.

The authors however point out the apparent shortcomings of the method despite eliminating the usual artefacts "*The spherical wave front reconstruction technique suffers from one main limitation. In evaluating a highly complex troposphere (i.e. ducts), smoothing out of the vertical field distribution may occur.*"

A comparison of a two methods aiming at producing the same results with regards to bending of propagation paths is reported by *Robertshaw* (1986), the two methods are the following: Ray Trace and Effective Earth Radius Model (EERM) methods. The evaluation

of the models is the object of the study, which investigated an example for both with a suitably chosen data set.

The author states, "*The purpose of this work is to show that suitable scale factors can be determined and employed to yield reasonable approximations for path parameters at higher altitudes, as would be encountered in airborne radar applications. In general, the scale factor is strongly dependent upon the source (transmitter) altitude and surface refractivity*".

A short description of the methods involved is necessary for further comparison.
An atmospheric ray trace exponential shell model is applied with geometrical progression in shell thickness. More shells at the lower altitudes are needed to accommodate larger refractivity gradients and to maintain the accuracy of the algorithm for the ray trace method. Each shell, or stratum contains a constant value of refractivity assumed that is measured at the middle of the layer. Propagation within shell boundaries is assumed along straight lines. The ray bending is perceived to take place according to Snell's law of refraction at the boundaries of each stratum, as if they were slabs with different dielectric constants.

The EERM method assumes a propagation path along a straight line from source to terminus. It takes into account atmospheric refraction at low altitudes where the refractivity profile is almost linear. The effective earth radius needs to be properly scaled to provide for propagation along a straight line. This is a "fictitious" model aimed at using the simplest possible geometry yielding the same output results as the previous method. It makes use of averages, and assumes constant values of the refractivity gradients, and thus the k-factor.

In order to evaluate the methods "*results produced by the ray trace model are used to determine the altitude dependence of k and the accuracy of the EERM for higher altitude paths*".

The first comparison of the predictions is based on the assumption of a single value of N of 300 at a surface height of 1 kft. There are three different altitudes 15, 45, 60 kft, and three

different k-factor values 1.209, 1.116, 1.089, producing comparable ranges of the grazing angles for the depression angles at source. The accuracy of comparison between the ranges and the angles at the surfaces for initially higher depression angle values is very good but for decreasing input values the differences become larger between these two methods. The second comparison is organised differently at 1 kft terrain elevation for source altitudes from 4 to 90 kft for three different values of refractivity, namely N_s = 200, 300, 400, corresponding to different k-factor values. The comparison is repeated for a terrain elevation of 2 kft with similar results. The differences between the two cases remain minimal. The author tries to find the best fit for the results by finding the appropriate k-factor in terms of the "*ground range*" and the "*slant range*". It is concluded that a k-factor of 4/3 is very different from the values required in both these cases.

An important concluding comment found in the paper states, "*The factors tend to converge for high altitude sources since N_s influences the refractivity profile only up to altitudes of 9 km*". Earlier it was pointed out that, "*The gradient for the N_s = 200 case has a sharp discontinuity at 9 km*".

Airborne radar propagation requirements are analysed by *Denny* (2000) in order to assess the main operational parameters involved, such as Range to Horizon, Effective Earth Radius, Radius of Curvature, and Straight Line Propagation Losses. Mathematical modelling of propagation by refraction, as applicable to airborne sources of radiation (transmitters), and which have sufficient accuracy for modern radar capabilities, needs much more detailed knowledge of the propagation mechanism than before. Snell's Law of Refraction is formulated in a novel way, namely as the "*microscopic form of Snell's Law*" and the "*macroscopic form of Snell's Law*". This model has been applied to the atmosphere, where the refractive index depends upon altitude, in order to calculate the curved paths along which the radio waves travel.

The author makes an interesting comment regarding the current status of the k-factor, "*The effective earth radius concept is more complicated than is usually presented in textbooks*". If the transmission direction of the main beam is greater than 2 degrees off the horizontal, the k-factor value will have to be calculated according to a specific formula proposed, otherwise k = 4/3 is considered to be sufficiently accurate.

Abnormal propagation conditions of ducting can result in very long propagation distances, which in turn lead to multiple images of the target (mirages). This may be treated numerically to determine the ray paths for all refractivity profiles. The author remarks, "*Only simple profiles admit analytic solutions*".

Operational characteristics of airborne transmitters are of interest, and are discussed by *Almond* (1983) for England and the North Sea region. The author is concerned with radio propagation at different altitudes particularly for specific propagation modes of elevated ducting and super-refraction. Properties of the troposphere and features, which may cause severe disruptions to operational radio systems, are discussed. However, users may also turn these aspects to a tactical advantage.

Major radio systems are discussed, in terms of being the main users of the information required for their successful functioning. The best available radio refractive data are required, and the means of gathering such intelligence are briefly considered. Computerised prediction methods, current at the time, are referred to, along with their input requirements. This is done against the background of the main problems expected. Shortcomings of existing technology are discussed. New techniques were needed particularly to account for the horizontal homogeneity of the atmosphere predictions, as well as to be able to extend the results of soundings at discrete locations to the area in between, in order to obtain the full picture of the geographical area of interest.

The last comment made by the author is significant. "*For a user to be able to avoid problems caused by anomalous propagation or to put it to his advantage, he must be aware of its presence, and what effect it may have on his operational system. Thus, a near real time detection and prediction method is called for, which positively addresses the problem of horizontal extent. Without, this form of technique it seems unlikely that users will be able to exploit anomalous propagation with any degree of confidence*".

2.5.3 Discussions of the ducting mode

A statistical approach to propagation in evaporation ducts is given by *Hitney and Vieth* (1990) for two different environments.

A set of four different frequencies, namely 1.0, 3.0, 9.6, and 18.0GHz were used in the Aegean Sea between the two Greek islands of Naxos and Mykonos, where the path from transmitter to receiver was 35.2 km long and entirely over water. Transmitters for the first three frequencies were elevated at 4.8 m above sea level and 4.5 m for the last one at18GHz. At the receive site, the first three receivers were placed at heights of 19.2m and the last one at 17.8 m above sea level.

The second set of measurements took place in the North Sea between Weddewarden at the north coast of Germany and the island of Helgoland, the frequencies used were 0.6, 2.3, 6.8 GHz. The transmitter antennas were elevated at 35, 28, 29 m, and the receiver antennas on the island at 32, 31, 33 m above sea level respectively. The distance between them was 77.2 km. In both cases the links monitored were longer than the standard atmosphere radio horizon, which in the first case was about 27 km and in the second case 46 km.

The results of monitoring were presented as path-loss distribution for each frequency and placed separately as a function of loss in dB resulting in the percentage of time of occurrence for events. The plots were compared with the calculated values by means of the MLAYER computer program based on the underlying theory by *Budden* (1961). The modal equation was for the vertical refractivity profile.

Finally, in both cases path loss was plotted against the height of the evaporation duct and the histogram of evaporation duct height occurrence given. The accepted general knowledge that duct heights are greater in the lower latitudes and higher in the higher latitudes confirms that conclusion as the histograms are visibly shifted.

An historic review of different theoretical models as reported in the literature, and which are useful for the analysis of ducts in the troposphere is given by *Jha, et al.* (1989). Duct propagation mechanisms are briefly described and the difference between ducting as a form of guided transmission of energy, in comparison with other modes of propagation, is discussed. The frequency cut-off formula is mentioned for a duct, which is treated as a dielectric wave-guide.

Six different methods are given to calculate the vertical refractivity profile in order to analyse ducting properties for further propagation predictions.

The first one, the Wave Guide Mode Method, is presented in a form of a field strength solution for two different polarisations (vertical, horizontal), "*In ducting mode, the attenuation, increases very slowly with the number in the multilinear case. Thus hundreds of modes may have to be included to yield stable results which give rise to difficulties in obtaining cut-off for the number of modes required in the mode sum*". The remaining series in the wave-guide mode theory may converge fast under particular conditions but this method is limited to plane, or spherically stratified refractivity models.

The second model is the Phase Integral Method. This has a long history and has evolved through different stages under a few researchers. In its present form it offers two field solutions. The first is for a surface duct, the second for an elevated duct. These solutions are expressed in terms of Airy functions and assume approximately linear variations of the refractive index. "*The expressions for surface duct are valid only for slowly varying medium. In practice, refractivity profile departs from linearity i.e. the medium is too rapidly varying, or mathematically the quantity 1/q (dq/dz) is not small, the method fails. In particular if q becomes zero at some point in the medium, phase integral approach is ideal*".

The third model is the Initial Value Method. Boundary conditions lead to the formulation of two solutions, one for surface duct other for an elevated duct. The differential equation is integrated using an iterative technique until a value is reached satisfying the boundary conditions. "*However the use of this model is time consuming and needs larger computation time*".

The fourth model is the Continuation Method. This is in fact an extension of the previous approach and has the ability to accommodate a definition of complex mode numbers. It is even more computation time intensive, but the method is ideal for obtaining Eigen values and Eigen functions at greater altitudes. The authors comment that, "*this method fails in the medium having non-homogeneous strata, which is always observed in the tropospheric medium*".

The fifth model is the Coupled Mode Method. This is a two-dimensional, cylindrical model, which is employed in a laterally non-uniform tropospheric duct for the normal modes.

James Wait (*Wait,* 1980) solved Maxwell's equations in cylindrical co-ordinates for the mode coupling in a non-uniform tropospheric duct. The postulated form of the solution to the problem leads to typical expressions for the fields formulated in series of ordered terms. "*This method of mode degeneracy is suitable to explain surface duct propagation over rough surfaces but is rather complicated*".

The sixth, and last, model is the Finite Difference Method. Its application as described is mainly to an approximate function of the refractivity profile. "*For more complex profile, purely numerical techniques can be used to predict better value and the process can be repeated to find all desired solutions but these methods are computationally extensive*". In order to use the finite difference method the range of large profile heights needs to be transformed to a finite domain, namely $0<X<1$, by a suitable scale height like Z_o. This is done by an exponential transformation in a form $X = e^{-(Z/Zo)}$, then the domain of $0<X<1$ in divided into "m" equal steps "h" , namely, $h = m^{-1}$. The convergence and accuracy are the main considerations of the method used "*The only limitation of this method is that the refractivity profile is modelled by a function*".

In conclusion, a comparison of different theoretical models and methods as described in the literature along with their shortcomings and limitations suggests that the Finite Difference Method is the most appropriate model to define the refractivity profile in the troposphere.

Craig (1988) describes the use of a parabolic equation instead of ray tracing or mode theory, to predict the field strength in a ducting environment. The approach is reported as an alternative method. It is based on the solution to the Maxwell's equations with the modification that an initial elliptic equation is reduced to a parabolic one. Practically, one-dimensional refractivity index profiles are tractable. Typical profile implementations in computer modelling of the troposphere are confined to analytical profiles. Despite the fact that parabolic equations have been around for more than half a century, they became useful

in numerical methods for calculations and modelling only recently with the advent of cheap powerful computers.

The results presented in the paper by *Craig* (1988) represent 1GHz vertically polarised transmitters with a of Gaussian radiated beam in a100 N-unit 300m duct height at the beginning, tapering to 100 m at a range of 100km. Further results show different duct characteristics for a horizontal layer. It is therefore difficult to compare these two cases. The third case considered shows radio-coverage with a 5GHz horizontally polarised antenna beam elevated to 25 m and immersed in a duct of 70 m thickness. The pattern obtained is complicated one. It contains holes and covered islands in the coverage drawn for the 6 dB contours off the median value signal.

In conclusion, the effects of elevated ducting layers may be predicted easier and cheaper by obtaining coverage diagrams with the parabolic equation produced from a model able to handle two dimensional refractive index profiles.

Solutions of the modal equations for tropospheric profiles are given and discussed by *Levy* (1987) in order to comment on the properties of wave-guide propagation. Two cases are considered. The first is a linear case, where the profile is approximated by a holomorphic function leading to a limited number of the non-diffractive modes. The second is a non-linear case, where the profile is approximated by a piecewise continuous functions. However the derivatives have discontinuities of the first order. Therefore, in effect, non-holomorphic functions are considered. Solutions were obtained in both cases by a means of Airy functions. These are discussed together with conditions for their existence the mathematical proofs are presented in the appendixes to the article.

In conclusion the author stressed the instability of the solutions as a function of the approximating profiles, remarking on the practical consequences that, "*total field calculations should not be effected by small changes in the refractive index profile, even though the set of modes is unstable*". A conjecture "*that multilinear refractive profiles behave like the second type profile*" is offered and future work to fit a holomorphic profile to the data and only compute the diffractive modes was planned.

2.5.4 Examples in Broadcasting

Evaluation of the empirical methods used for field strength predictions in terrestrial broadcasting in the VHF and UHF bands, is compared with measurements obtained from monitoring by *Isola and Riccardi* (1988).

At the time the paper was developed, a digital terrain model for Italy had become available. This triggered an immediate interest in computer-aided design and calculations, especially to determine the coverage area of high-power transmitters for television and FM radio broadcasting. Of particular interest to the propagation study program in Italy was a large coverage design for those transmitters situated on tops of the mountains, and which were intended to provide for reception in a very uneven and rough area. The existing empirical methods, considered for their accuracy, were examined in all modes of propagation by comparing the predicted results with field strength measurements.

An important feature here was the expression of the k-factor in terms of percentage of time of occurrence for events, as a way of earth profile analysis. This has lead to a determination of the required field strength values for the wanted signal and for the spillover signal, which was needed for interference calculations.

Formulas are given for the attenuation in each propagation mode, and discussed for the purpose of the model presentation. The main concern of the study was the possibility to control the accuracy of the calculated predictions for specific applications depending on the terrain.

In conclusion the authors state, "*The method proposed for the prediction of field-strengths over true path profiles between the transmitting and receiving points enables more precise results to be obtained than can be achieved by statistical methods*".

An interesting review of the concepts of "the percentage of locations" and "the antenna height gain" is discussed by *Fairbrother et al.* (1986). The concepts are illustrated with broadcasting examples presented as different sets of measurements in the VHF band,

namely, between 95 and 200 MHz and effective isotropic radiated powers (EIRP) of 22 and 50kW for the FM and TV transmitters respectively.

The Bell Telephone Company 1944 propagation curves are referred to. These are used to predict field strength at a receiver some distance from a transmitter depending on the frequency, EIRP, percentage of time for events, percentage of time for locations, transmit-receive antenna heights, and terrain roughness. The CCIR Recommendations and Reports are referred to as a limited source of information regarding use and interpretation of the above ideas for implementation to field strength predictions and measurements.

The following three campaigns to conduct measurements took place with the aim to extend present the knowledge of Height Gain and possible range of applicability, not only to broadcasting but also to the mobile services:

The 1983 Survey in S-E England
The 1985 Survey in Essex
The 1986 Survey in Southminster

The results are summarised according to approximate frequency, polarisation, the path type (land, sea), and environment category (urban, suburban, rural, mixed). Also indicated are antenna heights used. There is an important result showing how much the gain of the deployed antenna is augmented when its height doubles.

In conclusion, the authors point out that, "*The data presented in this paper aim to augmenting the existing height gain information available in the technical literature. In particular, their applicability to heights above the urban clutter could be of benefit in the planning of mobile services as regards base station sites, which are typically located at heights exceeding 20m. Hitherto, no height gain data are readily available specifically addressing receiver antenna heights above 10m*".

2.5.5 Review of Appropriate Engineering Models

2.5.5.1 The Okumura-Hata Model

With the advent of microcell coverage planning needs, especially for the cellular telephony systems, it become important to evaluate previously known models for this new purpose *Harley* (1989). The Okumura-Hata model (*Okumura*, 1968), (*Hata,* 1980) has particular limitations regarding its applicability. For example, it is valid over distances of 1 to 100 km for antenna heights from 30 to 1000m and the frequency range from 150 to 2000 MHz.

Two sets of measurements in the city of Melbourne were taken for 5 m and 9 m antenna heights, and below 1 km in distance, clearly outside the range of the Okumura-Hata model. In both cases the results of the signal field-strengths were plotted against distances of less than 1 km, and for antenna heights less than 30 m. Further analysis by the author of the existing propagation formula led to discovery of a new feature named "*the turning point*" in the measured characteristic.

The new distance marked by "the turning point" leads to an empirical model based on it, being an extension to Okumura-Hata method, attributing different formulae for attenuation in cases whether they are distances calculated before or beyond that point.

Harley states in conclusion, "*The measurements have been compared to the results of Okumura with the result that a new propagation model is required to explain microcell propagation along city streets, particularly, since a turning point in the attenuation slope is apparent. Further results are needed to verify the accuracy and coefficients of the model for other cities with different building types and with different city topologies*".

2.5.5.2 Longley-Rice and Johnson-Gierhart Models

The Longley-Rice and Johnson-Gierhart *Rice et al.* (1967) tropospheric propagation programs are useful in predicting propagation losses for paths over irregular terrain *Weiner, M.M.* (1986). These programs use an empirical database to statistically weigh

knife-edge diffraction losses with losses from multipath interference, smooth-spherical Earth diffraction, and troposcatter modes of propagation.

The paper provides a perspective concerning the use of the two programs with the emphasis being placed on the regions of applicability for the programmes and on factors that must be considered in selecting the input parameters. These programmes are written around the prediction models. However, an explicit comparison of the properties and regions of applicability of the two models has not been found to date in the literature. The article aims at comparing the numerical results from the programs against the common inputs and discussing their suitability for different possible scenarios.

2.5.5.3 Jenkinson and Van Dijk

Vertical profiles of refractive index were measured using a microwave refractometer in a light aircraft and reported by *Jenkinson and Van Dijk* (1969). Profiles were obtained by flying in ascending and descending spirals and assuming a horizontally stratified atmosphere for measurements between 500 and 5000 feet. The measurements took place between the island of Tasmania and Australia's Victoria State during summer at two frequencies of 173 and 1900 MHz. A set of air refractivity height profiles was gathered and analysed for the purpose of establishing the structure of atmosphere for propagation studies.

A super-refractive layer near 3000 feet was detected. This produced an enhanced signal on 173 MHz due either to some reflection from the layer, or possibly trapping. At 1900 MHz a similar situation was observed, most likely due to trapping. The measurements were based on meteorological observations of temperature, humidity and pressure from the aircraft, supplemented by routine readings from radio-sonde balloons.

Results are discussed as a sequence of events that took place during flights over these three consecutive days in terms of the values of refractivity, its gradients and the k-factor. All elevated trapping super-refractive layers were found and explained for these two frequencies. The relation between them and fading was commented on, and the possibility of reflection from this type of layer investigated.

Finally a super-refractive layer formation due to a subsidence inversion was documented, and its influence on propagation conditions demonstrated on the two frequencies in the VHF and UHF bands.

"The refractive index profiles show that during both January and March 1966, the average effective earth radius factor k under 1.30, being 1.25 and 1.28 respectively, for the atmosphere below 1500 feet, which is the region of most interest to radio systems."

2.5.5.4 Harvey's work

Harvey (1987 a) reported on the modelling of sub-refractive fading, as a project of the Research Laboratories of Telecom Australia in the Province of Queensland. Links were monitored in two different parts of the province, namely, at Julia Creek situated in the N-W part of the province, and Dalby close to Brisbane. The relevant information concerning the radio-meteorological conditions was gathered in two ways, firstly by monitoring the weather conditions in the areas, secondly by monitoring the links' performance, particularly with regards to sub-refractive fading conditions.

Sub-refraction has a specific feature that the rays are bent upward under these conditions. This is because the upper part of the troposphere is denser than the lower part. Therefore the speed of the radio waves is greater at the earth surface that bends them up, thus distorting the wave front to cause propagation away from the earth.

The process of sub-refraction is interpreted, from the k-factor point of view, as a so-called earth bulging phenomenon where the effective earth radius is smaller than the true earth radius. Effectively the k-factor is less than one and greater than zero.

In conclusion, the following was said: *"A meteorological model of the sub-refractive fading mechanism, has been established. The lowest (worst) signal levels correspond to positive linear refractive index gradients, which then allow a lower bound of the effective k value to be estimated. A number of events have been used to test this model of estimating k_e (min) from surface meteorological parameters and these are compared with those derived from fading on microwave paths. Considering the limited number of meteorological stations and observations, reasonable agreement is achieved".*

A further paper by *Harvey* (1987 b) deals specifically with the estimation of sub-refractive statistics using synoptic meteorological data. The effective k-factor values were obtained during nights from monitoring the links operated at Julia Creek and from Lands End to Gilliat at 4 GHz. It was observed that sub-refractive propagation takes place during nights and that the k_e (minimum) values are observed mainly at that time. Plots of $k_{e\ min}$ versus time have a characteristic V shape. Different fading phenomena depend on the behaviour of the k-factor values within the sub-refractive region, namely, for cases where the refractivity gradient assumes positive values. The nocturnal sub-refractive fading may be separated into different components such as selective multipath fading, and scintillation fading.

A linear refractivity gradient was assumed as a function of altitude between the ends of the radio path. *"The effective k-value k_e is that value of k that gives the same received field as if the refractive index gradient was linear and uniform along the length of the path". "If the linear gradients at points along the path differ in slope then k_e will represent an average gradient along the path".*

The characteristics obtained are mainly the result of the meteorological record analysis of event shape modelling and the long-term event extraction. The crucial information is presented in two figures depicting the *"Cumulative distribution of effective k-factor value (40km path)-comparison of Julia Creek measurement data with meteorological based estimates at stations to east and west".* And the *"Cumulative distribution of effective k-factor values (40km path)-Chartervile and Longreach, worst year and month".*

The first figure shows that, *"The sub-refraction is seen to be more severe towards the eastern (Richmond) side with Julia Creek and Cloncurry having similar statistics."*
The second figure is interpreted to indicate, *"cumulative distribution of effective k-factor values for the worst year, 1976, and the worst month Dec. 1976, for meteorological stations Charleville and Longreach".*

2.5.5.5. The EHF Telecommunication System Engineering Model (ETSEM)

The EHF Telecommunication System Engineering Model (ETSEM) has been created to assist in engineering of line-of-sight radio links. It was designed to operate in the frequency range of 10 GHz to 100 GHz, using a desktop computer, implementing the models of propagation (*Allen,* 1986).

Besides the propagation effects modelled to predict performance of the microwave terrestrial radio systems, extensive specifications of the input parameters including the equipment technical characteristics have to be supplied. In order to determine the cumulative distributions of the bit error rate in digital links, and the cumulative distributions of the worst channel signal-to-noise ratio in analogue links.

Primarily, the software was developed for the U.S. Army Information Systems Engineering Agency. It is therefore firmly based on the military radio standards. Since the Military Manuals, quoted in the paper, were declassified, many benefits for the non-military applications have followed from the use of these manuals.

The whole system may be divided into units: System Installation Models, Propagation Models, and System Performance Models.

The first part comprises of the Earth Geometry Module, which defaults to the International Spheroid for the specified Great Circle distance calculations and related data tabulation.

The second part contains the Path Profile and Ray-Path Modules. Its goals are the optimum selection of antenna heights in order to estimate the radio path reliability.

The propagation models cover the following features: Rain Attenuation Module, the Clear-Air Absorption Module, Multipath Fading Module, Combined Cumulative Distribution Module, and the Climatological Databases.

The first module contains three secondary models, such as the rain attenuation algorithm *"First of those predicts cumulative distribution of point rain rate. The second model converts the cumulative distribution of rain rate into a cumulative distribution of attenuation for the path (point-to-path conversion) using third model of raindrop size distribution"*.

In the second module, *"The model of clear-air absorption can be broken into two parts. The first part is due to molecular oxygen and varies with time by only a few percent in dB. The second part is due to water vapour and accordingly varies widely with time, season, and climate"*.

The third, Multipath Fading Module, is one of the models specifically developed for frequencies above 10 GHz by *Crombie* (1983). *"The author does not know of any method for scaling from the worst month to the other months of the year. Thus the model would be expected to normally overpredict the amount of multipath fading for an arbitrary interval of month"*.

The fourth part, the Combined Cumulative Distribution Module, is used to compute a combined cumulative distribution of attenuation with the link budget, in order to determine the received level signal (RLS) cumulative distribution.

The overall link attenuation cumulative distribution is made up of three contributions. These are from the multipath fading attenuation cumulative distribution, the attenuation of the water vapour cumulative distribution, and rain attenuation cumulative distribution. *"Once the cumulative distributions for the three propagation effects are determined, it is necessary to estimate the overall cumulative distribution of the RLS from them in order to predict the availability of the communication system"*.

The fifth module is the Climatological Databases, which requires input of all the climatological parameters needed by other propagation models. However, a part of this module constitutes the climatological databases for North America and Europe containing all necessary details provided by the meteorological stations with observations and monthly mean statistics.

"When the data bases are used, the averages of the transmitter and receiver latitudes and longitudes are computed to estimate the bearing of the centre of the path."

The obtained co-ordinates make it possible to interpolate from the database, which is searched for the closest two stations around the centre of the path.

"This method of interpolating from the database was selected because of its simplicity. The weighting, order of the polynomial, and maximum distance of stations from the path were all examined and selected to give the minimum standard error when interpolating mean monthly precipitation."

The System Performance Models are meant to predict the performance of the analogue and digital communication systems by means of the cumulative distribution of the RSL.
The Link Equipment Gain Module is meant to check the budget of the link by providing the input of the module with all listed operational parameters, and the characteristics of the equipment. The output of the module gives a calculated RSL and computed carrier-to-noise ratio (C/N).

The Analogue Modulation Performance Modules have two purposes. The first is to compute the FM/FDM single channel transfer function of the receiver, while the second module computes the availability of a channel in a FM/FDM system.

Furthermore, different kinds of noise sources are reviewed. These include thermal and intermodulation effects, and the behaviour of the signal to noise channels in multiplexed transmission, and the pre-emphasis and de-emphasis techniques to transmit such signals. Formulas to determine signal to noise ratio are given with comments regarding the relevant measurements, together with the noise generated by the equipment.

Frequent examples make reference to the military standards mentioned earlier, particularly regarding the hypothetical reference circuit and the annual outage time allowable.

The Digital Modulation Performance Module is to predict the availability of digital links, i.e. *"the fraction of time that the bit error rate (BER) is less than some required performance standard"*

According to MIL-STD-188-322 digital LOS microwave terrestrial radio links must comply with the design objective, *" to have a 30 dB minimum fade margin on all paths. All radio links are required to have a minimum annual path availability of 0.99995 for maintaining a bit error-rate of $5*10^{-9}$ for operations below 10GHz. All radio links are also required to have a minimum annual path availability of 0.99998 for maintaining a bit error rate of $1*10^{-2}$."*

In the present specification these objectives are taken up to 100 GHz as a long-term requirement, but for the short-term availability still remains at 0.99995 for BER less than$5*10^{-9}$. *"Long-term or median path performance (for error rates substantially less than $5*10^{-9}$ are not meaningful since such low error rates are generally a function of equipment performance, not propagation effects."*

Digital radio systems, using orthogonal modulation schemes, working against the background of Gaussian noise, would still retain the same shape of their transfer functions. However, the BER threshold will change from one receiver to another.

In order to compare the performance of a digital receiver to an equivalent analogue one the complementary error function containing the characteristic factors of BER, Pr (representing thermal noise), and K_0 (equipment dependent) must be solved for Pr.
In conclusion: *"The cumulative distribution of the bit error rate for digital links and cumulative distribution of the worst channel signal-to-noise ratio for FM/FDM links are predicted. These measures of performance are predicted for any interval of months out of the year."*

2.5.5.6 Ground wave propagation over an irregular earth surface

Ground wave propagation over irregular earth surface is reviewed historically and illustrated by a number of applications as examples of computer programs by *Rotheram, et*

al. (1985). The Marconi Research Centre (MRC) validated developments in the field of propagation for the lower VHF and HF frequency ranges. The MRC had published results of comparison for some known older and also some new programmes. These latter programmes employed algorithms to predict field strength values calculated by these programmes based on different formulas.

The initial phase of the theoretical development is due to Sommerfeld, who at the beginning of previous century developed the famous Sommerfeld flat earth theory *Sommerfeld*, (1909).
Further work came from Watson, who proposed the transformation known today by his name, and which resulted in the residue series, which constitutes a basis for the modern theoretical developments that followed.

The 1930s revived interest in these theories. Computational methods based on the algorithms were proposed, and the results finally verified by measurements of the radio fields.

An important contribution was made by *Millington* (1949), who developed a formula handling propagation over a mixed path, partially over land and over water. *"Further developments of the theory involved the extension to inhomogeneous atmospheres and irregular surfaces."*

This method is still in use but since then a more general theory has been proposed by Furutsu, which allows for different electrical properties of the path, different antenna heights, and for three-piece profiles.

Finally the theory developed by *Ott,* (1970) must be mentioned, as it is applicable to propagation over slowly undulating surface of the terrain. The final algorithm is presented in the form of a Volterra integral equation of the first kind, which is solved by the programme WAGNER.

All three methods yield numerical results that are obtained for similar conditions, meaning the input values. In particular the output values for the FURUTSU and NEWBREM programmes are compared and presented in a graphical form.

The curves initially used for predictions of the field strength are a function of distance and frequency within the range 10 kHz to 10 MHz, and were produced with the assumption of a linear refractive index variation with altitude.

Assuming an exponential character of refractivity, which would no doubt be more representative than a linear one, the ground-wave propagation curves then could be corrected. The MRC has done this by use of the GRWAVE program. *"The traditional ground-wave theory allowed the inclusion of gross atmospheric refractive index variations through the use of an effective earth's radius, equivalent to a linear refractive index variation. For average atmospheric conditions, the refractive index of the troposphere varies exponentially with heights."*

In conclusion, the paper documents the work on ground-wave propagation in the VHF and HF frequency bands, which has been conducted by the MRC building using concepts known to date, and associated with practical computational aspects. Gaps and shortcomings of the algorithms are pointed out and the scope for further work indicated.

2.5.5.7 Parabolic Equation Method

This method is a fairly new technique. Slingsby (1991) refers to the fact that the method was first applied in 1946 by Leontovich and Flock for propagation over a spherical earth in a vertically inhomogeneous atmosphere. The method was extended to the situation of a two-dimensional inhomogeneous atmosphere, yielding a parabolic partial differential equation for the field.

In the same paper the author mentions that a closed form solution of the wave equations, which govern realistic physical representation of the troposphere, can only be obtained in very simple cases. However, more complicated propagation problems can be handled numerically by making approximations to these equations.

The method was originally developed for application in underwater acoustic propagation problems to solve a parabolic equation identical in form to that applicable in tropospheric propagation. Use of the technique allows a full-wave solution without the large computational overheads of previous full-wave solutions. It is this aspect of the proposed method, which is of interest to researchers for application to terrestrial telecommunications problems.

As mentioned, the Soviet scientists M.A. Leontovich and V. A. Vock, from Vladivostock, originally proposed the method and closed form solution in 1946. The method works directly with field strength and the refractivity index, in N units, as a function of height and distance. Cylindrical coordinates are used. The field strength is expressed in three dimensional space co-ordinates and time, in the form of a simple hyperbolic wave equation. A transition is made to the Helmholtz Equation in elliptic form by dropping the time variable and assuming time to be a harmonic function.

An elliptical space variable equation in three dimensions is obtained. This leads to a parabolic equation by simply discarding one of the terms. Boundary conditions are applied. The first of these relates to the earth's electrical characteristics. Both media (ground and air) are assumed to act as dielectrics above 100 MHz.

The second boundary condition is usually at some arbitrarily adopted height of, for example, 1 km above the ground. In typical radar case considered the range of the radar is usually 300 to 400 km, or in a broadcasting case some 50 to 100 km depending on power (effective isotropic radiated power), mast height, and the terrain contour.

The range and character of solutions are discussed in Levy (1995) and a history of the latest developments in the field is given. In previous approaches the parabolic equation was solved by means of a range dependent marching method. The frequency, propagation angles and domain size affected the integration times. In some cases solutions are required over long ranges. For example, in a defence radar application one is interested in frequency, propagation angles, ranges up to 400 km, and heights up to 10 km. Larger domains are of interest in the case where one is modelling earth satellite communications paths. In these cases parabolic equations can become computationally intensive.

Levy points out developments and difficulties encountered, and also refers to current contributions. It is asserted that strong variations in the refractivity index seldom occur above a kilometre or so, and for practical purposes become standard above a certain height. Accordingly researchers have been interested in finding efficient methods to extend the parabolic equation method to high altitudes. The relatively slow standard parabolic equation methods are reserved for calculations in that portion of the domain where the atmospheric irregularities occur. A hybrid technique combining the parabolic equation method and ray tracing has been developed.

This method however remained a dormant concept until the advent of powerful computers when further work on its application commenced. Since then other mathematical techniques such as the finite element method, the fast Fourier transform method, the split-step method, etcetera, have been introduced and developed.

Today computational cost is hardly a factor, given the power of modern desktop computers. Instead the time required to calculate radio coverage on an electronic map is given. Despite the technological advances, the problem of using a two-dimensional refractivity index which varies over an area and with height remains. A successful approach to this problem must still be found.

Conclusions offered by Levy and Craig (1989) are still valid today. They assert that application of the parabolic equation method used with refractivity data obtained from modern radiosondes (minisondes) is a powerful tool for the prediction of radio fieldstrength. Calculated fieldstrengths are in good agreement with measured results even in the presence of noisy refractivity data. It is now possible to consider the effects of random fluctuations in either the measurements or in the propagating medium since these effects are quantifiable. It is suggested that because of statistical studies the field should be described in stochastic terms rather than deterministic ones.

Two major centres of scientific research and development of the parabolic equation method are outstanding in the field; these are the Appleton Laboratory in the UK, and John's Hopkins University in the US. The smaller centres are at the San Diego Naval Base

in California. Occasionally papers from France, Turkey and Italy have also been published.

2.5.5.8 Ray Tracing method

The method is exclusively applicable to terrestrial line-of-sight microwave radio links, where the transmitter and receiver can be connected by a continuous trajectory-line indicating a path along which propagation in the troposphere takes place.

This line is neither straight nor an arc, but is usually curved in some way as the refractive index changes along the path according to meteorological conditions. Often several ray paths may be found for the waves travelling from the transmitter to the receiver. Because the waves could arrive along ray paths of different length there is usually some time delay between them. This could result in either constructive or destructive interference, depending on the phase difference. In the case of destructive interference the result could be fading of the signal. In the case of reflections from ground or the sides of hills or mountains, interference between the direct and reflected rays could also occur.

Often the method is used to determine the angle-of-arrival at the receiving antenna and this in turn provides information on the required tilt of the antenna.

The method requires a vertical profile of the refractive index of the troposphere and it is often used to analyse for ducting conditions. This assists with the design of a line-of-sight terrestrial radio links in the presence of elevated and surface ducting conditions in the area. The areas may have different climatic conditions subject to seasonal changes. This could be conducive to duct creation. In turn this could cause the rays to be reflected or defocused and could result in different kinds of fading, which could disrupt signals at the receiver sites (Costa, 1991).

Therefore, it is important, from the design point of view, to determine the correct heights of towers for any given link at least to avoid signal disruption by a duct if it cannot be turned to an advantage. One of the conclusions by Webster (1983) is to the effect that,

"The occurrence of multipath fading might well be reduced by the deliberate mounting of antennas at significantly different heights above the local terrain."

The present literature survey occasionally covers titles on this technique, where a prominent author Alan R. Webster proposed a vertical refractivity profile in the form of an arc tangent function of height that provides for an elevated tropospheric layer (Webster, 1983). Characteristics of the layer may easily be described by the parameters of the arc tangent function. These are the thickness, elevation and the steepness of the refractivity change across the slope or a trough if a refractivity gradient is contemplated. Existence of such a layer between transmitter and receiver results in multiple ray propagation caused by refractivity variation. Frequency sensitive fading may arise because of this condition.

This method is not applicable to very long distance over the horizon propagation where a wave approach is necessary. It may however be used on shorter distance line-of-sight links to assess the ranges of delay times, amplitudes and angle-of-arrival to be expected (Webster, 1983).

This specific approach relates particularly to clear-air propagation, which, according to some researchers, is not yet fully understood.

Some important conclusions are mentioned by Webster (1983) as, *"Single-path fading can be produced by a layer forming below the transmitter and/or receiver heights which has the appearance of being due to multipath propagation. While it might be argued that a "fade is a fade," a significant difference is that such single path fading is not frequency selective and hence does not produce abrupt phase changes across the band which is a feature of multipath fading."*

2.5.6 Historic background where propagation development is validated

Arnold (1986) gives a contemporary review of geometrical theories of wave propagation. *"The review begins with a brief historical overview to place a perspective on current work, and ends with an assessment of future directions for geometrical techniques."*

Propagation of radio waves has always been visualised most effectively by geometrical interpretations of the ray trajectories and the wave fronts travelling along lines not always necessarily straight.

Geometry plays a particularly important role in the development and use of techniques in the propagation of waves by exploring the effects in scientific radio planning. The most important of the concepts found here is undoubtedly the k-factor, which is based on the idea of waves travelling in straight lines as a form of mapping these ray trajectories, which are not necessarily straight but are straightened by using the concept of the Effective Earth Radius.

The paper in fact deals with much more general assessment of patterns in knowledge by saying, *"The interaction, which exists between geometry and physics has been the deepest and richest theme in the development of science since antiquity, and this relationship is nowhere exemplified better than in the field of optics. The maxim that "light travels on straight lines" which forms the basis of all elementary treatments of the subject already exhibits the complete unity of the concepts of light propagation. The geometry of space, a unity, which is only enhanced by modern replacement of "geodesic" for "straight line" following Hamilton and Einstein."*

Despite propagation in outer space, everything basically refers to gravitational force that curves space, or in case of planet Earth attracts the atmosphere permanently, thereby, allowing the permanent existence of refractivity, which shapes trajectories of rays in the terrestrial radio-wave propagation. The mutual influence of geometry and physics brings particularly fruitful development to both sciences, *"To be more specific, we should try to relate problems of current interest in geometry and wave propagation."*

The author envisaged the purpose of the paper as querying to what extent new mathematics could be applied to solving problems in wave propagation theory. He stressed the importance of the intuitive character of geometry, which makes it the most fundamental of all mathematical disciplines.

However, mention is also made that the last century (20th) witnessed a departure from the rational simplicity of Euclid and Pythagoras, for which classical geometry was known, but that that century also saw a postulatory, more abstract, approach that later prevailed. Problems of radio propagation formulated by a means of partial differential equations that are of more than one variable are usually solved by separation of the unknowns. As it is not always possible to separate the unknown variables the solutions may not be analytically obtained. Therefore, they are sought by approximated numerical methods. *"As the separability of the variables depends on the presence of symmetry in the geometry of the problem, this method has restricted utility."*

The review considers the state of research in geometrical methods suitable for solving problems in radio wave propagation.

The second paragraph opens a discussion on a problem of current interest, the non-uniformity of the classical theory of geometrical optics presented from the historical perspective of its research and development.

Next the Luneberg formulation of geometrical optics principles is considered. Different methods such as patching are mentioned to correct the shortcomings of Kirchhoff-Huyghens theory.

Inhomogenous-media propagation is addressed in terms of the theory of caustics as formulated by Maslov.

A ray-mode transform, which is based on the Poisson sum formula, addresses new techniques applicable to wave-guides.

Communications engineering is considered in terms of attempts to apply new theoretical models.

Finally the author speculates on the future role of geometry in wave theory.

The most important ideas and concepts relevant to the theme are, in fact, described earlier in the paper, and these will be discussed briefly now for the purpose of completeness and perspective of the review.

Specifically astronomical observations gave rise to different cosmologies, having a geometrical character, especially for describing trajectories of celestial bodies. *"Even the etymology of its name indicates the practical nature of geometry (earth-measure)."*

Throughout the Renaissance in Europe, the study of optics and mechanics were closely relating to geometry, culminating in Newton's *Principia Mathematica* and *Opticks* following geometrical arguments, which lead to his discovery of differential calculus. Differential calculus by Newton combined with Descartes co-ordinate geometry made it possible for Leibnitz's work *"on transformations of light ray caustics by curved reflectors, a prototypical application of differential geometry to optical physics"*.

Newton's legacy led the eighteen-century mathematicians, Euler, Lagrange and Laplace, to combine development of geometrical-mechanical synthesis.

Further work of "*Hamilton was able to show that the known laws of geometrical optics in particular Fermat's Principle of least optical path length between source point and observation point, for a medium with continuously varying optical in-homogeneity, could be expressed in an identical form to the laws of mechanics, as geometry in space."*

At the beginning of 19th century "quivering" of the "particles" of light was no longer a satisfactory explanation. Experiments by Young and Fresnel suggest a wave motion, rather than a particle motion. The final confirmation of the wave motion nature of light came from Fresnel who demonstrated the phenomenon of diffraction displayed by light. *"The necessary arrival of quantum mechanics in the early 20th century supplied the same linear background theory to classical mechanics as did Maxwell's equations for classical geometrical optics."*

The Schroedinger equation came into existence after the work contributed by Planck, Heisenberg, Bohr, and above all by Hamilton. It connects position of a point with its

momentum through the Planck constant, according to the Uncertainty Principle of Heisenberg, for certain boundary conditions like e.g. a potential well. The solution obtained comes as a wave function and is interpreted as a probability of finding the point-particle, according to its energy at a specific place.

The remaining question still concerns the physical interpretation of the wave function? *"In short: can quantum mechanics be uniquely constructed from classical mechanics?"* However, the similarity between quantum mechanics and geometrical optics leads to a question of fitting the wave functions to a given set of trajectories, which is a well-posed problem of correspondence in optics, and the quantum correspondence problem. *"In fact, it may be that the quantum correspondence problem should be posed in the same way as the optical correspondence problem: purely as an asymptotic relation between wave functions and trajectories."* This still remains an open question.

In conclusion the author states, *"The theory of wave propagation is fundamental to all of modern communications engineering, and to most of solid-state physics, and we have shown how geometrical insight continually manifests itself in the understanding of waves."* Of particular interest is the future of the k-factor in the propagation of radio waves. It is deeply geometric in nature, character and function as a real concept with its own meaning. It could still play a role as a unifying factor between geometry and waves in propagation studies.

"Inevitably the ideas in current vogue at the frontiers of theoretical physics will find their way into more practical areas of application, such as the exploitation of optical non-linearity in devices for optical signal processing."

2.5.7 Other Southern African Studies

Afullo et al. (2001) report on studies of the refractivity gradient and the k-factor values in Botswana. The paper indicates a wider African interest in the propagation studies in the troposphere on the continent, and includes a direct contribution from Namibia. New initiatives in the field in other parts of Africa are referred to. These took place from the

nineties to the present time in North West Africa and covered the radio spectrum from VHF to microwave.

Three years of measurements covering the period 1996 – 1998 is reported at Maun, in northern Botswana. This is at 945 m above sea level. Vaisala low-resolution radiosondes were deployed twice a day at 1 am and 1 pm. Because the sonde reported only at 10 sec intervals, the usual restricted altitude for radio meteorological work of 100 m was increased to 200 m above ground level in order to have more data points to work with to determine the median and the effective k-factor values.

The results obtained lead to plots expressing the refractivity gradient within the first 200 m as a percentage of time for events of the gradients changing from –200 to +100 N/km. The variation of the refractivity gradient and the cumulative distribution of the gradient are depicted. Both data representations include gradients appropriate for the ducting mode. In the discussion of the results, the median value of the refractivity gradient was determined as –20 N-units/km for the months of February (21%), May (46%), August (48%), and November (28%).

There is a pronounced tendency for sub-refractivity in winter rather than in summer when super-refractivity prevails. The reader is reminded that in the Southern Hemisphere wintertime is from May to August, while summer is regarded as occurring between November and February.

The authors present the k-factor distribution for February, May, August and September for Maun as the frequency occurrence with the median value of 1.1. They also give an effective value of the k-factor of $k_e = 0.7$, which is exceeded 99.9% of time. These values exclude the contributions of ducting refractivity gradients, therefore, the all-inclusive values will have a mean k-factor of 1.03 and an effective k-factor of $k_e = 0.61$.

2.6 Conclusion

The literature survey has been conducted with the objective of covering the body of knowledge as closely as possible with regards to the existing scholarship on the subject of

the k-factor. The main difficulty encountered during the literature review was that there appears to be a little known about the k-factor, from its initial conception to date, apart from the practical value of its application.

Over and above that, the concept is scattered across many publications ranging from the textbook definitions through various scientific reports, journals, and conference papers up to and including the ITU-R recommendations and reports.

Virtually all the sources deal with its applications and almost none is devoted to its concept and philosophy. Not even one monograph on the subject was found. A very limited volume of research appears to have been published over the last 45 years on the topic throughout the world. During the last 15 years there has been some progress, ironically, mainly in South Africa.

However, a recent conference publication made mention that *"The effective earth radius concept is more complicated than usually is presented in textbooks" Denny* (2000.). Apart from that, it has been acknowledged almost from the beginning that it is a valid and useful concept, even if very little is known about it as yet.

The original South African work made it worthwhile, and indeed possible, for the present effort to be undertaken and to take progress a step further.

Chapter 3

THE AVAILABLE SOUTH AFRICAN DATA SOURCES AND THE FIRST HYPOTHESIS

3.1 Introduction

Two sets of data, which are widely used in South Africa at present, are presented here. These are the SABC and the CSIR data as suggested for use by *Nel and Erasmus* (1986) and *Pauw* (1996) respectively. The data are presented as tables of the cumulative distribution of the radio refractive k-factor values expressed as a percentage of time of occurrence, in different parts of the country. These tables are listed below as Tables 3.1 and 3.2 respectively, and discussed in context in the appropriate sections 3.2.1 and 3.2.2. The copies of the original documents are presented here in a similar format, for purposes of analysis and comparison, and for better, more orderly and consistent presentation.

The third set of data is that presented by Nel in his MSc thesis *Nel* (1989). This set comprises tables of the average cumulative probability of occurrence for the gradient of refractive index, and the k-factor for each of 12 months for 8 stations at which radiosonde data were obtained during the period 1976 to 1986. This set has been subjected to a thorough regression analysis in order to identify its properties for the purpose of modelling.

The fourth set of data is based on original routine ground based observational data gathered by the South African Weather Service and further processed independently by means of fundamentally different method from that of Nel. Results from these two equal size sets are discussed and compared. The final outcome from both sets of results is assessed for their differences and similarities in order to formulate final conclusions and recommendations for the follow up work.

In this chapter, the first postulate of a simple formula to represent the cumulative probability that a particular value of the k-factor will be exceeded, will be made on the basis of the data initially available as the SABC and CSIR tables. In doing so it will be following the historical sequence of the work done in the development of the thesis. The

concept of the Eigen-functions and Eigen-values to force fit the proposed formula to the data at one point on the basis of a least mean square fit to the available data will be used. In later work the proposed distribution formula was evaluated in terms of regression analyses.

3.2 THE SOUTH AFRICAN DATA SOURCES

3.2.1 The SABC Data

The SABC data initially originated from the first report by *Nel and Erasmus* (1986). This report contained a table, given below as Table 3.1, which listed values of the k-factor for the cumulative percentage of occurrence of specific values for nine different major centres in South Africa and Namibia. These values are presented in terms of day/night conditions in order to facilitate radio planning for the best and worst propagation conditions.

3.2.2 The CSIR Data

The CSIR data suggested by *Pauw* (1996) was published after the previous data set became widely known and popular with local radio planners and users. It presented new and improved data, which was different from the previous set. This was expected to be much more accurate and reliable than the previous one. Further analysis of the data during the course of the work presented here confirmed this supposition. The data set is structured differently inasmuch as it presents fewer values of the k-factor corresponding to different percentages of occurrence, is symmetrical in its presentation and is given for only eight places in South Africa and Namibia as listed below in Table 3.2. In essence it presents the highest and lowest values to be expected for the k-factors, as an aid in evaluating the best and worst conditions with regards to communications and interference in the planning of communication systems.

It was found after detailed examination and comparisons with the complete set of data published by Nel in his MSc-dissertation, that in fact the CSIR data were extracted from this work *Nel* (1989). The CSIR data, therefore, constitutes a subset of the more

comprehensive data. As such it contains only the maximum and minimum values of the main set across all percentages and months.

3.2.3 The Comprehensive Set of Monthly Averaged Data

The two data sets referred to above are widely known to and accepted by the telecommunications community in South Africa. They have been used extensively because of their simplicity and universality for radio telecommunications planning. However, the most comprehensive data set of the observed cumulative distributions for the k-factor is that due to *Nel* (1989). This set is tabulated as Tables A.1-A.8 *Nel* (1989), for twelve months of the year for each of the 8 observation stations where meteorological radiosonde data were taken. This set has been examined most extensively in the present work, in order to obtain an empirical model of the cumulative distribution of the k-factor, and also to determine the most valid model of spatial distribution for the k-factor over land and at the coast.

3.3 The First Hypothesis

After a careful appraisal of the data as listed in Tables 3.1 and 3.2, it was proposed that the fraction of time, Ψ, that the k-factor would exceed a particular value, k, of the k-factor could be represented in terms of some standard variance, σ^2, of k as follows:

$$\psi = \exp\left(-\frac{(k-1)^2}{2*\sigma^2}\right), \qquad (3.1)$$

Expression (3.1) applies for k greater than unity, and for a fraction of time of occurrence lying between 1 (for k = 1) and zero (for some value of k greater than 1). Examination of the data in Tables 3.1, and 3.2 shows that the k-factor could be less than one but that the cumulative probability of occurrence that this will be exceeded is high.

The process of evaluating an Eigen-value function to provide a least mean squares fit for a given variance is best illustrated by means of an example. Consider, for example, the SABC daytime data for Cape Town. Figure 3.1 illustrates a set of curves for the

percentages of occurrence from Table 3.1, for Cape Town, for various values of variance such that the curve for a particular percentage passes through a specific data point for the k-factor and percentage of occurrence. A least mean square fit was performed for each of the curves in terms of the available data points. The curve giving the lowest residual values was selected to represent the data trend. For the example being considered this resulted in the matched curve as shown in Figure 3.2, where the matched data point is at k=1.85 for the 10% probability level of being exceeded. In other words, there is a 10% cumulative probability that the k-factor will exceed 1.85. It was thus possible to find a unique matched curve for each of the sets of data shown in Tables 3.1 and 3.2, such that the curve for any particular set would pass through at least one data point. That curve was the one generated for each set and having the lowest residual mean squares error.

This concept of maintaining certain original values in each data set was conceived around the value of a variance, which offered the smallest error compared to all other Eigen-functions generated by the other given points. This way, at least one original value was preserved. It was now possible to recreate the data in Tables 3.1 and 3.2 with the least intervention in the SABC and CSIR data, in order, to investigate the third hypothesis, which is that the refractivity gradient reduced to the sea level is constant, almost everywhere.

The recreated tables corresponding to Tables 3.1 and 3.2 are shown as Tables 3.3 and 3.4 respectively.

Table 3.1 Cumulative distribution of day- and nighttime values of the k-factor expected to be exceeded for various percentages of time, as proposed for use by the SABC *Nel and Erasmus* (1986)

LOCATION	Percentage of time that specific values of the k-factor are exceeded during the daytime									
	0.10%	0.50%	1.00%	5.00%	10.00%	50.00%	90.00%	95.00%	99.00%	99.90%
Cape Town	2.95	2.73	2.50	2.12	1.85	1.42	1.27	1.22	1.18	1.05
Port Elizabeth	4.04	3.30	3.04	2.28	1.96	1.46	1.28	1.24	1.16	1.10
Alexander Bay	3.04	2.72	2.56	2.26	2.10	1.60	1.28	1.26	1.18	1.10
Upington	1.72	1.68	1.57	1.43	1.38	1.22	1.12	1.08	1.07	0.95
Bloemfontein	1.70	1.62	1.57	1.42	1.35	1.22	1.15	1.13	1.08	1.02
Durban	4.84	4.00	3.14	2.36	2.04	1.52	1.30	1.26	1.10	1.02
Pretoria	1.86	1.70	1.54	1.36	1.40	1.20	1.10	1.10	1.10	0.94
Bethlehem	1.90	1.84	1.72	1.56	1.50	1.30	1.18	1.16	1.12	1.02
	Percentage of time that specific values of the k-factor are exceeded during the nighttime									
	0.10%	0.50%	1.00%	5.00%	10.00%	50.00%	90.00%	95.00%	99.00%	99.90%
Cape Town	3.92	3.38	3.03	2.42	2.18	1.56	1.37	1.33	1.13	0.94
Port Elizabeth	3.94	3.28	3.08	2.38	2.09	1.50	1.30	1.27	1.18	1.13
Alexander Bay	3.57	3.34	3.13	2.63	2.36	1.72	1.42	1.30	1.14	0.97
Upington	2.56	2.16	1.93	1.66	1.57	1.37	1.24	1.21	1.12	1.02
Bloemfontein	2.11	1.95	1.85	1.68	1.60	1.41	1.30	1.27	1.23	1.12
Durban	4.40	3.82	3.19	2.25	2.03	1.55	1.38	1.33	1.14	1.01
Pretoria	2.00	1.90	1.78	1.62	1.56	1.37	1.29	1.24	1.20	1.04
Windhoek	2.04	1.91	1.82	1.66	1.58	1.37	1.25	1.23	1.15	1.12

Table 3.2 Cumulative distribution of day- and nighttime values of the k-factor, expected to be exceeded for various percentages of time, as proposed for use by the CSIR *Pauw* (1996)

LOCATION	Percentage of time that the k-factor is exceeded for communications availability studies						
	0.10%	1%	5%	50%	95%	99%	99.90%
Cape Town	2.33	2.16	1.91	1.44	1.25	1.20	0.99
Port Elizabeth	2.51	2.20	1.95	1.45	1.26	1.19	0.98
Alexander Bay	2.58	2.21	2.00	1.49	1.21	1.14	0.91
Upington	1.67	1.61	1.49	1.27	1.11	1.04	0.98
Bloemfontein	1.63	1.55	1.47	1.30	1.14	1.08	1.06
Durban	2.30	2.19	2.00	1.45	1.22	1.17	1.04
Pretoria	1.65	1.53	1.44	1.28	1.15	1.12	0.93
Windhoek	1.61	1.46	1.42	1.24	1.12	1.10	1.05
	Percentage of time that the k-factor is exceeded for communications interference studies						
	0.10%	1%	5%	50%	95%	99%	99.90%
Cape Town	5.43	3.16	2.42	1.52	1.29	1.25	1.23
Port Elizabeth	6.07	3.78	2.61	1.56	1.31	1.25	1.23
Alexander Bay	4.03	3.37	2.73	1.69	1.30	1.23	1.17
Upington	2.84	2.13	1.73	1.35	1.19	1.15	1.13
Bloemfontein	2.44	2.01	1.76	1.40	1.21	1.14	1.11
Durban	6.12	3.17	2.47	1.57	1.32	1.25	1.19
Pretoria	2.35	1.90	1.67	1.41	1.25	1.21	1.16
Windhoek	2.06	1.97	1.84	1.38	1.19	1.16	1.07

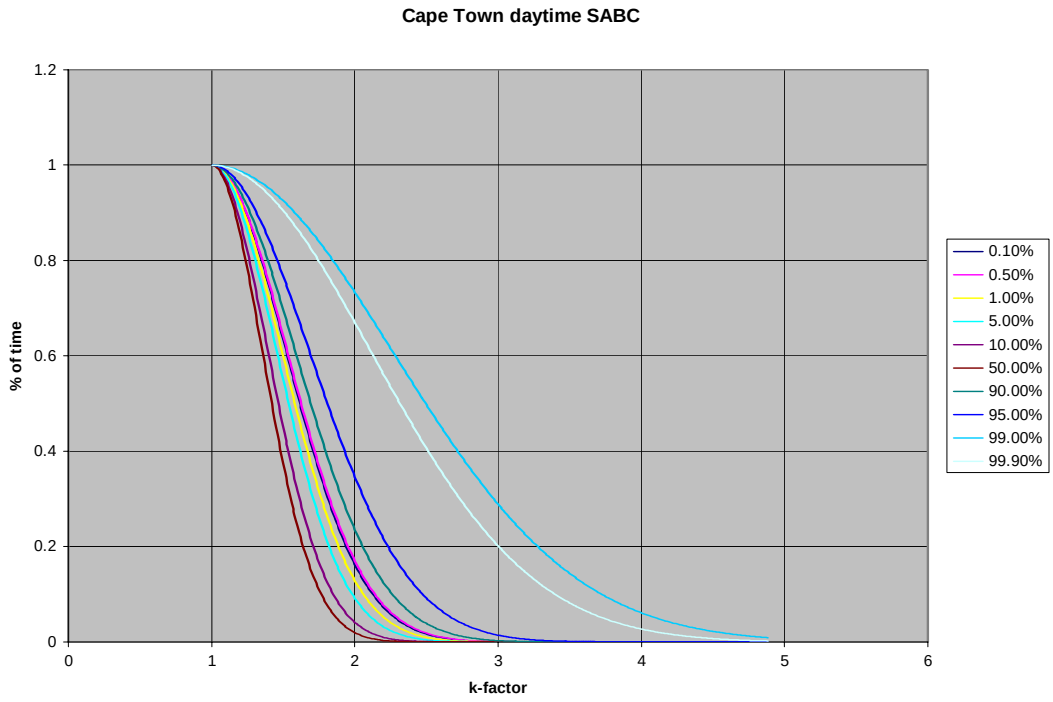

Figure 3.1 Sets of curves illustrating the percentage of time that a particular value of the k-factor will be exceeded as a function of different values of the variance selected to match the SABC data for Cape Town daytime (See Table 3.1)

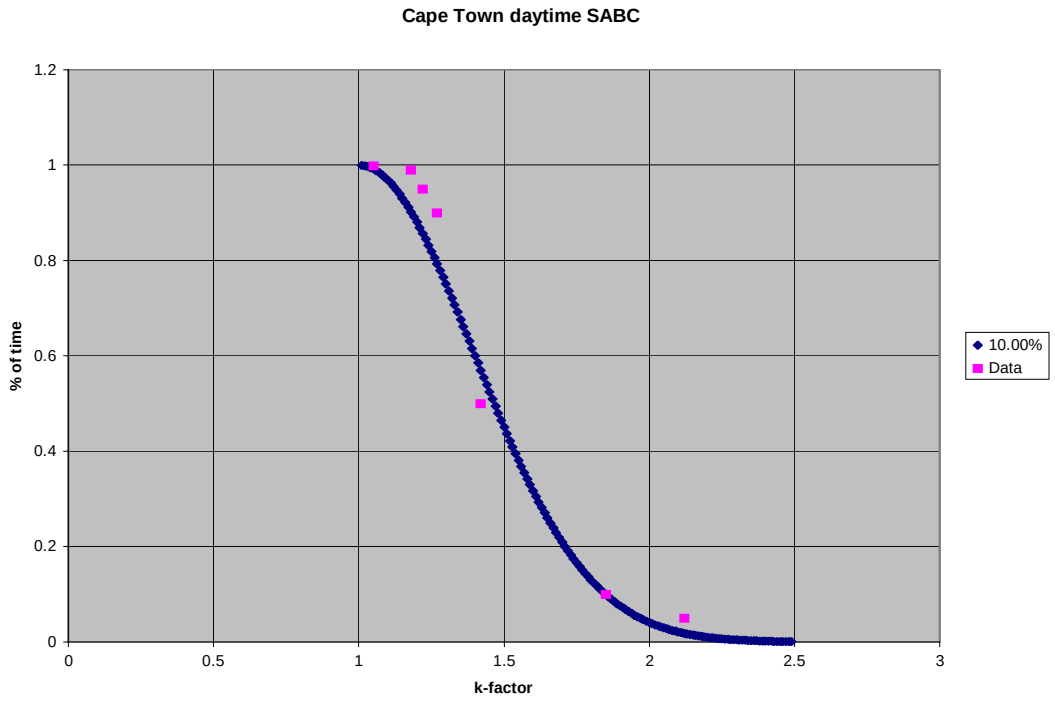

Figure 3.2 The selected "Eigen-function" curve providing the least mean squares residuals for the k=1.85, 10% probability of exceedence data point for the SABC daytime data for Cape Town (See Table 3.3).

Table 3.3 Recreated cumulative distributions of day- and nighttime values of the k-factor expected to be exceeded for various percentages of time, based on an "Eigen-function" analysis of the SABC data presented in Table 3.1

LOCATION	Predicted percentage of time that specific values of the k-factor are exceeded during the daytime									
	0.10%	0.50%	1.00%	5.00%	10.00%	50.00%	90.00%	95.00%	99.00%	99.90%
Cape Town	2.47	2.29	2.20	1.97	1.85	1.47	1.18	1.13	1.06	1.02
Port Elizabeth	2.66	2.46	2.36	2.10	1.96	1.53	1.21	1.14	1.06	1.02
Alexander Bay	2.96	2.72	2.60	2.29	2.13	1.62	1.24	1.17	1.07	1.02
Upington	1.70	1.61	1.57	1.46	1.40	1.22	1.09	1.06	1.03	1.01
Bloemfontein	1.71	1.62	1.58	1.47	1.41	1.22	1.09	1.06	1.03	1.01
Durban	2.80	2.58	2.47	2.19	2.04	1.57	1.22	1.16	1.07	1.02
Pretoria	1.66	1.58	1.54	1.44	1.38	1.21	1.08	1.06	1.03	1.01
Bethlehem	2.03	1.90	1.84	1.68	1.59	1.33	1.13	1.09	1.04	1.01
	Predicted percentage of time that specific values of the k-factor are exceeded during nighttime									
	0.10%	0.50%	1.00%	5.00%	10.00%	50.00%	90.00%	95.00%	99.00%	99.90%
Cape Town	3.04	2.79	2.67	2.35	2.18	1.65	1.25	1.18	1.08	1.02
Port Elizabeth	2.89	2.65	2.54	2.24	2.09	1.60	1.23	1.16	1.07	1.02
Alexander Bay	3.48	3.17	3.02	2.63	2.43	1.78	1.31	1.21	1.09	1.03
Upington	2.17	2.02	1.95	1.77	1.67	1.37	1.14	1.10	1.04	1.01
Bloemfontein	2.29	2.13	2.06	1.85	1.75	1.41	1.16	1.11	1.05	1.02
Durban	2.90	2.66	2.55	2.25	2.10	1.60	1.23	1.16	1.07	1.02
Pretoria	2.17	2.02	1.95	1.77	1.67	1.37	1.14	1.10	1.04	1.01
Windhoek	2.17	2.02	1.95	1.77	1.67	1.37	1.14	1.10	1.04	1.01

Table 3.4 Recreated cumulative distributions of day- and nighttime values of the k-factor expected to be exceeded for various percentages of time, based on an "Eigen-function" analysis of the CSIR data presented in Table 3.2

LOCATION	Predicted percentage of time that the k-factor is exceeded for communications availability studies						
	0.10%	1.00%	5.00%	50.00%	95.00%	99.00%	99.90%
Cape Town	2.42	2.16	1.94	1.45	1.12	1.05	1.02
Port Elizabeth	2.51	2.23	1.99	1.48	1.13	1.06	1.02
Alexander Bay	2.58	2.29	2.04	1.50	1.14	1.06	1.02
Upington	1.85	1.70	1.56	1.27	1.07	1.03	1.01
Bloemfontein	1.95	1.77	1.62	1.30	1.08	1.04	1.01
Durban	2.52	2.24	2.00	1.48	1.13	1.06	1.02
Pretoria	1.65	1.53	1.43	1.21	1.06	1.02	1.01
Windhoek	1.76	1.62	1.50	1.24	1.07	1.03	1.01
LOCATION	Predicted percentage of time that the k-factor is exceeded for communications interference studies						
	0.10%	1.00%	5.00%	50.00%	95.00%	99.00%	99.90%
Cape Town	3.16	2.76	2.42	1.68	1.19	1.08	1.03
Port Elizabeth	2.77	2.44	2.16	1.56	1.15	1.07	1.02
Alexander Bay	3.18	2.78	2.43	1.69	1.19	1.08	1.03
Upington	2.11	1.91	1.73	1.35	1.10	1.04	1.01
Bloemfontein	2.26	2.03	1.83	1.40	1.11	1.05	1.02
Durban	3.23	2.82	2.47	1.71	1.19	1.09	1.03
Pretoria	2.35	2.10	1.89	1.43	1.12	1.05	1.02
Windhoek	2.28	2.04	1.84	1.40	1.11	1.05	1.02

Examination of Tables 3.3 and 3.4 shows no values of the k-factor less than 1 for high values of exceedence. This is hardly surprising in light of the formula proposed in equation (3.1) and its assumed range of applicability.

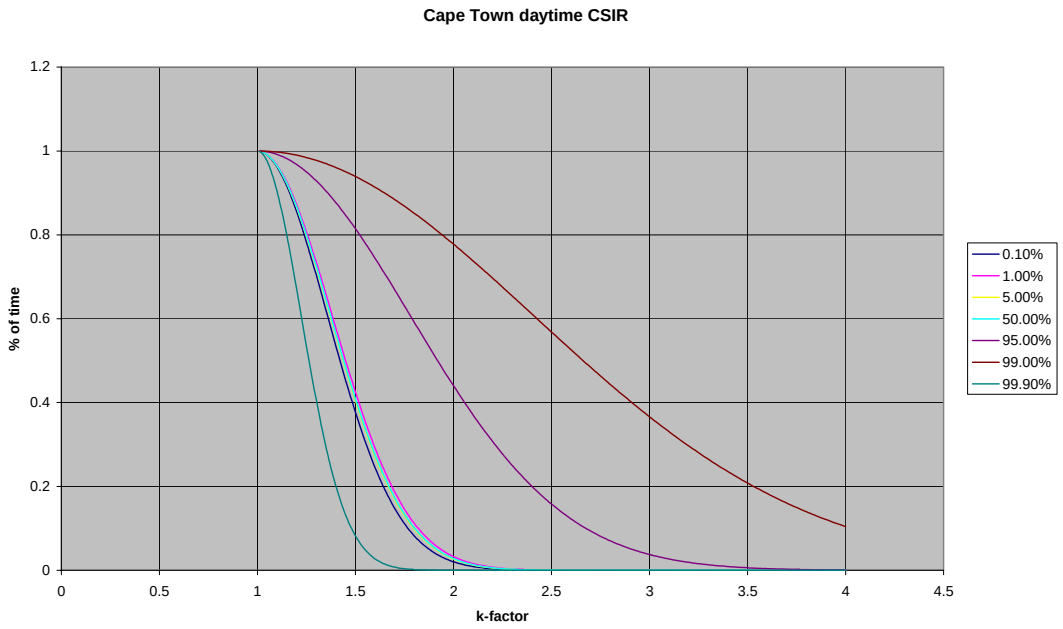

Figure 3.3 Sets of curves illustrating the percentage of time that a particular value of the k-factor will be exceeded as a function of different values of the variance selected to match the CSIR data for Cape Town daytime (See Table 3.2)

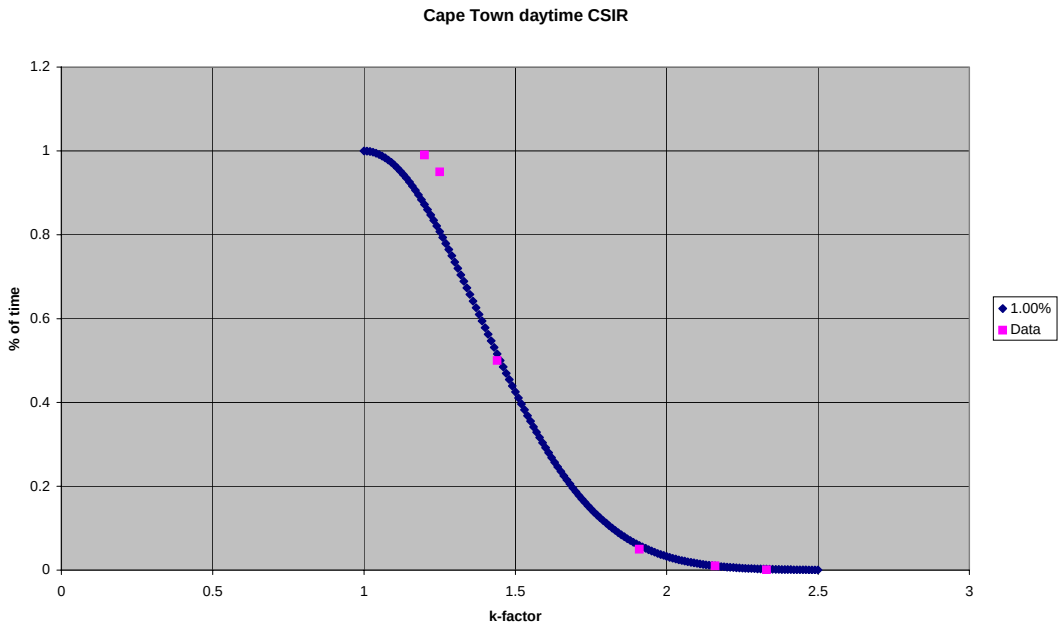

Figure 3.4 The selected "Eigen-function" curve providing the least mean squares residuals for the k=2.16, 1% probability of exceedence data point for the CSIR daytime data for Cape Town (See Table 3.4).

3.4 Regression Analysis of Nel's Data

The cumulative data, ψ, tabulated in Table A.1-A.8 of *Nel* (1989), for the monthly observed k-factors for Windhoek in Namibia, Upington, Bloemfontein, Pretoria, Alexander Bay, Cape Town, Port Elizabeth and Durban in South Africa were subjected to a simple regression analysis using the statistical analysis package MINITAB ©. The input data were subjected to a close examination for consistency because of a few obvious typographical errors. The gradient of refractive index and the k-factor values were recalculated using the other information provided in the table. These regression analyses were performed for the averaged monthly data, and the maximum, minimum and average values for the year as a whole. Results from these analyses were published by *Palmer and Baker* (2002).

The basis of the regression analyses was derived from expression (3.1), which yields,

$$\sqrt{\ln(1/\psi)} = (k-1)\frac{1}{\sigma\sqrt{2}} + c, \qquad (3.2)$$

where c represents a constant term in the regression analysis in order to compensate for any observed values of the k-factor which might be less than unity, and $1/(\sigma\sqrt{2})$ is the first predictor coefficient.

Examination of the resultant regression graphs for all stations for all months, typical examples of which are shown in Figures 3.5 - 3.8, (all generated from MINITAB ©), suggests that there appears to be a dominant term, which could correspond to the so-called "dry" term. And a second term, which appears to be seasonal, or climatic, and which could correspond the so-called "wet" term. *Hall* (1979) discusses the partition of the refractive index in terms of the "dry" and "wet" concepts, while *Nel, et al*. (1989) also refer to these terms. It is clear that there is much greater variability in the "wet" term, than in the "dry" term and that the "dry" term contributes significantly more to the refractive index than the "wet" term. In *Palmer and Baker* (2002) only the simple regression analysis is considered, thus ignoring the effect of a "wet" term contribution. The follow-up paper by *Baker and Palmer* (2002) considered the possibility of both terms in the regression analyses.

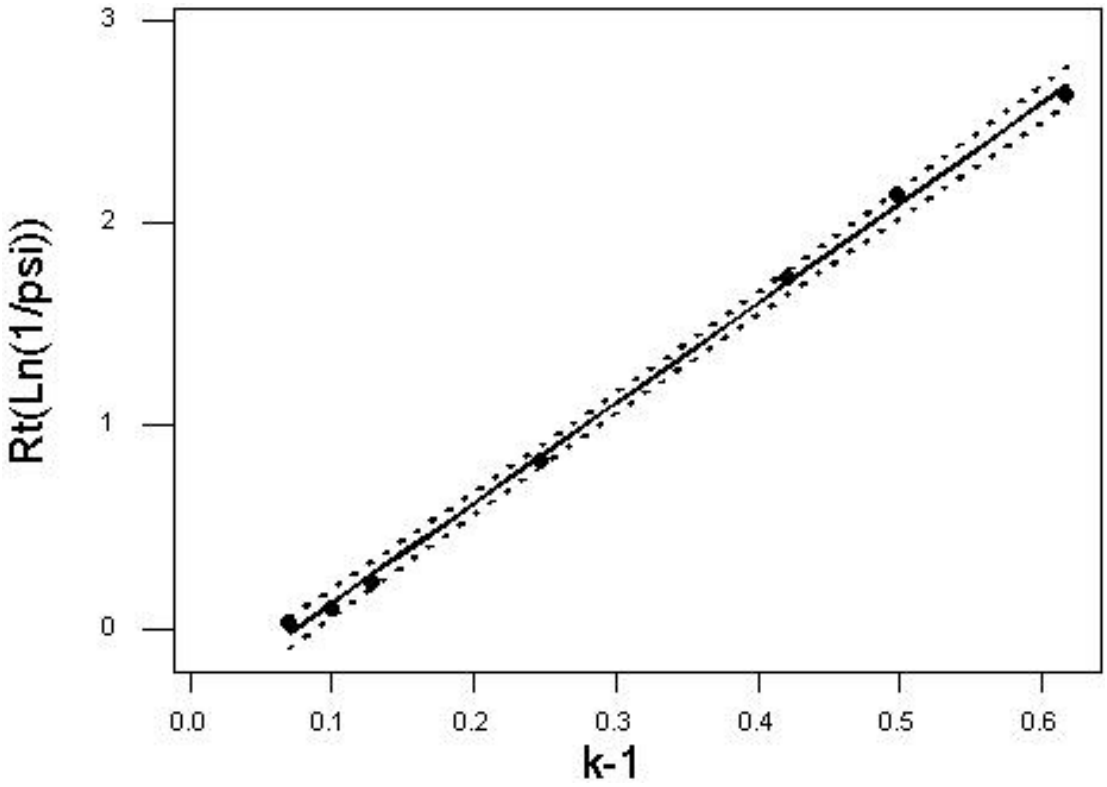

Figure 3.5 Simple regression analysis for average data for Windhoek best month - July

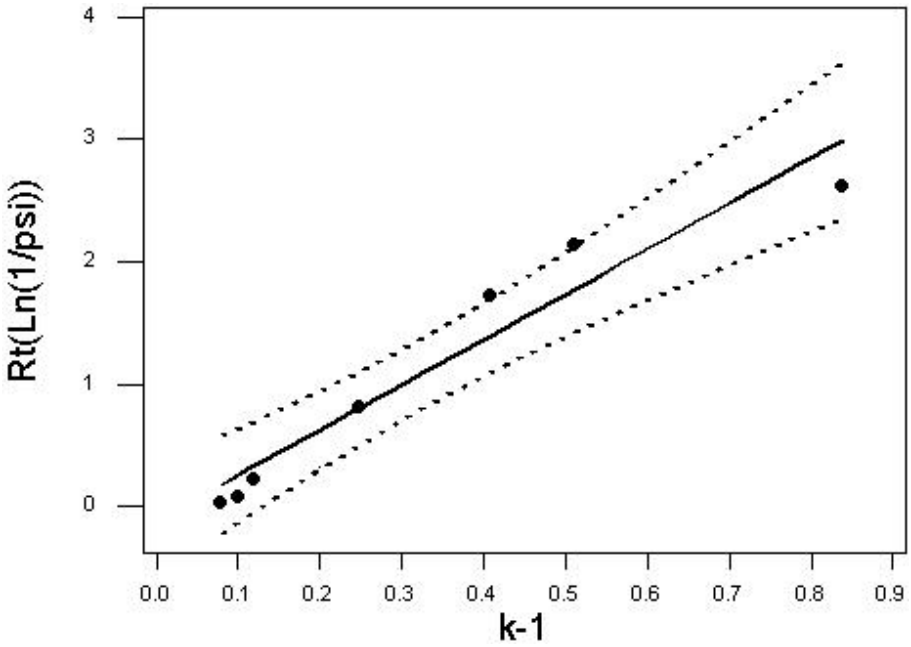

Figure 3.6 Simple regression analysis for average data for Windhoek worst month – September

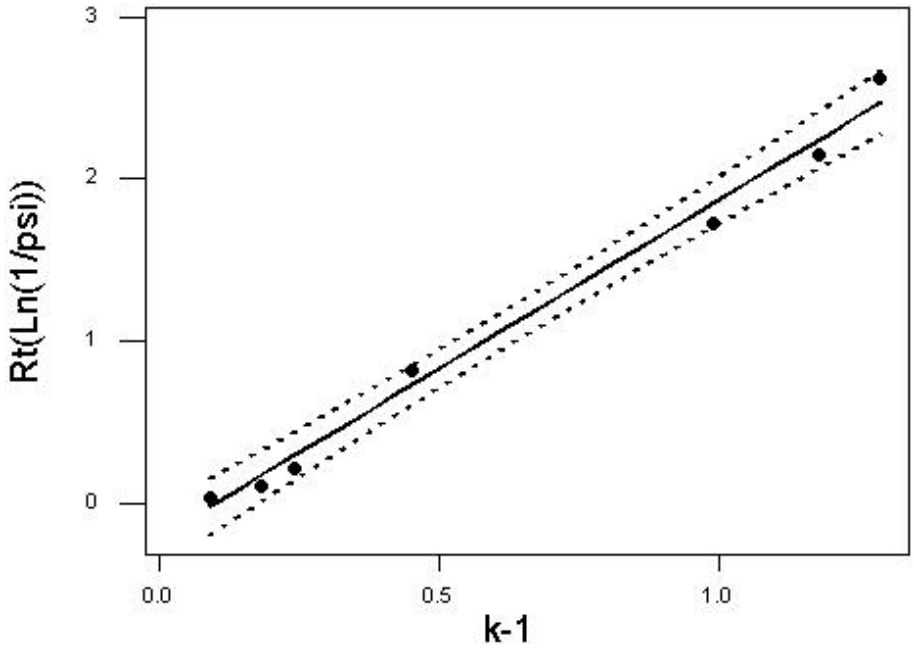

Figure 3.7 Simple regression analysis for average data for Durban best month – July

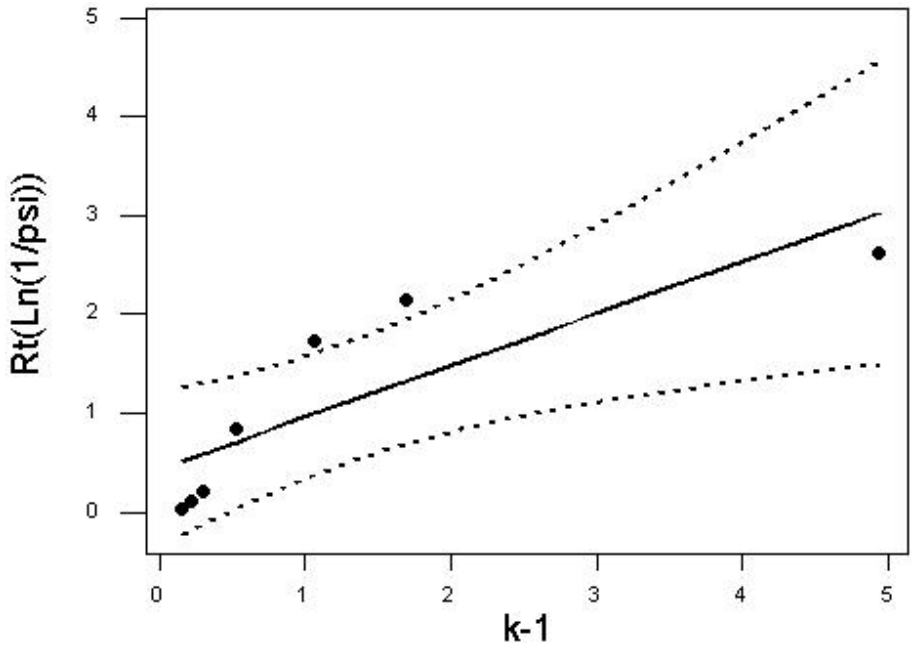

Figure 3.8 Simple regression analysis for average data for Durban worst month – January

The best overall match between the observed data and regression analyses, as evidenced by the Analysis of Variance (ANOVA) for the simple cases considered here and tabulated in Table 3.5 was obtained for Windhoek. Arguably the worst results obtained were for the regression analyses for Durban. In both cases the regression analyses were performed on the average data for the stations reported by *Nel* (1989), using expression (3.2).

Table 3.5. Comparison of regression analyses and ANOVA for the average data or k-factor distributions observed at different locations.

Location	Height	Constant Term				Predictor Term (P-val.=0.00)			ANOVA (P-val.=0.00)	
	(m)	Value	Stand. Dev.	T-statistic	P-value	Value	Stand. Dev.	T-statistic	F-statistic	R-Sq (Adj)
Durban	8	0.1348	0.1944	0.7	0.52	0.9551	0.1380	6.9	47.9	88.7%
Alexander Bay	21	-0.0718	0.0473	-1.5	0.19	1.3245	0.0409	32.4	1046.8	99.4%
Cape Town	44	-0.0356	0.1193	-0.3	0.78	1.3286	0.1061	12.5	156.7	96.3%
Port Elizabeth	60	0.0471	0.1507	0.3	0.77	1.0676	0.1130	9.5	89.3	93.6%
Upington	836	-0.0616	0.0857	-0.7	0.51	2.6911	0.1519	17.7	313.9	98.1%
Bloemfontein	1351	-0.2686	0.0468	-5.7	0.00	3.2794	0.0910	36.0	1298.2	99.5%
Pretoria	1524	-0.2945	0.1092	-2.7	0.04	3.3647	0.2160	15.6	242.6	97.6%
Windhoek	1712	-0.2769	0.0426	-6.5	0.00	3.6356	0.0915	39.7	1579.2	99.6%

With a 95% confidence interval, the constant term may be non-zero, for Windhoek (Namibia), Bloemfontein and Pretoria. The P-value for these cases is less than 0.05. For all other cases there is a possibility that the value of the constant could be zero. For the predictor term, the statistics suggest that the value is within the 95% confidence interval. In terms of the overall Analysis of Variance, the results are considered to be satisfactory, with a P-value of essentially zero for all stations.

3.5 Discussion of the combined model dry & wet – inclusion of the climatic term

Further analysis of Nel's data for all eight observation-sites, namely Alexander Bay, Cape Town, Port Elizabeth, Durban, Upington, Bloemfontein, and Pretoria, in South Africa, and Windhoek in Namibia, by means of the first hypothesis, which relates to the cumulative distribution for time percentage probability of occurrence, led to a new conclusion. This

was that the data, which does not follow the distribution formula for the first hypothesis contains additional information that could be retrieved and utilised. This situation was explored by, *Baker and Palmer* (2002b), and *Baker and Palmer* (2003).

It was noticed that there was a systematic distortion in the fit of the trend of the observed cumulative data points compared to that predicted by the regression analysis by means of (3.2), which is based on equation (3.1). This occurs predominantly during summer months and is most pronounced at the coastal stations and disappears almost entirely in winter particularly at the inland stations. The situation is illustrated in Figures 3.5 to 3.8.

It was proposed that the cumulative distribution could possibly be represented by the product of two independent cumulative distributions, one corresponding to a dry term and the second to a wet term, *Baker and Palmer* (2002b), *Baker and Palmer* (2003). In reformulating the cumulative distribution as represented by equation 3.1, it was proposed that the cumulative distribution, $\psi_{\text{eff}}(k)$, could be represented by,

$$\Psi_{eff}(k) = \Psi_{dry} \times \Psi_{wet}, \tag{3.3}$$

where

$$\Psi_{dry} = \exp\left(-\frac{(k'-1)^2}{2\sigma_{dry}^2}\right), \tag{3.4}$$

which is essentially the same expression as was used in (3.1), and

$$\Psi_{wet} = \exp\left(-\frac{(k'-k_{ref})^2}{2\sigma_{wet}^2}\right), \tag{3.5}$$

giving us

$$\Psi_{eff} = \exp\left(-\left(\frac{(k'-1)^2}{2\sigma_{dry}^2} + \frac{(k'-k_{ref})^2}{2\sigma_{wet}^2}\right)\right), \tag{3.6}$$

The variance is given by $\sigma^{2,}$ and the subscripts "dry" and "wet" identify the climatic conditions giving rise to the relevant terms. The reference value for the refractive index, k_{ref}, must be determined from the available data. It was specifically assumed in this formulation that the meteorological processes giving rise to these two terms were statistically independent, and that therefore equation (3.3) would be valid.

The "dry-wet" regression formula was similar to the simple regression used in *Palmer and Baker* (2002), but with the inclusion of the "wet" term. For the extended model, the regression formula thus became

$$\sqrt{\ln(1/\Psi)} = c' + m_1(k' - 1) + m_2 Abs(k' - k_{ref}), \qquad (3.7)$$

which can be rewritten as

$$\sqrt{\ln(1/\Psi)} = c + m_1 k' + m_2 Abs(k' - k_{ref}), \qquad (3.8)$$

In terms of the original assumption of the independence of the "dry" and wet" cumulative distribution terms in (3.3), and ignoring the constant term for the moment, the implication is that the cross product between the two exponent terms in (3.4) and (3.5) makes no significant contribution in the regression analysis. In effect, the sum of the squares equals the square of the sums in the combined exponent because we have assumed the correlation between the cross terms to be zero (See for example *Vardeman* (1999)). Thus replacing the "dry" and "wet" exponent terms in (3.6) by x^2 and y^2 respectively, we effectively have $(x^2 + y^2) \approx (x + y)^2$ for the regression analysis based on (3.6), thus giving rise to (3.8). This particular form maintained the desired sensitivity of the analyses for values of k close to unity, and resulted in ANOVA F-statistics for the regression analyses, which indicated high levels of acceptability. The regressor terms c and m_1 may be thought of as describing the properties of the "dry" component of the effective cumulative distribution, while m_2 may be identified with the "wet" or climatic component.

3.6 Analysis of the Annual Average Data

The monthly data for the cumulative distribution of the k-factor was averaged for each of the eight stations over the ten-year period 1976 – 1986 for which Nel's data were available. Multiple linear regression analyses were performed on the average data using values of the k-factor at 0.5 and 0.05 cumulative levels separately, as well as the average of these levels, as k_{ref}. It was also found that the best overall results were obtained with the average value of k at the 0.5 and 0.05 cumulative levels as $k_{ref.}$

Table 3.6 gives a preview of the results obtained in terms of equation (3.8) for the regression coefficients *m1*, *m2*, and the constant value of *c* for all the eight stations organised by their heights.

The relevant statistical information is included to provide some indication regarding the quality of these results. The T-statistics and P-values for *c*, *m1*, and *m2* can be used to decide the acceptability of the analysis. For the multiple regression analysis itself, the F-statistics and P-value for the Analysis of Variance (ANOVA) is given.

The T-statistics, F-statistics, and P-values give a measure of confidence that one could have in the analysis e.g. the T-statistics and P-values tabulated for all stations for *c* and *m1* suggest that the listed values are well within the 95% confidence limits. However, the T-statistics and P-values tabulated for *m2* suggest their acceptance for the coastal stations but not the same level of confidence for the inland stations. The F-statistics for the analysis of variance (ANOVA) for the overall analysis suggests that this approach is justified for the annual average situation.

Table 3.6 Summary of results for the regression analysis for the average annual data for all observation stations for the "wet-dry" model

LOCATION	Height (m)	Constant Term (c) (P-val. = 0.000)			1st Coefficient (m1) (P-val. = 0.000)		
		Value	Stand. Dev.	T-statistic	Value	Stand. Dev.	T-statistic
Durban	8	-0.9670	0.0796	-12.2	1.3944	0.0616	22.7
Alexander Bay	21	-1.2583	0.0385	-32.7	1.3477	0.0155	87.2
Cape Town	44	-1.2931	0.0821	-15.8	1.5361	0.0556	27.7
Port Elizabeth	60	-1.0290	0.0633	-16.3	1.3761	0.0466	29.5
Upington	836	-2.6727	0.1533	-17.4	2.7972	0.1093	25.6
Bloemfontein	1351	-3.4724	0.1347	-25.8	3.2841	0.0846	38.8
Pretoria	1524	-3.5703	0.2657	-13.4	3.4443	0.1862	18.5
Windhoek	1712	-3.8252	0.0857	-44.6	3.6594	0.0578	63.6

LOCATION	Height (m)	2nd Coefficient (m2)				ANOVA (P-val.=0.000)	
		Value	Stand. Dev.	T-statistic	P-Value	F-statistic	R-Sq (Adj)
Durban	8	-0.9075	0.1049	-8.7	0.001	414.9	99.3%
Alexander Bay	21	-0.2595	0.0448	-5.8	0.004	3947.5	99.9%
Cape Town	44	-0.6906	0.1259	-5.5	0.005	548.7	99.5%
Port Elizabeth	60	-0.7731	0.0913	-8.5	0.001	712.3	99.6%
Upington	836	-0.6996	0.2600	-2.7	0.056	352.9	96.6%
Bloemfontein	1351	-0.2936	0.2187	-1.3	0.251	754.0	99.6%
Pretoria	1524	-0.7628	0.4301	-1.8	0.151	174.9	98.3%
Windhoek	1712	-0.4725	0.1595	-3.0	0.041	2021.0	99.9%

From Table 3.6 the following conclusions may be drawn, regarding the coastal stations only:

1.) The constant term (*c*) values may be paired, because of their similarity, for Durban and Port Elizabeth, while those for Cape Town and Alexander Bay are also similar. The two-paired groups however differ between themselves.

2.) The first coefficient, *m1,* looks similar for Durban, Port Elizabeth and Alexander Bay but differs quite a bit from the value for Cape Town.

3.) The second coefficient, *m2*, displays a large scatter for all stations. However for the inland stations it appears that it may be height independent.

4.) There appears to be height dependence for the first two coefficients, namely *c* and *m1*, while there is no similar clear trend for m2, as noted in 3) above.

In *Baker and Palmer* (2002) height dependent regression analyses were performed on *c*, *m1*, and *m2*, using simple linear regression of the form

$$c = m_{ch} * h + c_{ch} \tag{3.9}$$

where m_{ch} and c_{ch} are the regression coefficients and constants appropriate for c, for the example, for the regression analysis in terms of the height h.

The results suggested an offset in the best-fit curves for the coastal stations for *c* and *m1* compared with the trend for inland stations. The results for *m2* suggest that there is no height dependency. A closer examination of the results in Table 3.6 suggests a restriction of these to the inland stations for the purpose of the simple regression analysis.
Figures 3.9, 3.10, and 3.11 illustrate best-fit curves obtained for c, *m1*, and *m3* for these stations. The 95% confidence intervals are included as dashed lines. The corresponding height dependent regression coefficients are tabulated in Table 3.7. The T-statistics and ANOVA results confirm that there appears to be a height dependence for c, m1, nut NOT for m2. The regressor terms from Table 3.7 suggests the possibility of using a similar expression to (3.8) to predict the values of c and m1 for the inland stations, and to compare them in terms of their values and the standard deviation. The results are shown in Table 3.8 for the predicted coefficients of c and m1. They correspond, without exception, to those given in Table 1 plus minus one standard deviation as derived in the regression analysis.

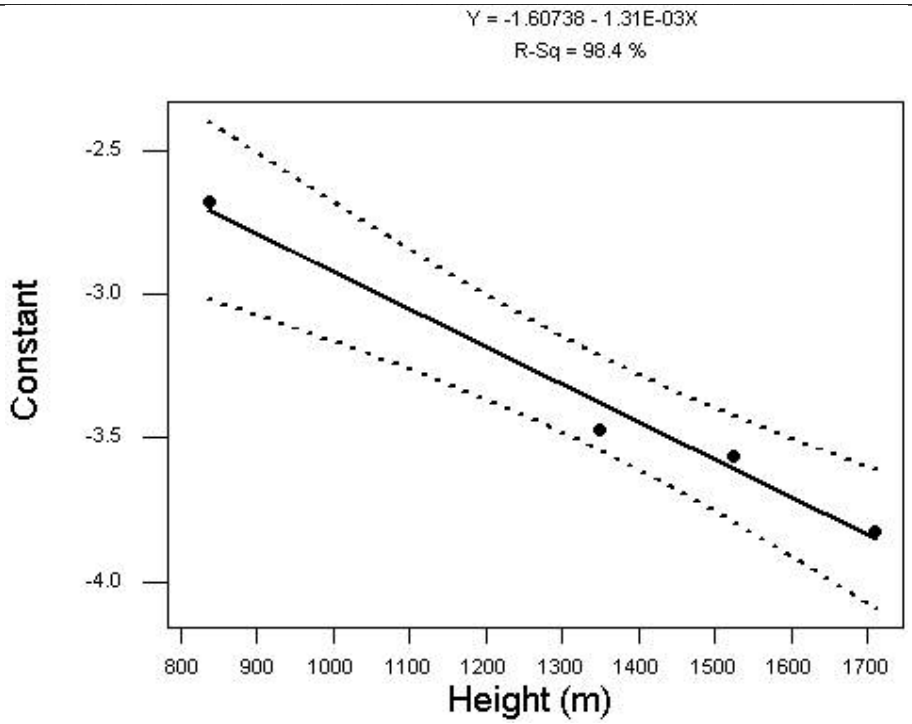

Figure 3.9 Variation of the constant term c in the regression as a function of height for the inland stations

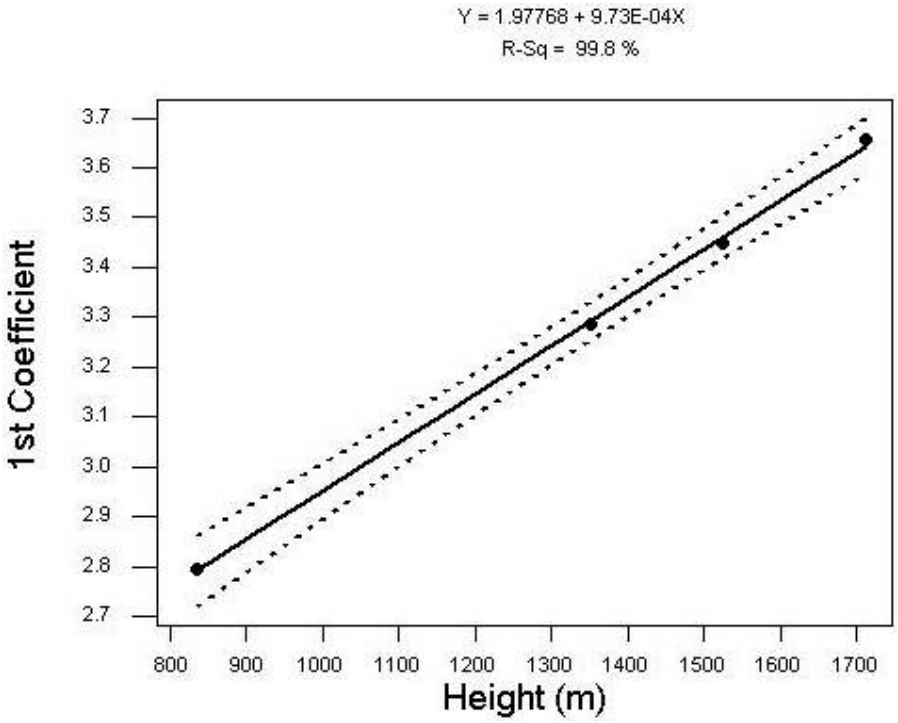

Figure 3.10 Variation of the first regression coefficient *m1* as a function of height for the inland stations

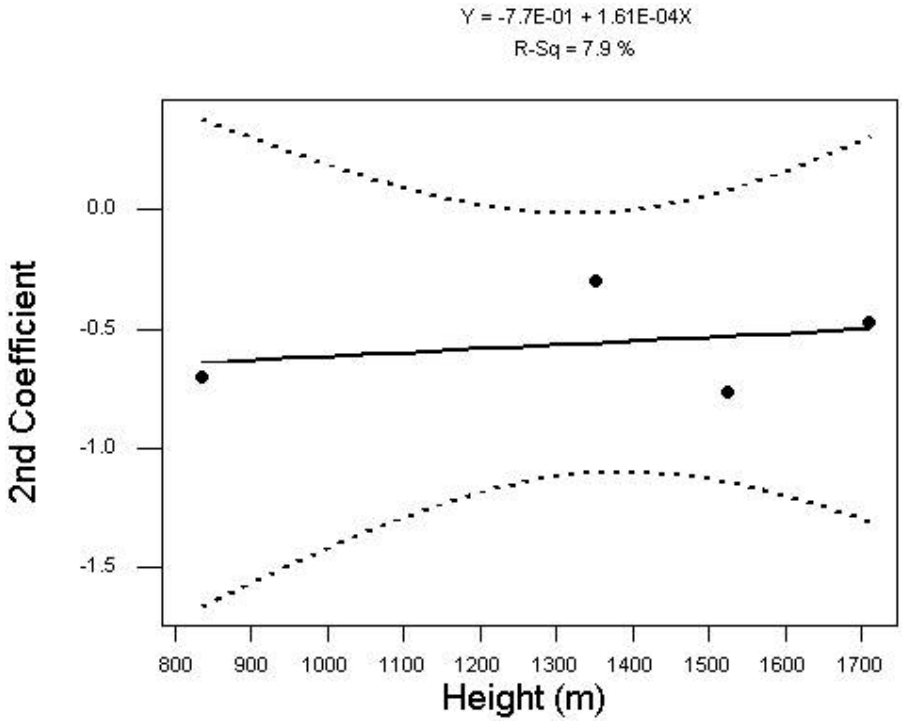

Figure 3.11 Variation of the second regression term *m2* as a function of height for the inland stations

Table 3.7 Summary of results for a height dependent regression analysis of the coefficients for inland stations listed in Table 3.6

Coefficients for "Dry-Wet" model	Constant Term				Height Coefficient				ANOVA		
	Value	Stand. Dev.	T-statistic	P-value	Value	Stand. Dev.	T-statistic	P-value	F-statistic	P-value	R-Sq (Adj)
Constant	-1.6074	0.1634	-9.8	0.010	-0.001311	0.0001	-11.2	0.008	125.2	0.008	97.6%
1st Coefficient (m1)	1.9777	0.0376	52.6	0.000	0.000973	0.0000	36.1	0.001	1300.0	0.001	99.8%
2nd Coefficient (m2)	-0.7749	0.5414	-1.4	0.289	0.000161	0.0004	0.4	0.719	0.2	0.719	0.0%

Table 3.8 Comparison of predicted values for the constant *c* and first coefficient *m1* obtained from the height dependent regression analysis with the expected ± 1 standard deviation ranges for these coefficients listed in Table 3.6

Station	Height (m)	Constant (c)			First Coefficient (m1)		
		Predicted	Expected Range		Predicted	Expected Range	
Upington	836	-2.7036	-2.5194	-2.8260	2.7908	2.9065	2.6879
Bloemfontein	1351	-3.3790	-3.3377	-3.6071	3.2916	3.3687	3.1995
Pretoria	1524	-3.6058	-3.3046	-3.8360	3.4599	3.6305	3.2581
Windhoek	1712	-3.8523	-3.7396	-3.9109	3.6427	3.7173	3.6016

3.7 Comparison of Predicted and Observed Cumulative Distributions for the Inland Stations

A comparison can now be made between the annual average cumulative distributions of the k-factor at the inland stations obtained by a means of regression analyses, and the observed cumulative distribution using height as a parameter. For the purpose of this discussion, this comparison is restricted to the inland stations only.

It was found that $k_{ref,}$ the average value of the k-factor at 0.5 and 0.05 cumulative levels to be used in equation (3.6), has a surprisingly small range. The average value for the four inland stations of their 12-month annual average for this parameter is 1.4395, with a standard deviation of only 0.0202. Further evaluation of the data, by comparison between the predicted and observed cumulative distributions, suggested that the k-factor maintained an acceptable agreement using the average value for the four inland stations. The average value of *m2* for the four inland stations is 0.5571, with a standard deviation of 0.2154. At first glance, this would appear to be a gross simplification that would result in a poor comparison between the predicted and observed annual average k-factor cumulative distributions. Nevertheless, the results shown in Table 3.9, with the exception of only three cases (highlighted), indicate all the predicted values are within only one standard deviation of the observed averages. These results are somewhat surprising but most gratifying. This essentially confirms the probable validity of the dual cumulative distribution model.

It is now possible to predict the expected annual average values of the k-factor expected to be exceeded, for example, for 0.001 of the time for the inland areas of South Africa by using DTM model, which is structured for 15 minutes of longitude and latitude. This represents roughly 25×25 km pixels for the gridlines on the contour map. The resultant map for the annual average for South Africa is shown in Figure 3.12. It is believed that this is largely applicable to the summer rainfall areas. Some of the predicted contours fall below of the altitude of the lowest observation station, Upington, at a height of 836 m. There is therefore some uncertainty that the contours obtained between, say, 800 m altitude and sea level extend adequately down to the coastal plains.

Table 3.9 Comparison of predicted and observed cumulative distributions for inland stations including the standard deviation for the annual averages, and differences between the predicted and observed values

Cumulative Probability		0.001	0.01	0.05	0.5	0.95	0.99	0.999
Upington	Predicted	2.03	1.81	1.63	1.30	1.11	1.08	1.06
836 m	Observed	2.06	1.80	1.58	1.31	1.15	1.09	1.03
	Difference	-0.03	0.01	0.04	-0.01	-0.03	-0.01	0.03
	Stand. Dev.	0.40	0.18	0.07	0.03	0.02	0.03	0.05
Bloemfontein	Predicted	1.90	1.73	1.58	1.30	1.15	1.11	1.09
1351 m	Observed	1.91	1.72	1.58	1.34	1.17	1.12	1.08
	Difference	-0.01	0.01	0.00	-0.03	-0.03	0.00	0.01
	Stand. Dev.	0.25	0.17	0.11	0.04	0.02	0.02	0.02
Pretoria	Predicted	1.87	1.71	1.56	1.30	1.15	1.12	1.11
1524 m	Observed	1.93	1.67	1.55	1.33	1.19	1.15	1.08
	Difference	-0.06	0.03	0.01	-0.03	-0.03	-0.02	0.02
	Stand. Dev.	0.25	0.12	0.09	0.05	0.03	0.03	0.06
Windhoek	Predicted	1.84	1.68	1.55	1.31	1.16	1.13	1.12
1712 m	Observed	1.82	1.66	1.53	1.29	1.15	1.12	1.08
	Difference	0.02	0.02	0.02	0.02	0.01	0.01	0.04
	Stand. Dev.	0.17	0.16	0.12	0.05	0.03	0.02	0.03

3.8 Discussion of hypotheses and Conclusion

A dual cumulative probability distribution has been postulated in order to describe the average k-factor distribution for eight observation stations in South Africa and Namibia, four of these being inland and four coastal. Despite the fact that the general model does not yet appear to satisfy the requirements for the coastal stations in terms of regression analyses it would seem that the model might have applicability in the inland summer rainfall regions of South Africa.

The regressor terms *c* and *m1*, which may be associated with the "dry" component of cumulative distribution showed a strong height dependency. Despite the fact that the "wet" or climatic regressor term, *m2*, showed no definite height dependency, and varied for four

stations, it was nevertheless possible to obtain a good comparison between the observed and predicted cumulative distributions for the k-factor by using an average value.

In general, the agreement was to within one standard deviation for the average annual value, at each of the tabulated values of the cumulative distribution. Discrepancies have been highlighted in Table 3.9.

In light of these promising results it is desirable to revisit the data at the South Africa Weather Service to see if would be possible to refine the existing database further, including data obtained since Nel and his co-workers undertook the original study.

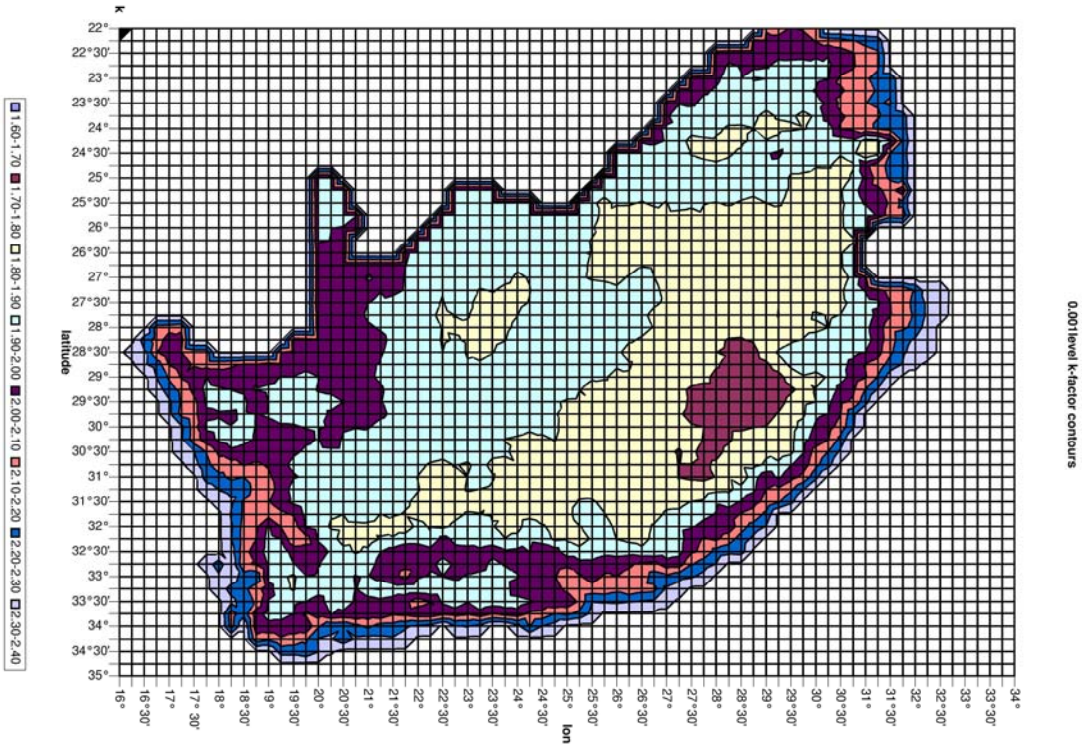

Figure 3.12 Predicted contours of the annual average k-factor expected to be exceeded 0.001 of the time for inland summer rainfall areas in South Africa (The Microsoft Excel © format required extensive video processing to re-orient)

What appears to be certain is that the models outlined above, and some of the other models to be discussed in Chapter 5 have the potential of significantly improving terrestrial radio telecommunications planning, than has been possible with any of the methods and/or models used in South Africa to date.

3.9 Discussion of the First Hypothesis and its Consequences

Schiavone (1981) used a normal distribution for the probability density functions of the refractivity gradients for mixed and stratified air regimes in the contiguous United States. More recently results obtained in Botswana over a period of about 3 years for the refractivity gradient and the k-factor suggest that a normal distribution for the probability density function is valid for central values around the median for observations made at Maun (*Afullo et al,* (2001).

The probability density function for the k-factor could thus be represented as:

$$f(k) = \frac{1}{\sqrt{2\pi}\sigma} \exp\left(- \frac{(k-\mu)^2}{2 * \sigma^2} \right), \tag{3.10}$$

for all k for $\sigma > 0$. The mean value of k is given by μ, and σ^2 is the variance of k.

The cumulative distribution function for k is given by:

$$\psi(k) = P(k \le k') = \int_{-\infty}^{k} f(k')dk', \tag{3.11}$$

where P is the probability that the random variable k will be less than k'.

Computationally equation (3.11) is not suitable for implementation in general calculations. It was therefore proposed *Palmer and Baker* (2002) that the cumulative distribution function for k should be represented by:

$$\psi(k) = P(k \geq k') = \exp\left(-\frac{(k-1)^2}{2*\sigma^2}\right), \qquad (3.12)$$

where Ψ(k) is the probability that k will be greater than some value k', and is valid for dΨ(k)/dk>0. This is a condition defined for our cut off point. For the present data at hand we are only interested in values of k>1 in terms of our restrictive condition. The change in the use of the inequality is essential.

The value of the variance may be determined by the value, which provides the best match of Ψ(k) to the observed data. Differentiation of (3.12) would lead to a different form of the probability density function than that given in (3.10). The expression is also seen to be symmetrical around k=1. The cumulative distribution for k represented by (3.12) will be shown to provide acceptable results when comparing observed and predicted data.

Equation (3.12) relates to the cumulative distribution. The average value of k should not be interpreted as being equal to unity. Instead, as the equation stands, setting k=1 suggests that k would exceed unity 100 % of the time.

Substituting in (3.12) for k from (2.1), and setting the cumulative distribution function Ψ to 0.5 one obtains:

$$\frac{1}{2} = \exp\left(-\left(\frac{1}{1+\frac{dN}{dh}/50\pi} - 1\right)^2 / 2\sigma^2\right), \qquad (3.13)$$

$$\psi(k) = 2^{-((1-k)*(1+50\pi/\frac{dN}{dh}))^2}, \qquad (3.14)$$

Setting Ψ(k) = ½, and solving for k, one obtains two solutions for k, namely, (3.15) the familiar expression and (3.16) the new one.

The first formula for the k-factor is the familiar one, namely:

$$k_1 = \frac{1}{1 + \left(\frac{dN}{dh}\right)/50\pi}, \tag{3.15}$$

the second, new formula, for the k-factor is:

$$k_2 = 1 + \frac{\left(\frac{dN}{dh}\right)/50\pi}{1 + \left(\frac{dN}{dh}\right)/50\pi}, \tag{3.16}$$

Setting (dN/dh)/50π = -¼, the typical normalised gradient expected at sea level, one obtains two separate values for k for the effective earth radius k-factor, namely, 4/3 and 2/3 for k_1 and k_2 respectively for the same amount of time for percentage events.

A consequence of the formulation of the cumulative distribution of k following on the first hypothesis is that a second expression for the k-factor has been found. As already reported in the published paper by *Palmer and Baker* (2002) the second set of branches implied by the new formula may be added. This may be interpreted graphically, and visualised as described below.

Existing known plots of the k-factor, such as represented by equation (3.15) above, are fairly well described in the literature, *Hall* (1979), *Mojoli, et. al.* (1985*), Imbeau, et. al.* (1993) and is illustrated in Figure 3.13. Equations (3.15) and (3.16) are illustrated in Figure 3.14 by way of comparison.

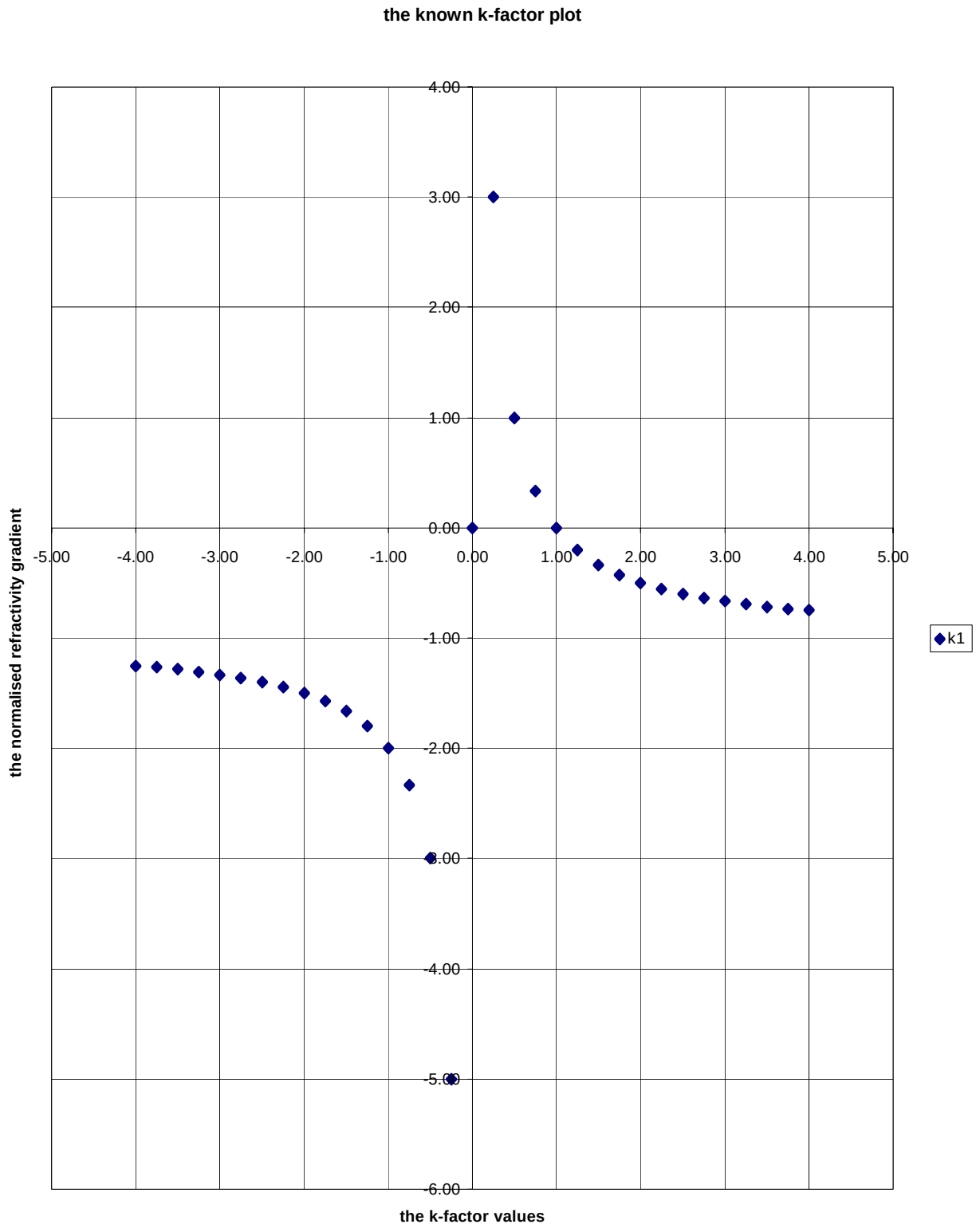

Figure 3.13 The known k-factor plot against the normalised refractivity gradient from the known expression.

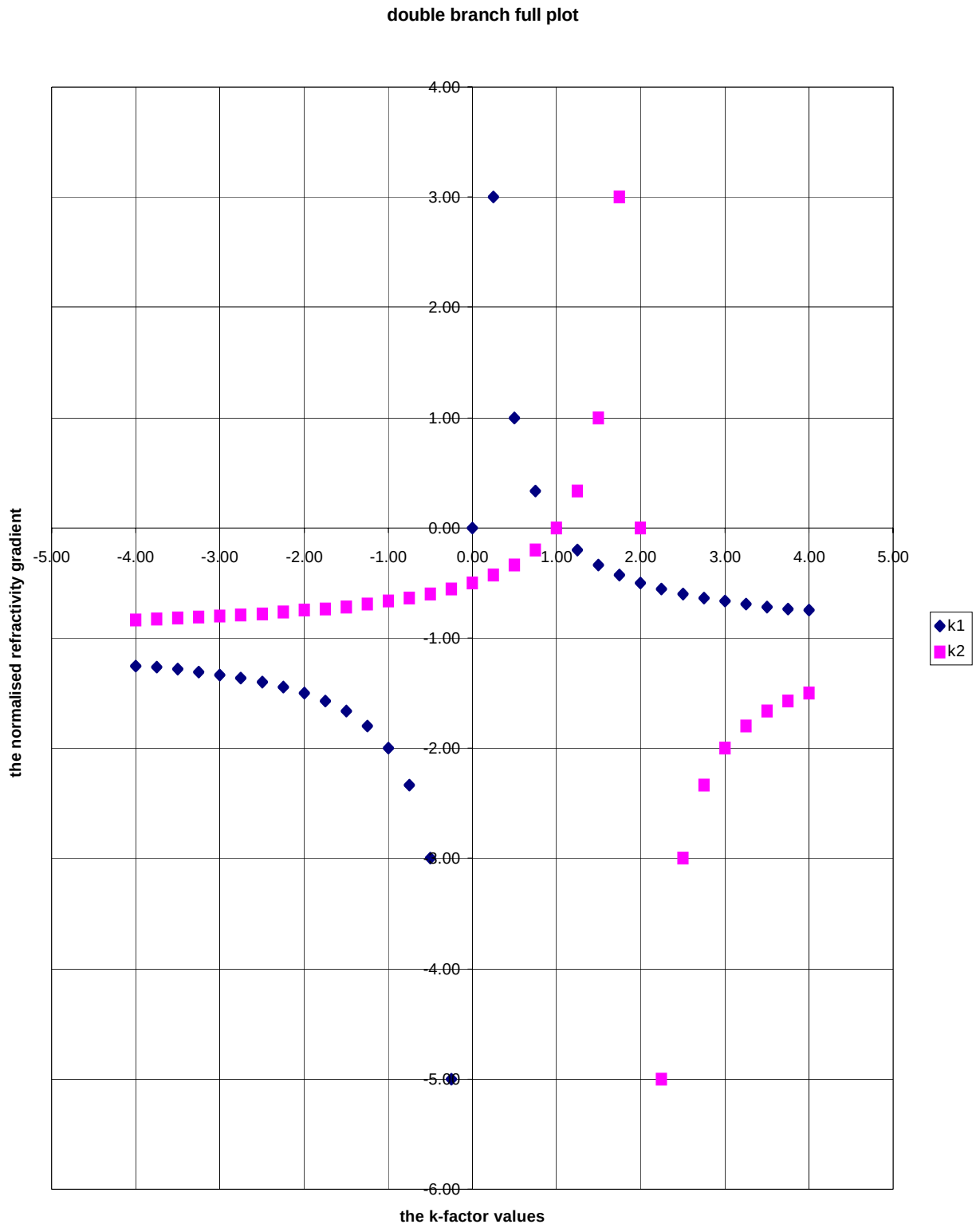

Figure 3.14 Old and new k-factor expressions together showing a more symmetrical appearance, use of both formulae simultaneously is required to produce the plot.

Of particular importance is the classification of the propagation modes, in terms of the familiar plot. The accepted classification of the propagation modes are given below for completeness:

$\{ 0 < k < +4/3 \} \times \{ -1 < (dN/dh)/50\pi < +\infty \}$ range of sub-refraction;

$\{ 4/3 < k < +\infty \} \times \{ -1 < (dN/dh)/50\pi < -¼ \}$ range of super-refraction;

$\{ -\infty < k < 0 \} \times \{ -\infty < (dN/dh)/50\pi < -1 \}$ range of ducting;

Where × denotes the conditions for the ranges for k and dN/dh, which must be simultaneously satisfied for the propagation mode described *Hall* (1979).

3.10 New data from the SA Weather Service

A new set of data was acquired from the SA Weather Service at the beginning of 2003. This set contained data for a period of ten years between 1976 and 1986 for twelve months in each year, and was confined to the same sites as were used by *Nel* (1989) in his M-thesis, namely Cape Town, Port Elizabeth, Durban, Alexander Bay, Upington, Bloemfontein, Pretoria, Windhoek (Namibia). The data files for each of these places also contained the following entries: the air pressure, the water vapour content given as a percentage in the relative humidity, and temperature.

These data were gathered three times a day, namely, at eight o'clock in the morning, at two o'clock on the afternoon, and at eight o'clock at night. In addition to that, the average daily maximum and minimum temperatures were supplied for each month. The data were made available in suitable format for processing on a spreadsheet. This made it convenient to obtain suitable results for comparison between values of the k-factor and/or the refractivity gradient derived from radiosonde observations, the proposed model based on regression analyses, or groundbased observation.

3.11 New Data Processing & Results

In order to convert the observed ground based climatological data to values of the refractivity of the atmosphere, the refractivity gradient, and finally the k-factor values, the data have to be processed further.

The reader is reminded that the refractive index in N-units is given by equation (3.17) as (see for example *Hall* (1979)):

$$N = 77.6\frac{P}{T} + 3.73\times 10^5\,\frac{e}{T^2} \qquad (3.17)$$

Where P = atmospheric pressure,
e=water vapour pressure, and
T = temperature (K).

The relative humidity value H (%) from the SA Weather Service data must be converted to a water vapour pressure **e** for use in the formulas of the refractivity value and its gradient, from which the k-factor could in turn be calculated. The formulas for converting the relative humidity to the water vapour pressure in the atmosphere are conveniently given by equations (7.2) and (7.3) in *Hall* (1979), and are repeated here as equations (3.18) and (3.18). The reader's attention is drawn to the fact that in equation (2.3) on page 15 of this reference, the negative sign should be changed to plus sign. A search of various web sites on the Internet has confirmed this correction. The water vapour pressure is thus given as (7.3) with (7.2), which is an additional formula given separately here for converting the relative humidity, expressed in (%), to **e** according to the maximum possible saturated vapour pressure, $\mathbf{e_s}$, at an air temperature **t**.

$$e_s = 6.11\times \exp\left(\frac{19.7\times t}{t+273.15}\right), \qquad (3.18)$$

$$e = H \times e_s \tag{3.19}$$

where

e_s = saturated water vapour pressure at the air temperature t (C),

e = water vapour pressure (hPa), and

t = ambient temperature measured in C deg (the SA Weather Service readings are recorded in the Celsius degrees)

H = Relative humidity of the atmosphere in %

The refractivity gradient is obtained easily by simple differentiation of this empirical formula over the altitude and is quoted in *Bem* (1973) as

$$\frac{dN}{dh} = 77.6 \times \left(\left(\frac{1}{T} \right) \times \left(\frac{dP}{dh} \right) - \left(\left(\frac{P}{T^2} \right) + 9620 \times e \times \left(T^3 \right) \right) \times \left(\frac{dT}{dh} \right) + \left(\frac{4810}{T^2} \right) - \left(\frac{de}{dh} \right) \right), \tag{3.20}$$

where

$$dP/dh = - g*P/(R*T), \tag{3.21}$$

$$de/dh = -g*e/(R*T), \tag{3.22}$$

T = absolute temperature = t + 273.15 (K deg/km),

R = 287, and is the ratio of the universal gas constant r equal 8310 (joule/kmol*K) and the mole mass of the air M = 29 (kg/kmol),

g = 9.81 (m/sec^2) earth gravitational acceleration,

P = air pressure (hPa),

One can rewrite 3.20 as,

$$\frac{dN}{dh} = -77.6 \times \left(P + 4810 \times \frac{e}{T} \right) \times \left(\frac{1}{T^2} \right) \times \left(\frac{g}{R} \right) - 77.6 \times \left(P + 9620 \times \left(\frac{1}{T^3} \right) \right) \times \left(\frac{dT}{dh} \right), \tag{3.23}$$

dP/dh = air pressure gradient, (hPa/km)

de/dh = water vapour pressure gradient (hPa/km),

dT/dh = temperature gradient (K deg/km),

N = refractivity of the troposphere (N-units), and

dN/dh = refractivity gradient of the troposphere (N-units/km).

Equation (3.23) above represents the refractivity gradient. The equation is organised such that the first term represents a gravitational part of the formula, which remains altitude independent. However, the second term of the formula it is altitude dependent, and contains the temperature gradient as a strong altitude function.

The above expressions were used to calculate the averages of the atmospheric refractivity, the refractivity gradient, and the k-factor for various months for the eight-radiosonde observations sites noted previously.

The temperature gradient is probably the most important function in equation (3.23), which represent the refractivity gradient. As such it represents the strongest influence in the model of distribution of the refractivity gradient with altitude.

The scale height for air is given in many textbooks (for example *Davies* (1965)), and is given by H = RT/Mg (km), all parameters in the expression are defined above.

The scale height for wet air must be determined in terms of the relative components of dry air and water vapour. A typical value for the scale height of water vapour is given as 2.5 km (*Hall and Barclay,* 1989).

The problem of what value to use for the temperature gradient remains. Theoretically this is about –10 degrees per km. However, experimentally this is found to be about 6.5 degrees per km at ground level (*Preston-Whyte and Tyson,* 1993).

It is clear that the scale heights discussed above, and the temperature gradient should be examined more carefully in future work, particularly for ground level observations, and in terms of the influence of moisture content.

3.12 Comparison between different models

The new values of the k-factor and the refractivity gradient, both of which may be obtained independently from the SA Weather Service's, ground observation data by the method outlined above, may be compared with the previous results from *Nel* (1989), and predictions based on the empirical model formulated in this work and derived using regression analyses of Nel's data. The comparison applies for the average or 50% cumulative values from Nel's data.

The results are in general comparable as can be seen in Table 3.10, except for the gradient results for Alexander Bay. For the other 7 stations, the greatest difference is some 5.9 % at Port Elizabeth during April. This result is indeed most satisfactory from the point of view of using ground based climatic data in support of communications planning. Month number presents data with January corresponding to month 1, February to month 2, etc.

The case of Alexander Bay is worthy of further investigation. It is believed that the temperature and/or humidity gradient here may be strongly influenced by the cold Benguela current sweeping up the West Coast of Southern Africa. Reference has been made to anomalous propagation conditions, in this part of the country by *Lourens and Jury* (1988). These conditions could be ascribed to long lasting ducting conditions induced by this ocean effect. Similar anomalous propagation conditions have been noted on the west coasts of continents by *Morita* (1980).

Table 3.10 Comparison between Nel's average (50% cumulative probability) data and the Weather Service (WS) data obtained using ground based meteorological data for the eight radiosonde-stations.

CAPE TOWN		Height (m)	44									
Month	1	2	3	4	5	6	7	8	9	10	11	12
N from WS	339.6	341.2	339.7	338.6	333.5	329.7	329.1	328.9	329.7	331.0	334.5	337.8
N from Nel	337.5	340.6	338.4	338.8	333.6	330.2	329.4	328.8	328.9	329.2	333.2	337.6
Difference	2.1	0.6	1.3	-0.2	-0.1	-0.5	-0.3	0.1	0.8	1.8	1.3	0.2
Month	1	2	3	4	5	6	7	8	9	10	11	12
dN/dh Calc.	-48.5	-48.8	-48.8	-48.9	-48.4	-48.0	-48.0	-47.9	-47.9	-47.8	-48.0	-48.4
dN/dh from Nel	-51.6	-53.7	-50.9	-51.3	-49.2	-48.1	-48.6	-49.2	-48.3	-49.4	-50.4	-50.1
Difference	3.1	4.9	2.1	2.4	0.8	0.1	0.6	1.3	0.5	1.7	2.4	1.8
Month	1	2	3	4	5	6	7	8	9	10	11	12
k from WS	1.45	1.45	1.45	1.45	1.45	1.44	1.44	1.44	1.44	1.44	1.44	1.45
k from Nel	1.49	1.52	1.48	1.48	1.46	1.44	1.45	1.46	1.44	1.46	1.47	1.47
Diff. WB / Nel %	2.8	4.5	1.9	2.2	0.7	0.0	0.5	1.2	0.4	1.5	2.2	1.6
WINDHOEK		Height (m)	1712									
Month	1	2	3	4	5	6	7	8	9	10	11	12
N from WS	265.6	275.5	272.3	259.1	248.2	245.8	242.9	238.5	237.3	242.0	246.0	252.6
N from Nel	277.1	276.9	274.9	265.5	254.6	251.1	249.4	246.0	243.7	249.2	246.3	256.0
Difference	-11.4	-1.4	-2.7	-6.4	-6.5	-5.2	-6.5	-7.6	-6.4	-7.2	-0.3	-3.5
Month	1	2	3	4	5	6	7	8	9	10	11	12
dN/dh Calc.	-37.4	-39.1	-38.7	-36.8	-35.4	-35.2	-34.8	-33.8	-33.2	-33.8	-34.2	-35.2
dN/dH from Nel	-42.8	-40.4	-40.1	-38.0	-33.7	-32.4	-31.2	-30.3	-31.3	-33.4	-30.7	-39.5
Difference	5.4	1.3	1.4	1.2	-1.7	-2.9	-3.6	-3.5	-1.9	-0.4	-3.5	4.3
Month	1	2	3	4	5	6	7	8	9	10	11	12
k from WS	1.31	1.33	1.33	1.31	1.29	1.29	1.28	1.27	1.27	1.27	1.28	1.29
k from Nel	1.31	1.33	1.33	1.31	1.29	1.29	1.28	1.27	1.27	1.27	1.28	1.29
Diff. WS / Nel %	-0.05	-0.04	-0.04	-0.04	-0.03	-0.03	-0.03	-0.03	-0.03	-0.03	-0.03	-0.04

DURBAN		Height (m)	8									
Month	1	2	3	4	5	6	7	8	9	10	11	12
N from WS	366.1	368.1	364.6	356.6	342.8	333.7	334.3	340.7	345.0	348.8	355.8	360.6
N from Nel	366.2	367.8	364.4	356.2	339.9	330.6	332.5	339.5	345.1	349.3	354.5	360.6
Difference	0.1	-0.3	-0.3	-0.3	-2.9	-3.1	-1.8	-1.2	0.1	0.5	-1.2	0.0
Month	1	2	3	4	5	6	7	8	9	10	11	12
dN/dh Calc.	-52.2	-52.4	-52.0	-51.0	-49.2	-48.0	-48.1	-49.0	-49.5	-50.0	-50.9	-51.4
dN/dh from Nel	-54.3	-54.0	-53.7	-56.7	-52.6	-49.5	-48.8	-51.0	-50.1	-50.3	-52.6	-54.5
Difference	2.2	1.5	1.7	5.7	3.5	1.5	0.6	1.9	0.6	0.3	1.7	3.0
Month	1	2	3	4	5	6	7	8	9	10	11	12
k from WS	1.50	1.50	1.50	1.48	1.46	1.44	1.44	1.45	1.46	1.47	1.48	1.49
k from Nel	1.53	1.52	1.52	1.56	1.50	1.46	1.45	1.48	1.47	1.47	1.50	1.53
Diff. WS / Nel %	2.0	1.4	1.6	5.4	3.2	1.3	0.6	1.8	0.5	0.2	1.6	2.8
PORT ELIZABETH		Height (m)	60									
Month	1	2	3	4	5	6	7	8	9	10	11	12
N from WS	349.3	353.0	349.5	343.9	334.0	327.9	328.2	330.3	333.9	337.7	341.7	346.1
N from Nel	348.0	352.2	348.2	342.8	333.1	326.8	327.0	329.3	331.6	335.9	340.5	344.9
Difference	1.2	0.8	1.4	1.2	0.9	1.1	1.2	1.0	2.3	1.8	1.2	1.2
Month	1	2	3	4	5	6	7	8	9	10	11	12
dN/dh Calc.	-49.9	-50.6	-50.2	-49.5	-48.2	-47.5	-47.6	-47.9	-48.3	-48.7	-49.1	-49.6
dN/dh from Nel	-54.1	-56.1	-54.9	-55.9	-52.2	-51.2	-51.5	-48.2	-49.1	-50.8	-52.6	-54.3
Difference	4.1	5.6	4.7	6.4	4.0	3.7	3.9	0.3	0.8	2.0	3.5	4.7
Month	1	2	3	4	5	6	7	8	9	10	11	12
k from WS	1.47	1.48	1.47	1.46	1.44	1.43	1.44	1.44	1.44	1.45	1.46	1.46
k from Nel	1.52	1.56	1.54	1.55	1.50	1.48	1.49	1.44	1.45	1.48	1.50	1.53
Diff. WS / Nel %	3.8	5.2	4.4	5.9	3.6	3.4	3.5	0.2	0.7	1.8	3.2	4.4

ALEXANDER BAY		Height (m)	21									
Month	1	2	3	4	5	6	7	8	9	10	11	12
N from WS	341.6	342.8	339.2	336.7	330.3	326.8	325.5	326.5	329.3	331.7	335.1	339.4
N from Nel	342.0	343.5	339.3	337.8	332.6	329.2	328.7	329.0	330.0	331.7	335.3	339.8
Difference	-0.3	-0.7	-0.1	-1.1	-2.3	-2.4	-3.2	-2.5	-0.8	0.0	-0.1	-0.4
Month	1	2	3	4	5	6	7	8	9	10	11	12
dN/dh Calc.	-49.0	-49.3	-48.9	-48.6	-47.7	-47.2	-47.1	-47.3	-47.6	-47.9	-48.3	-48.8
dN/dh from Nel	-64.0	-62.9	-62.1	-58.6	-57.4	-53.1	-51.6	-51.6	-53.4	-58.7	-65.5	-61.8
Difference	15.0	13.6	13.2	10.0	9.7	5.9	4.5	4.3	5.7	10.7	17.3	13.0
Month	1	2	3	4	5	6	7	8	9	10	11	12
k from WS	1.45	1.46	1.45	1.45	1.44	1.43	1.43	1.43	1.44	1.44	1.44	1.45
k from Nel	1.69	1.67	1.65	1.59	1.58	1.51	1.49	1.49	1.51	1.60	1.72	1.65
Diff. WS / Nel %	13.8	12.6	12.2	9.2	8.8	5.3	4.1	3.9	5.2	9.8	15.8	12.0
UPINGTON		Height (m)	836									
Month	1	2	3	4	5	6	7	8	9	10	11	12
N from WS	284.6	292.5	294.0	289.8	283.4	281.8	279.9	276.7	276.5	277.3	277.0	278.9
N from Nel	277.2	284.9	287.5	285.7	282.2	281.8	281.4	275.5	277.0	276.8	275.3	277.0
Difference	7.4	7.6	6.5	4.1	1.3	0.0	-1.5	1.2	-0.5	0.5	1.7	1.8
Month	1	2	3	4	5	6	7	8	9	10	11	12
dN/dh Calc.	-39.3	-40.7	-41.2	-41.0	-40.6	-40.7	-40.4	-39.7	-39.2	-38.8	-38.5	-38.5
dN/dh from Nel	-37.0	-40.4	-38.7	-39.0	-38.3	-38.9	-37.5	-37.8	-37.0	-33.5	-33.4	-34.7
Difference	-2.3	-0.2	-2.5	-2.0	-2.3	-1.8	-2.9	-1.9	-2.1	-5.3	-5.1	-3.8
Month	1	2	3	4	5	6	7	8	9	10	11	12
k from WS	1.34	1.35	1.36	1.35	1.35	1.35	1.35	1.34	1.33	1.33	1.32	1.33
k from Nel	1.31	1.35	1.33	1.33	1.32	1.33	1.31	1.32	1.31	1.27	1.27	1.28
Diff. WS / Nel %	-2.1	-0.3	-2.3	-1.8	-2.0	-1.6	-2.5	-1.7	-1.9	-4.5	-4.3	-3.3

BLOEMFON-TEIN		Height (m)	1351									
Month	1	2	3	4	5	6	7	8	9	10	11	12
N from WS	284.8	290.4	287.2	277.9	268.9	266.6	264.5	263.3	266.4	272.7	274.8	278.1
N from Nel	288.3	295.9	291.8	280.1	272.0	270.3	268.6	266.6	269.5	275.1	277.6	284.0
Difference	-3.5	-5.5	-4.5	-2.2	-3.1	-3.7	-4.1	-3.4	-3.1	-2.3	-2.8	-5.8
Month	1	2	3	4	5	6	7	8	9	10	11	12
dN/dh Calc.	-40.3	-41.3	-41.1	-40.1	-39.2	-39.2	-38.8	-38.3	-38.2	-38.9	-39.0	-39.3
dN/dh from Nel	-42.7	-44.2	-44.5	-40.5	-37.0	-37.1	-37.1	-36.1	-36.5	-38.6	-38.9	-41.5
Difference	2.4	2.9	3.4	0.5	-2.2	-2.1	-1.7	-2.2	-1.8	-0.3	-0.1	2.3
Month	1	2	3	4	5	6	7	8	9	10	11	12
k from WS	1.35	1.36	1.36	1.34	1.33	1.33	1.33	1.32	1.32	1.33	1.33	1.33
k from Nel	1.37	1.39	1.40	1.35	1.31	1.31	1.31	1.30	1.30	1.33	1.33	1.36
Diff. WS / Nel %	2.0	2.4	2.8	0.3	-1.9	-1.8	-1.5	-1.9	-1.5	-0.3	-0.1	1.9
PRETORIA		Height (m)	1524									
Month	1	2	3	4	5	6	7	8	9	10	11	12
N from WS	300.0	298.5	296.2	284.9	274.5	270.2	270.2	269.7	274.3	284.0	291.1	295.2
N from Nel	296.4	296.2	291.6	278.1	267.0	263.8	262.9	262.7	268.0	279.5	288.0	292.7
Difference	3.6	2.2	4.6	6.8	7.5	6.4	7.3	7.0	6.3	4.5	3.1	2.5
Month	1	2	3	4	5	6	7	8	9	10	11	12
dN/dh Calc.	-42.7	-42.5	-42.3	-40.8	-39.5	-39.2	-39.2	-38.7	-39.1	-40.4	-41.4	-42.0
dN/dh from Nel	-45.5	-44.8	-42.6	-38.0	-34.7	-35.3	-34.2	-34.8	-35.8	-38.7	-42.2	-43.7
Difference	2.7	2.3	0.3	-2.8	-4.8	-4.0	-5.0	-4.0	-3.3	-1.7	0.7	1.8
Month	1	2	3	4	5	6	7	8	9	10	11	12
k from WS	1.37	1.37	1.37	1.35	1.34	1.33	1.33	1.33	1.33	1.35	1.36	1.37
k from Nel	1.41	1.40	1.37	1.32	1.28	1.29	1.28	1.28	1.30	1.33	1.37	1.39
Diff. WS / Nel %	2.4	1.9	0.2	-2.5	-4.2	-3.4	-4.3	-3.4	-2.8	-1.5	0.6	1.5

3.13 Discussion of the empirical model based on Nel's results

The data from *Nel* (1989) had been analysed and corrected where possible for consistency, with a view to evaluation in terms of the first hypothesis for the cumulative distribution of the k-factor in terms of time occurrence of events. The variation of the k-factor as a function of altitude, and therefore also effectively the refractivity gradient in terms of equation (3.15) which relates the two, was considered.

The resultant empirical model appears to be linear in terms of height given the restricted data set, at least for the altitudes analysed, and may be formulated as a two-term linear expression, one altitude dependent, and the other altitude independent.

This model used Nel's published cumulative probability data for the gradient of the refractive index, and the resultant k-factor as the input. While in no way detracting from the value of Nel's contribution it must be mentioned that there seems to be a few typographical errors in the published tables. In most cases it has been possible to correct these errors either by interpolation or reference to other data presented in the tables. In general the tabulated values of the k-factor exceed unity. Nel does not specify exactly how the data, which formed the basis of these tables, were processed, other than that they are based on radiosonde observations made by the South African Weather Service.

Considerable time was spent on trying to match the observed cumulative percentage of time of occurrence distributions to a suitable formula, such as discussed in section 3.3, using the "Eigen" value approach. After applying a suitable transformation the resultant truncated Gaussian formula was converted to a linear one suitable for use in regression analysis. The regression analysis based on equation (3.1) was applied to Nel's data and regression coefficients derived for each station. These regression coefficients were in turn subjected to a further analysis in terms of a linear height model. The resultant height dependent coefficients permitted the prediction of the k-factor in terms of what was believed to be the equivalent of the so-called "dry" and "wet" terms. It was noted that the coastal observation sites do not conform fully to this model, presumably because of the

strong ocean effect. For this reason, the current model is proposed only for use in the summer rainfall area and for heights from the inland coastal plains upwards.

It is believed that this empirical model, based as it is on Nel's data, and supported by the Weather Service's ground data for the same eight stations, gives a much better indication of propagation conditions for Southern Africa than the simplistic 4/3rds effective earth radius average condition or 2/3rds effective earth radius worst case conditions typically used. Further work is, however, needed to explore the validity of the model more fully.

3.14 Comments on the New Model Derived from SA Weather Service Data

Application of equation (3.23), which represents the "point" form of the refractivity gradient directly, by using the meteorological readings of temperature, relative humidity, and the air pressure and various assumptions, is in itself not sufficient to determine the model of distribution of the refractivity gradient or k-factor as a function of the terrain heights. This statement is made despite the apparent good agreement found between the various models derived according to different approaches, and compared in Table 3.10.

The formula obtained by differentiation of the empirical expression for the atmospheric refractivity contains four terms that may be organised in two sub-expressions, which would be characterised as temperature gradient dependent, and gravitation dependent (temperature gradient independent).

The model requires additional knowledge regarding the behaviour of the gradient terms in this formula with elevation and climatic conditions. Readings need to be taken at different meteorological stations, for various heights. The resultant data must first be analysed, and assessed for to determine any linear or non-linear characteristics with altitude. Only then can a more suitable and possibly more accurate model of the k-factor, and the refractivity gradient distribution be proposed for the subcontinent.

The profile presented below in Figure 3.15 represents an average k-factor obtained from the mean data for ten years supplied by the SA Weather Service for 30 stations. Each value contributing to the average is for a specific month of each year between 1993 and 2002.

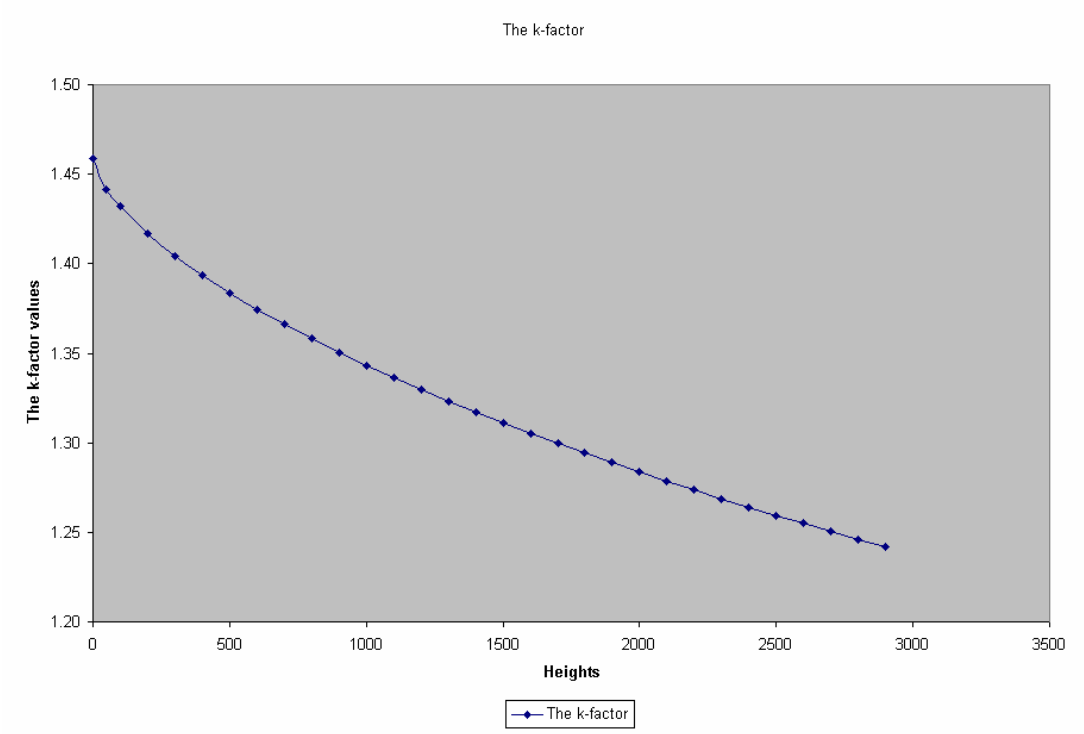

Figure 3.15 The plot represents a profile of the k-factor distribution used on the DTM to produce a map (Fig. 3.16) from the semi-empirical model. It uses the elliptic function to provide a height reference, and calculated refractivity gradient values for the regression analysis leading to that profile.

The map presented below in Figure 3.16 represents the k-factor distribution, obtained from the semi-empirical model found from meteorological data for thirty stations received from SA Weather Service and processed by a means of the formula (3.16). The refractivity gradients produced were derived for several meteorological stations referred to their heights above sea level. Information on the stations used is provided in Table 3.11, which shows their geographic parameters. The elliptic model, described in Chapter 5 Section 3, and which uses two variables, namely, the altitude and geographic latitude, was used to determine a predicted reference gradient at sea level for all thirty points for comparison with gradient values already obtained by empirical means. Further details regarding the model used are given below for clarity and consistence.

$$\frac{dN}{dh}/50\pi = a * \left(\left(\frac{h}{h_t} \right)^{\frac{2}{3}} - 1 \right), \tag{3.24}$$

$$h_t = \left(\frac{3}{2} - \left(\frac{X}{90} \right)^{\frac{2}{3}} \right) * 12km \tag{3.25}$$

$$\frac{dN}{dh}/50\pi = a * \left(\left(\frac{h}{\left(\frac{3}{2} - \left(\frac{X}{90} \right)^{\frac{2}{3}} \right) * 12km} \right)^{\frac{2}{3}} - 1 \right), \tag{3.26}$$

The X is geographical Latitude, **a** is a value of the refractivity gradient at altitude zero e.g. for the k-factor of 4/3 it would be –1/4. The height of the tropopause is given by h_t, and h is the ground level height for which predictions are required.

This model is known as double elliptic model as the idea to accommodate the geographic latitude and altitude is performed by this concept twice. It leads to the reduction of values

of the refractivity gradient obtained from the formula (3.23) to the sea level value by dividing these two sets one by the other. Further an average value is calculated and used to distribute the k-factor with height using a DTM, and to produce the average contour map presented in Figure 3.16. It must be stressed that these k-factor values are obtained from the ten years average taken over each month of every year.

Further regression analysis by the MINITAB © confirmed a good linear fit to the elliptic model, showing that at altitudes below 2km above sea level both function are almost identical estimates, meaning that a linear model is fully acceptable.

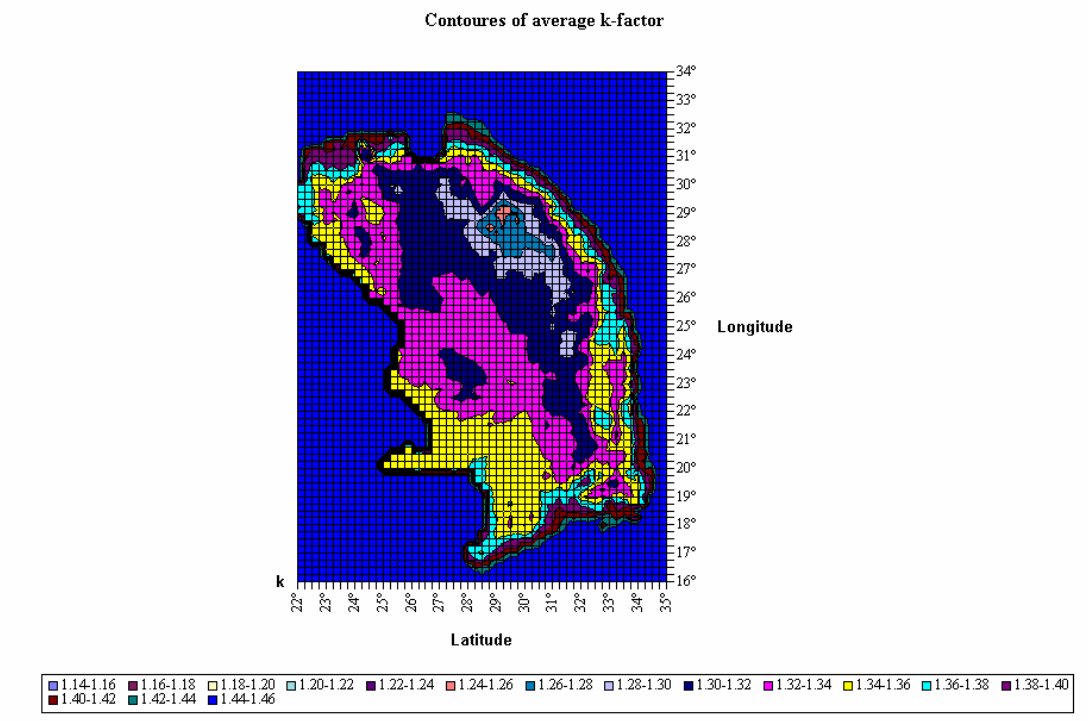

Figure 3.16 Average k-factor contours as derived from the semi-empirical model using the elliptic function to provide a height reference, and from the calculated "point" refractivity gradient values, processed further by regression analysis in terms of height. (Output format determined by EXELL ©)

Table 3.11 Average refractivity gradient data as derived from SA Weather Service information, and the refractivity gradient reduced to sea level after processing by means of the double Elliptic Model (last column).

Place	Latitude	Altitude St	Ref. Grad.	Normz.Gr.
PORT NOLLOTH	-29.23	4	-0.2982	-0.2996
TSITSIKAMMA	-34.03	5	-0.3106	-0.3123
CAPE AGULHAS	-34.83	8	-0.3071	-0.3095
DURBAN WO	-29.97	8	-0.3172	-0.3196
MALMESBURY	-33.47	101	-0.2864	-0.2989
PHALABORWA	-23.93	407	-0.3121	-0.3464
GRAHAMSTOWN	-33.28	642	-0.2816	-0.3288
LAINGSBURG	-33.20	655	-0.2494	-0.2918
PIETERMARITZBURG	-29.63	672	-0.2971	-0.3472
UMTATA WO	-31.53	742	-0.2759	-0.3269
GRAAFF - REINET	-32.20	791	-0.2655	-0.3174
ALLDAYS	-22.68	840	-0.2809	-0.3342
UPINGTON WO	-28.42	841	-0.2346	-0.2813
NELSPRUIT	-25.50	883	-0.2793	-0.3357
BEAUFORT-WES	-32.35	902	-0.2363	-0.2877
CALVINIA WO	-31.48	975	-0.2363	-0.2907
SPRINGBOK WO	-29.67	1006	-0.2402	-0.2961
POMFRET	-25.83	1182	-0.2343	-0.2945
KIMBERLEY WO	-28.80	1197	-0.2411	-0.3054
PIETERSBURG WO	-23.87	1237	-0.2538	-0.3204
MAFIKENG WO	-25.78	1282	-0.2381	-0.3037
VENTERSTAD	-30.78	1283	-0.2527	-0.3255
DE AAR WO	-30.67	1287	-0.2289	-0.2950
PRETORIA	-25.73	1310	-0.2485	-0.3182
KLERKSDORP	-26.90	1324	-0.2520	-0.3241
BLOEMFONTEIN WO	-29.10	1359	-0.2375	-0.3084
VEREENIGING	-26.57	1481	-0.2524	-0.3316
VREDE	-27.43	1670	-0.2355	-0.3184
BETHLEHEM WO	-28.25	1686	-0.2443	-0.3318
ERMELO WO	-26.50	1766	-0.2407	-0.3291
Average	-29.05			-0.3143

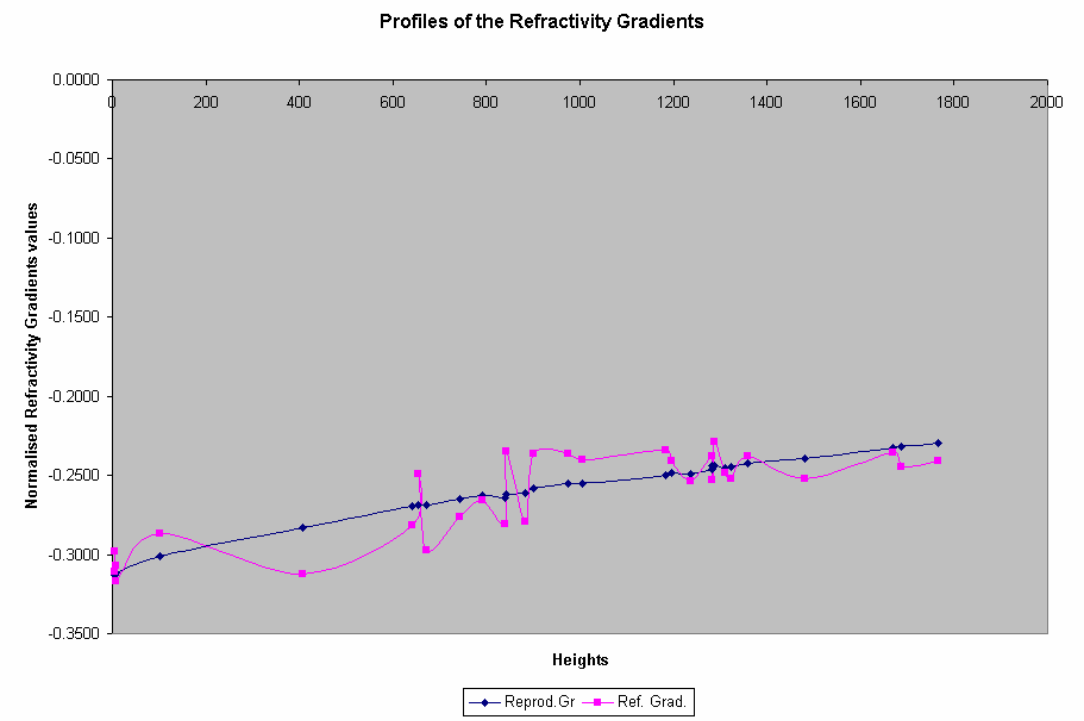

Figure 3.17 The plot represents profiles obtained from raw data as provided by SA Weather Service processed by a means of formula 3.20 and the reproduced refractivity gradient (the smooth one) by the regression analysis from the double Elliptic Model. (Output format determined by EXEL ©)

Table 3.12 Data profile used to extrapolate the average k-factor values over terrain elevation using a DTM for South Africa.

Altitude	The k-factor
0	1.46
50	1.44
100	1.43
200	1.42
300	1.40
400	1.39
500	1.38
600	1.37
700	1.37
800	1.36
900	1.35
1000	1.34
1100	1.34
1200	1.33
1300	1.32
1400	1.32
1500	1.31
1600	1.31
1700	1.30
1800	1.29
1900	1.29
2000	1.28
2100	1.28
2200	1.27
2300	1.27
2400	1.26
2500	1.26
2600	1.25
2700	1.25
2800	1.25
2900	1.24

3.15 Discussion of Results and Conclusions

Values of the refractivity gradient in Southern Africa can be derived from radiosonde observations, which measure temperature, air pressure, and the relative humidity as a function of height. By its very nature this technique is costly and time consuming, and is therefore applied only at a limited number of stations. The resultant values of the k-factor are accordingly highly localised and difficult to extend to other areas.

In fact, in the whole of South Africa there are over a hundred meteorological stations of different status, some of them taking ground based measurements three times a day, some two times a day, and some only once a day. These ground based data may be used to predict the long term and monthly average refractivity gradient and k-factor, and will thus result in a much better understanding of just how the average value of the k-factor varies across the country under different climatic conditions during different seasons.

It would be worthwhile to investigate the possible use of satellite technology to see if it is possible to measure or estimate the water vapour pressure and temperature variation as a function of height. If this could be done, it would be possible to monitor actual propagation conditions across Southern Africa using atmospheric morphological mapping similar in some respects to the mapping of ionospheric morphology using GPS techniques.

Chapter 4

GEOGRAPHIC EXTENSION OF THE DATA ACROSS SOUTH AFRICA

4.1 Introduction

The third hypothesis, in principle, deals with the gradient value of refractivity reduced to sea level. This value then remains constant for the area of the subcontinent undergoing the diurnal and seasonal changes only.

The second hypothesis, which was a possibility of extending the existing results representing values of the k-factor geographically to all places, was formulated before the DTM become available. Therefore, it remained only a proposition to extend the existing values of the k-factor and the refractivity gradient in order to create a two-dimensional map. Extending the existing neural network algorithm to a two-dimensional form and applying a great circle measure for distance has been done successfully below. However during this process a third hypothesis crystallised. This was that all values extended along the altitude from a model could be derived from a single point value given at sea level. The model will be applied on the DTM for the heights distribution but then the second hypothesis reduces to a simple research question.

The present chapter is concerned with the modelling of the refractivity gradient and the k-factor values for the new distribution model over land and sea. This is done in order to extend the application of the existing data to the Southern Africa region as a whole, using the limited data available, and to interpolate the data in between the observed values at the known observation sites. The extension is done without consideration of terrain elevation above sea level. It is purely a two dimensional map, outlining the estimated modelled values in between given points, and is done explicitly without DTM support.

4.2 Analysis of the SABC and the CSIR Recommended Data

In order to demonstrate how the existing data can be used to interpolate between the observation points, some examples will be considered. The values recommended by the

SABC for use during day and night are given in Table 4.1 and Table 4.2 respectively *Nel and Erasmus* (1986). The values recommended by the CSIR are shown in Table 4.3 and Table 4.4 *Pauw* (1996), and may be used in a similar way to the SABC data. In these tables the best estimates of the published values are chosen by a means of the Eigen-value method described in the previous chapter.

4.3 Algorithm Selection and Implementation

The algorithm, which will be applied to extend the recommended values to new areas is the Generalised Regression Neural Network (GRNN) as described by *Greene* (1999) and *Dobija* (1978). This has been extended to the two-dimensional case to handle the situation under consideration.

All distances involved in the calculations by the formulas are great circle ones. The Z is a value of the function going through the given points and is used for estimating values between given points. The formula is given below:

$$Z = \frac{\sum_{i=1}^{i=n} z_i * e^{-(x-x_i)^2/2*\sigma_1^2} * e^{-(y-y_i)^2/2*\sigma_2^2}}{\sum_{i=1}^{i=n} e^{-(x-x_i)^2/2*\sigma_1^2} * e^{-(y-y_i)^2/2*\sigma_2^2}}, \qquad (4.1)$$

The statistical indicators used in the formula above may be compared with expressions for variance divided by *n*, the number of observation sites. They are then known as unbiased estimators. Terms in 4.1 are define below.

Table 4.1 Selected data from the recreated SABC tables in Chapter 3 for daytime use to obtain the refractivity gradient values from the best Eigen value estimates. These are needed for extending values of the k-factor geographically in between the observation points.

	Altitude	Latitude		Latitude				
Place	Km	Degrees	Minutes	Decimal Degrees	%time	k-factor	Refractivity gradient	grad*50pi N-units/km
Cape Town	0.044	35	58	35.97	0.1	1.85	0.3	52.51
Port Elizabeth	0.06	33	59	33.98	0.1	1.96	0.4	56.64
Alexander Bay	0.021	28	34	28.57	0.005	2.72	0.5	71.40
Upington	0.836	28	26	28.43	0.01	1.57	0.2	34.01
Bloemfontein	1.351	29	6	29.10	0.005	1.62	0.2	38.02
Durban	0.008	29	58	29.97	0.1	2.04	0.4	57.32
Pretoria	1.372	25	45	25.75	0.01	1.54	0.2	33.50
Bethlehem	1.68	28	14	28.23	0.005	1.84	0.3	50.51
Average						1.89	0.31	49.24

Table 4.2 Selected data from the recreated SABC tables in Chapter 3 for nighttime use to obtain the refractivity gradient values from the best Eigen value estimates. These are needed for extending values of the k-factor geographically in between the observation points.

	Altitude	Latitude		Latitude				
Place	Km	Degrees	Minutes	Decimal Degrees	%time	k-factor	Refractivity gradient	grad*50pi N-units/km
Cape Town	0.044	35	58	35.97	0.1	2.18	0.4	67.34
Port Elizabeth	0.06	33	59	33.98	0.1	2.09	0.4	62.34
Alexander Bay	0.021	28	34	28.57	0.5	1.37	0.2	26.95
Upington	0.836	28	26	28.43	0.01	1.37	0.1	23.18
Bloemfontein	1.351	29	6	29.10	0.5	1.41	0.2	34.85
Durban	0.008	29	58	29.97	0.05	2.25	0.4	63.39
Pretoria	1.372	25	45	25.75	0.5	1.37	0.2	30.65
Bethlehem	1.712	22	29	22.48	0.5	1.37	0.2	30.60
Average						1.68	0.27	42.41

Table 4.3 Selected data from the recreated CSIR tables in Chapter 3 for daytime use to obtain the refractivity gradient values from the best Eigen value estimates. These are needed for extending values of the k-factor geographically in between the observation points.

	Altitude	Latitude		Latitude				
Place	Km	Degrees	Minutes	Decimal Degrees	%time	k-factor	Refractivity gradient	grad*50pi N-units/km
Cape Town	0.044	35	58	35.97	0.1	2.16	0.4	59.75
Port Elizabeth	0.06	33	59	33.98	0.1	2.51	0.4	65.66
Alexander Bay	0.021	28	34	28.57	0.5	2.58	0.4	63.78
Upington	0.836	28	26	28.43	0.01	1.27	0.1	22.38
Bloemfontein	1.351	29	6	29.10	0.5	1.3	0.2	26.41
Durban	0.008	29	58	29.97	0.05	2	0.3	53.65
Pretoria	1.372	25	45	25.75	0.5	1.65	0.2	35.72
Bethlehem	1.712	22	29	22.48	0.5	1.24	0.1	20.71
Average						1.84	0.28	43.51

Table 4.4 Selected data from the recreated CSIR tables in Chapter 3 for nighttime use to obtain the refractivity gradient values from the best Eigen value estimates. These are needed for extending values of the k-factor geographically in between the observation points.

	Altitude	Latitude		Latitude				
Place	Km	Degrees	Minutes	Decimal Degrees	%time	k-factor	Refractivity gradient	grad*50pi N-units/km
Cape Town	0.044	35	58	35.97	0.1	2.42	0.5	74.28
Port Elizabeth	0.06	33	59	33.98	0.1	1.56	0.3	40.91
Alexander Bay	0.021	28	34	28.57	0.5	1.69	0.3	45.60
Upington	0.836	28	26	28.43	0.01	1.73	0.3	45.43
Bloemfontein	1.351	29	6	29.10	0.5	1.40	0.2	34.11
Durban	0.008	29	58	29.97	0.05	2.47	0.5	71.11
Pretoria	1.372	25	45	25.75	0.5	2.35	0.4	64.61
Bethlehem	1.712	22	29	22.48	0.5	1.84	0.3	52.46
Average						1.93	0.34	53.56

where

$$\sigma_1 = \sqrt{\frac{1}{n*(n-1)}\sum_{i=1}^{i=n}(x_i - \bar{x})^2}, \tag{4.2}$$

$$\sigma_2 = \sqrt{\frac{1}{n*(n-1)}\sum_{i=1}^{i=n}(y_i - \bar{y})^2}, \tag{4.3}$$

The expressions below represent the sample mean, which is always used to calculate variance.

$$\bar{x} = \frac{1}{n}\sum_{i=1}^{i=n} x_i, \tag{4.4}$$

$$\bar{y} = \frac{1}{n}\sum_{i=1}^{i=n} y_i, \tag{4.5}$$

Application of the GRNN on the spreadsheet is a straightforward affair, namely, the first row on the spreadsheet is defined in terms of the geographical longitude with the values of the known points and certain new step values in between.

The first column is calibrated with the geographical latitude of the values of the given points and the chosen step values in between, preferably corresponding in value to the first ones for scale consistency. In order to replicate the existing known points, and to estimate values of the new points in between, the formulas given above need to be accommodated in each cell for all eight given observation points. This is done easily by typing the formulae in the first cell and then copying it into all other cells for the full range to be covered.

The formulas are convenient for use in a spreadsheet and the work necessary to obtain the numeric results is not complicated.

However, Kriging (*Clark,* 1979), and (*Clark and Harper,* 2000), which was another technique considered, is much more difficult to apply. Kriging involves matrix manipulation techniques for each and every point. It is thus very cumbersome to use conveniently in a spreadsheet. Customised software must therefore first be developed.

Despite this disadvantage, a variogram, which is a measure of spatial variability of the samples, was obtained from the data set available for analysis. The results were inconclusive. A standard application of Kriging was therefore ruled out.

However, there is unique research conducted by Dr. J. Carr at University of Nevada, who works with Kriging using a great-circle distance algorithm, for sparsely populated data, or for under-sampled systems (*Carr, et al.,* 1985). This approach might be worthwhile following up at some stage in future work.

Further investigation of this kind is very important to the evaluation of the Neural Network Regression Analysis algorithm. This is at this stage the only known, viable, method for applying to this type of sparse data sampling.

The Great-Circle formula applied in the present work

The great circle distance between two points, s (source) and d (destination), is given by

$$Dis\tan ce = \cos^{-1}\left(\sin\left(LAT_s\right)\times\sin\left(LAT_d\right)+\cos\left(LAT_s\right)\times\cos\left(LAT_d\right)\times\cos\left(LNG_d - LNG_s\right)\right)\times 111.111[km], \quad (4.6)$$

where

LAT_s and LNG_s = latitude and longitude of the source point,
LAT_d and LNG_d = latitude and longitude of the destination point.

The formula is particularly convenient for Southern Africa where all points are found to have south and east designation only.

4.4 Geographic Data Extension by means of the Elliptic Model

The Elliptic Model is primarily based on a distribution of a single value of the refractivity gradient at sea level at a specific time, for the whole country, changing with geographic latitude and altitude of the terrain with reference to the height of tropopause above sea level. The altitude is normalised along the height of the tropopause this is a reference in the classic exponential model of the troposphere as given in *Recommendation ITU-R P.453-7.*

The values of the refractivity gradient vary according to diurnal and seasonal changes. The tables should be obtained at least for the highest and the lowest values, in order to facilitate planning of the wanted values of signals and their interference spillover. Therefore, it is in principle possible to determine from the existing data the average values of the refractivity gradients for the country for the two cases considered, namely day and night in summer and winter. The concept will be extended further in the next chapter to the concept of an elliptic function model to extrapolate the refractivity away from the observation sites, to a larger territory.

The CSIR data should therefore rather be considered as a more representative guide and be used to obtain a preliminary Elliptic Model. This set is to be extended geographically exactly the same way as the previous sets of values.

It is evident from the SABC data set that these may not be accepted as a true reflection of the radio meteorological situation for the country, since the night figures of the refractivity gradient may not be lower than the day values.

Much of these comments apply to the k-factor, which reaches higher values during nights. Therefore, the radio transmissions spillover at night goes far beyond their normal coverage area. For these reasons the night values of the k-factor are used to calculate the interfering transmissions signals in order to minimise this harmful interference.

Tables 4.1, 4.2, 4.3, 4.4 contain values of the k-factor as recreated from the best estimates in Chapter 3 by the Eigen-value method. The values have been converted and confined to the

50% of time for events for the purpose of averaging and extending them geographically into locations away from the reference observation points. This has been done by use of the GRNN algorithm, which is able to accommodate the existing known point-values and extrapolate them further afield.

The GRNN in this specific application is defined as a two-dimensional function using Great Circle distances between all known-points. However, the problem encountered here is more difficult than previously reported in the literature because the sampling is sparse. Therefore an effort to apply the Kriging technique proved to be inconclusive as opposed to the GRNN, which was used in fact to produce the map contours. Nevertheless, some unique research of undersampled applications study using Great Circle distances with Kriging has been reported by *Carr, et al.* (1985) in research on earthquake occurrence predictions.

The idea to apply the GRNN was conceived at the time when the DTM was not yet available. At that time it was not known whether it would be possible to get one and what the limitations on it might be for this type of work. Thus this proposition was identified as a second hypothesis, because of the limitations and uncertainty of the outcome of its results. However, now it would appear to be a research question that produced an encouraging result, and which may still be explored in future work. This is so particularly in the case of the terms in the k-factor and the refractivity gradient, which are altitude independent. Therefore in those cases, which do not require a DTM and may be mapped separately and independently for any reason, it may still remain a viable option to visualise the results. The results representing sets of contours for different values of the k-factor in Figures 4.1 to 4.6 are devoid of the coastline and the national borders and therefore they may be difficult to read. The DTM itself, besides offering the above missing features, also does not provide any indications as to where there are rivers, towns, etc. The heights are presented only according to a selected pixel size of 15×15 minutes of arc, corresponding to approximately 25×25km pixel sizes.

It is important to illustrate how the process of interpolation and extrapolation of the k-factor values takes place. In the case of the SABC data (Tables 4.1 and 4.2) and the CSIR data (Tables 4.3 and 4.4) the spreading takes place directly from the given k-factor values, respectively for daytime (Figures 4.1 and 4.3) and nighttime values (Figures 4.2 and 4.4).

However, the Elliptic Model (Tables 4.5 and 4.6) is more involved requiring as it does the following steps. Firstly, the exponential model recommended by the ITU (*Recommendation ITU-R P.453-7*), has been used to reduce all the values of the refractivity gradients, at the 8 observation sites to sea level values, where according to the third hypothesis they are supposed to be equal at any given point in time. Unfortunately, these values do not come out equal for different reasons such as the fact that the exponential model is not perfect but only an approximation of a real one. The accuracy of the readings may be limited, amongst other possible reasons.

Secondly, an average value of all the converted readings is taken and used to produce a uniform spread of values, assuming the CSIR data sets (Tables 4.3 and 4.4) as more representative than the SABC ones. The contours for points in between the observation sites are obtained according to the chosen grid dividing the geographical co-ordinates in the east and south directions. The given points remain intact and reproduce their own values at places where they belong.

The third hypothesis, it should be mentioned, is applicable to the question of interpolating and extrapolating the k-factor values to some extent indirectly. In other words it assumes constant values of the refractivity gradients at sea level and at the tropopause level at a given point in time. This gradient always equals zero at the tropopause but its values change at sea level during night and day and for seasons of winter-summer. There is a number of possible models that could be used to interpolate/extrapolate the values as a function of altitude using these boundary conditions. In the engineering practice of radio planning the most important parameters are the best and the worst radio-meteorological conditions represented ultimately as the lowest and the highest k-factor values.

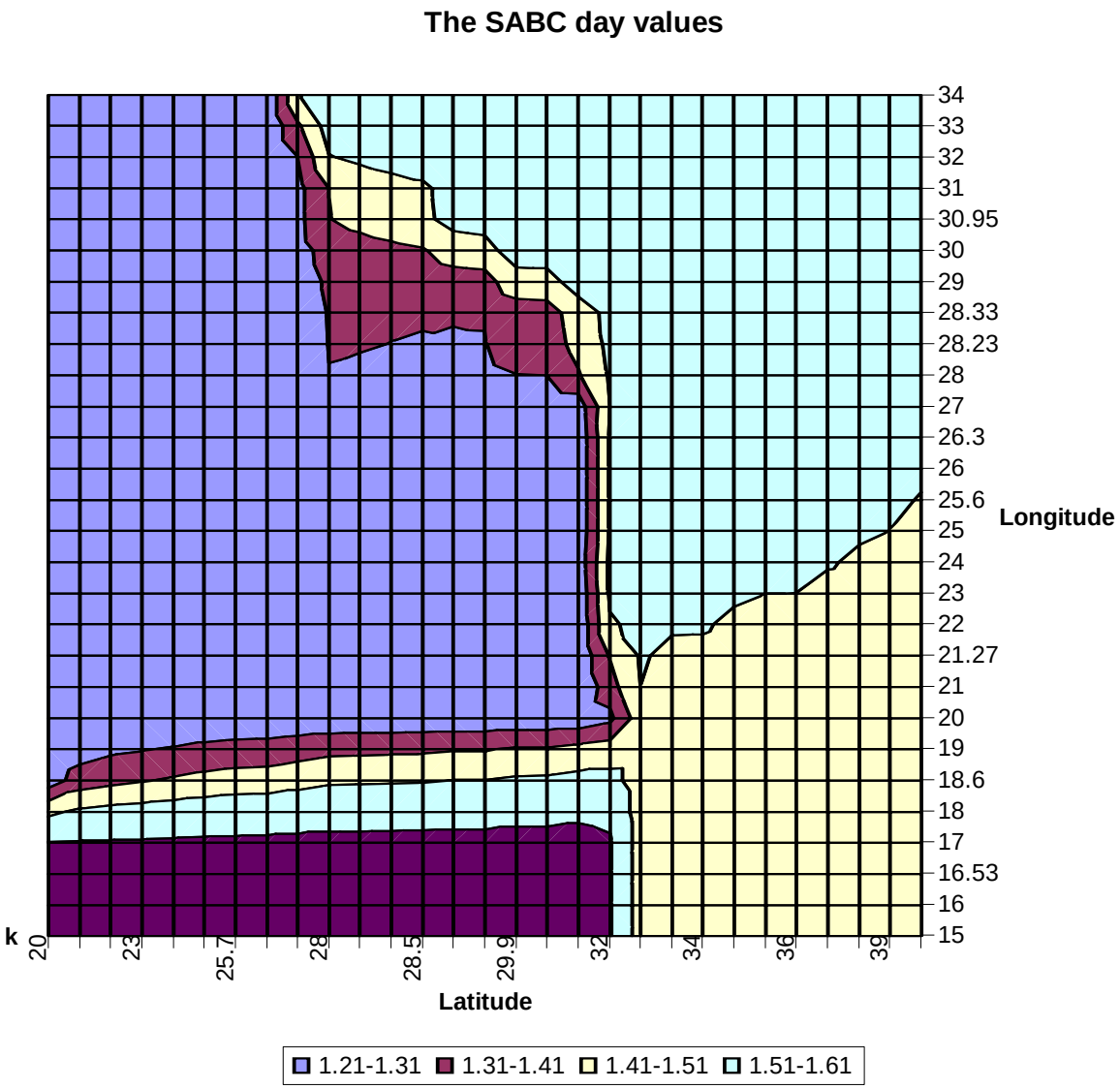

Figure 4.1 The SABC daytime values from Table 4.1 are used to produce the k-factor values for 50% of time for events, away from the points of measurement by extrapolating them geographically with the GRNN algorithm. (Output format determined by EXCEL ©)

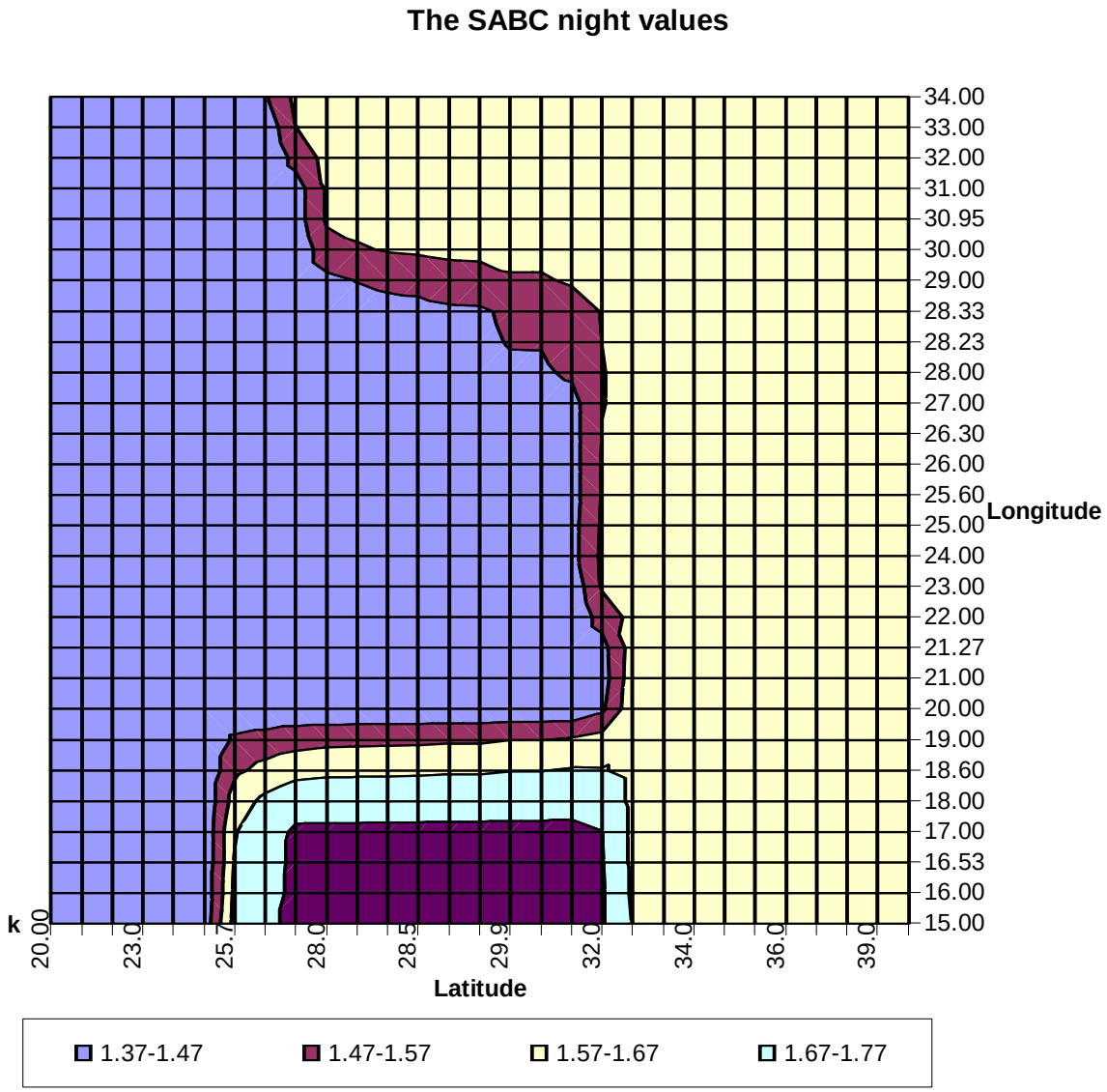

Figure 4.2 The SABC nighttime values from Table 4.2 are used to produce the k-factor values for 50% of time for events, away from the points of measurement by extrapolating them geographically with the GRNN algorithm. (Output format determined by EXCEL ©)

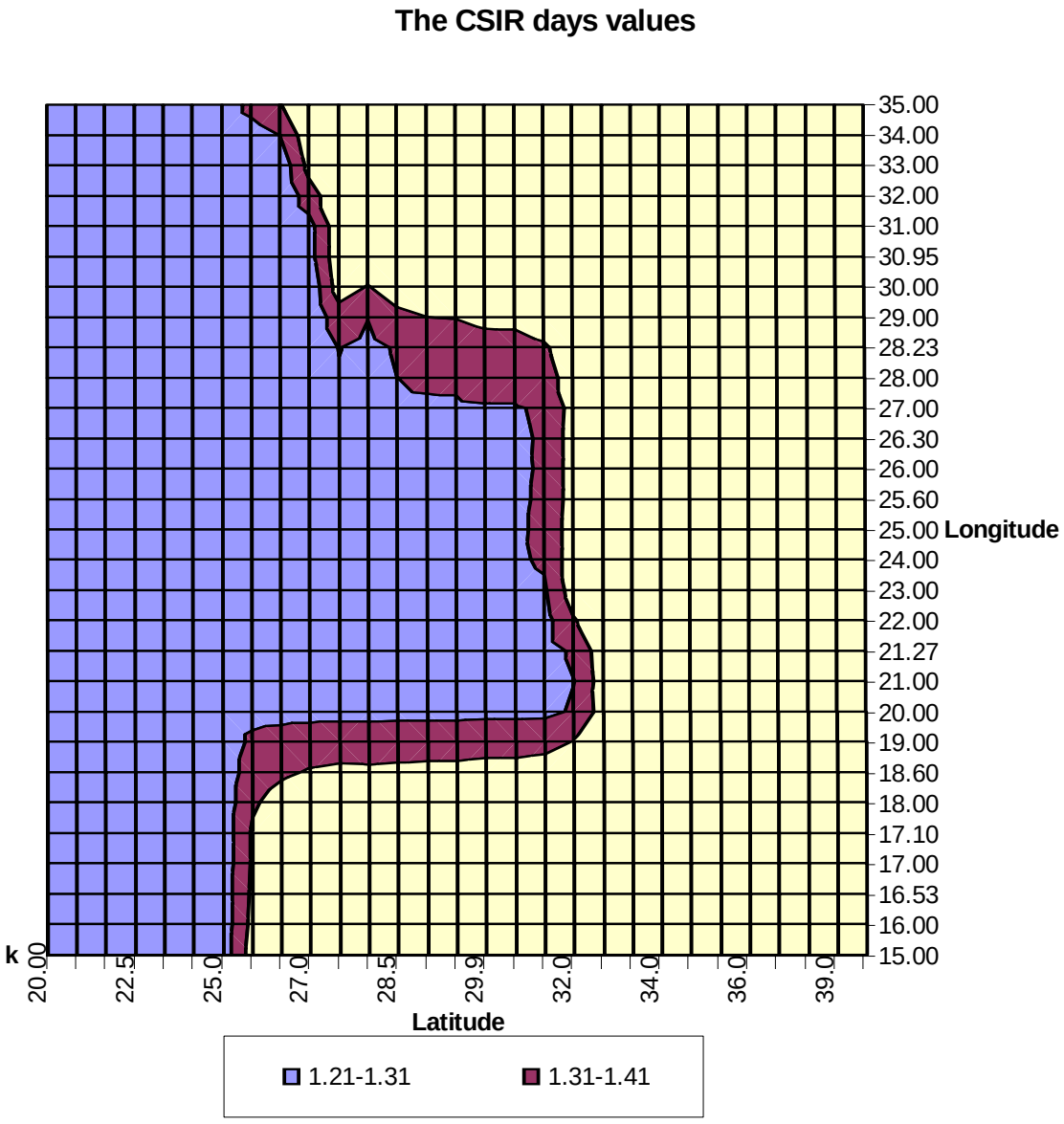

Figure 4.3 The CSIR daytime values from Table 4.3 are used to produce the k-factor values for 50% of time for events, away from the points of measurement by extrapolating them geographically with the GRNN algorithm. (Output format determined by EXCEL ©)

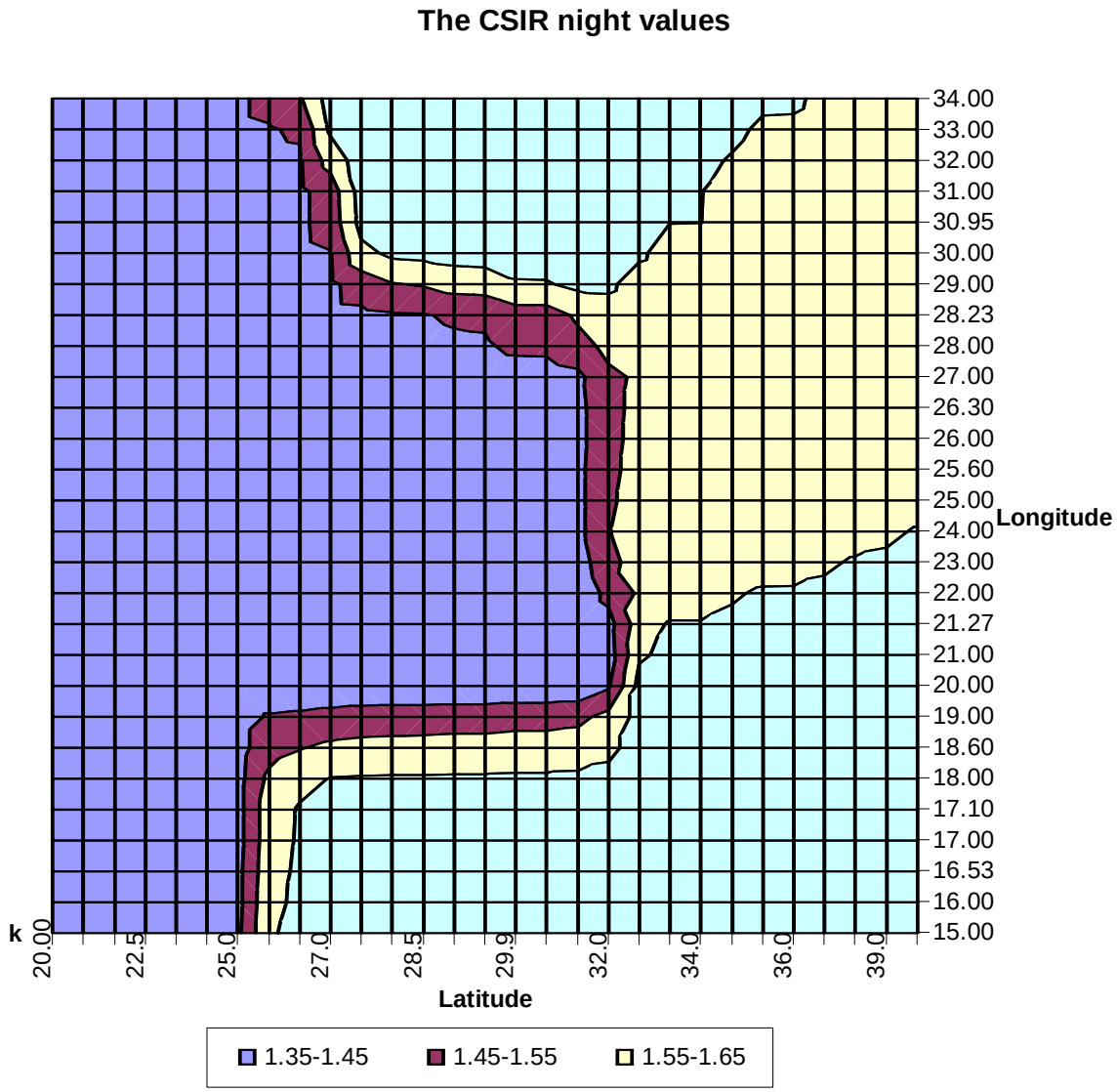

Figure 4.4 The CSIR nighttime values from Table 4.4 are used to produce the k-factor values for 50% of time for events, away from the points of measurement by extrapolating them geographically with the GRNN algorithm. (Output format determined by EXCEL ©)

Table 4.5 This presents selected data from the spread of the chosen averaged value for daytime use, obtained by estimates attributable to places in the CSIR data, using the Elliptic Model. These are needed for extending values of the k-factor in between the given points geographically as shown in Figure 4.5 below in the same manner as in both previous cases.

	Altitude	Latitude		Latitude				
Place	Km	Degrees	Minutes	Decimal Degrees	%time	k-factor	Refractivity gradient	grad*50pi N-units/km
Cape Town	0.044	35	58	35.97	0.5	1.39	0.1927	30.27
Port Elizabeth	0.06	33	59	33.98	0.5	1.40	0.1937	30.42
Alexander Bay	0.021	28	34	28.57	0.5	1.43	0.1950	30.63
Upington	0.836	28	26	28.43	0.5	1.40	0.2008	31.55
Bloemfontein	1.351	29	6	29.10	0.5	1.38	0.2078	32.65
Durban	0.008	29	58	29.97	0.5	1.42	0.1953	30.67
Pretoria	1.372	25	45	25.75	0.5	1.38	0.1995	31.34
Windhoek	1.680	22	29	22.48	0.5	1.40	0.2067	32.47
Average						1.40	0.1989	31.25

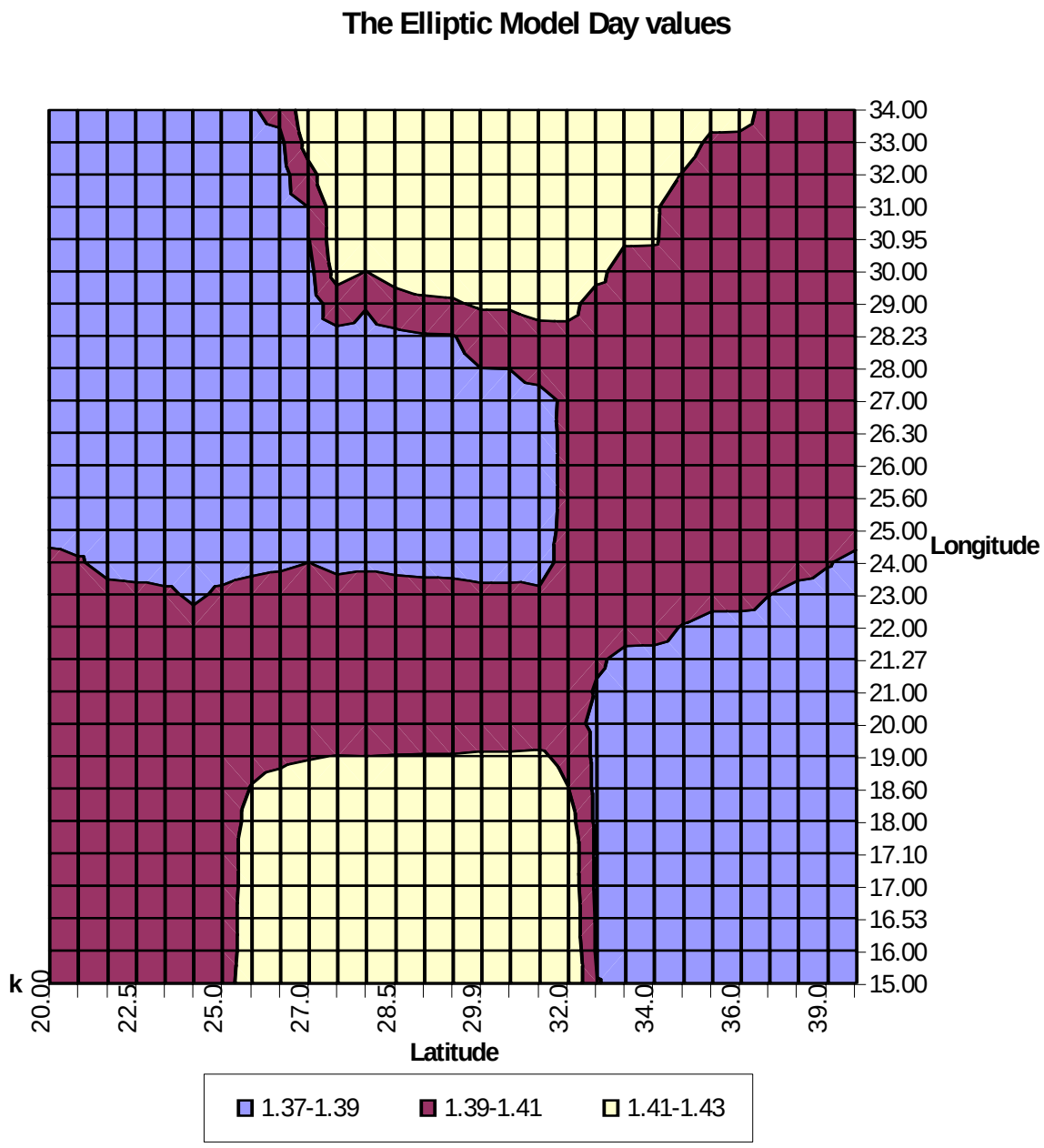

Figure 4.5 The Elliptic Model daytime values from Table 4.5 are used to produce the k-factor day values for 50% of time for events, away from the points of measurement by extrapolating them geographically with the GRNN algorithm. (Output format determined by EXCEL ©)

Table 4.6 This presents selected data from the spread of the chosen averaged value for nighttime use, obtained by estimates attributable to places in the CSIR data, using the Elliptic Model. These are needed for extending values of the k-factor in between the given points geographically as shown in Figure 4.6 below in the same manner as in both previous cases.

	Altitude	Latitude		Latitude				
Place	Km	Degrees	Minutes	Decimal Degrees	%time	k-factor	Refractivity gradient	grad*50pi N-units/km
Cape Town	0.044	35	58	35.97	0.5	1.47	0.2272	35.69
Port Elizabeth	0.06	33	59	33.98	0.5	1.48	0.2286	35.90
Alexander Bay	0.021	28	34	28.57	0.5	1.52	0.2306	36.23
Upington	0.836	28	26	28.43	0.5	1.48	0.2370	37.23
Bloemfontein	1.351	29	6	29.10	0.5	1.46	0.2450	38.49
Durban	0.008	29	58	29.97	0.5	1.51	0.2309	36.27
Pretoria	1.372	25	45	25.75	0.5	1.46	0.2352	36.95
Windhoek	1.712	22	29	22.48	0.5	1.48	0.2449	38.46
Average						1.48	0.2349	36.90

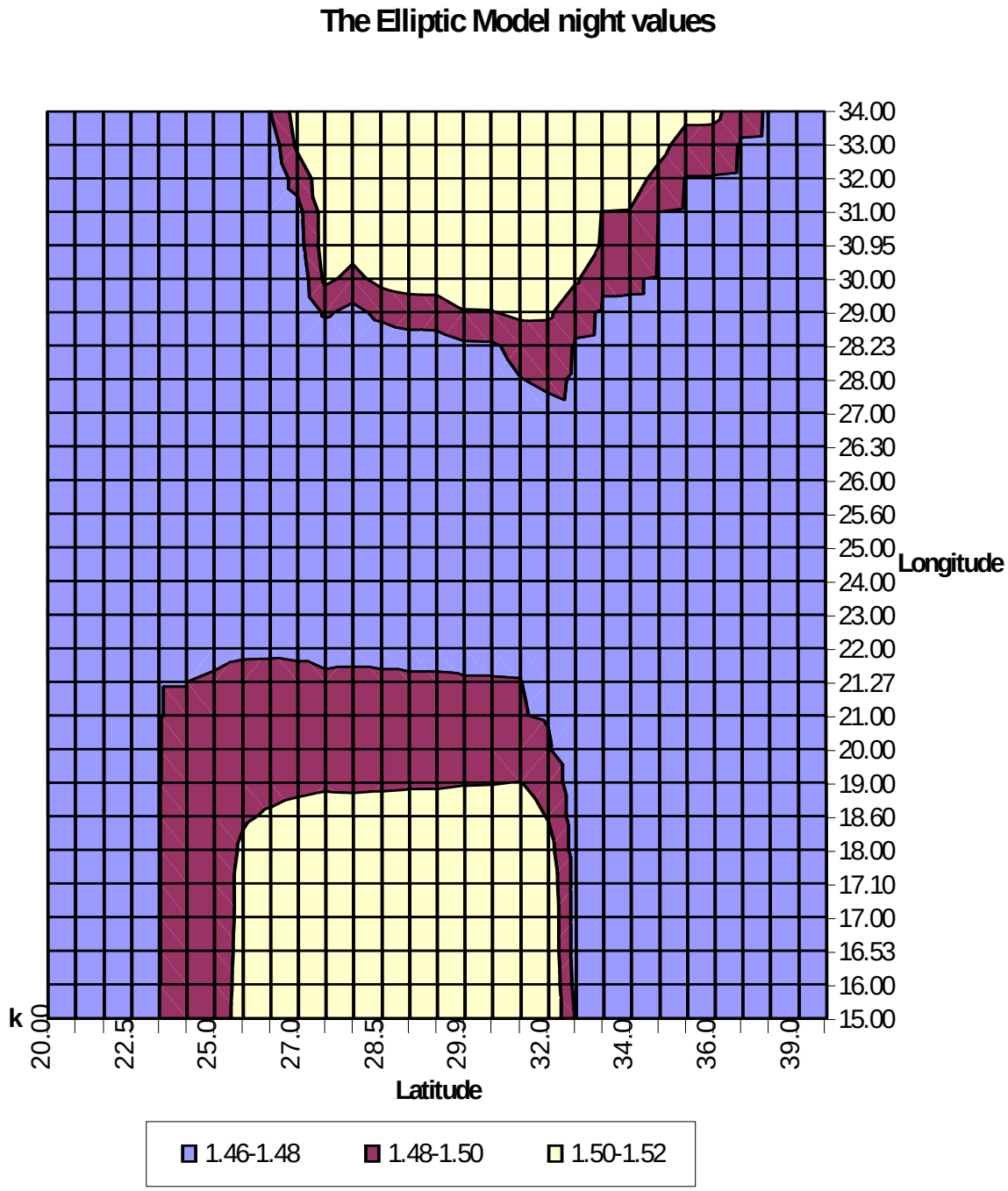

Figure 4.6 The Elliptic Model nighttime values from Table 4.6 are used to produce the k-factor values for 50% of time for events, away from the points of measurement by extrapolating them geographically with the GRNN algorithm. (Output format determined by EXCEL ©)

4.5 Conclusions

In Chapter 4 the second hypothesis was reported. This leads to a geographical extension of the known data at eight points, to the area of the land in between them, irrespective of the terrain elevation. This, finally reduced to a research question. This, in fact, allowed the production a two-dimensional map of the k-factor and the refractivity gradient values. This was done on the basis of extending the known one-dimensional formula of the neural network algorithm. Extending the data thus becomes a very mechanistic exercise.

In this process however, the available data have been analysed and the third hypothesis formulated. That was the model for extending the refractivity gradient, or the k-factor values from a single value point determined at sea level for the whole area. This was in turn used to obtain the average constant values such as those listed in Table 4.5 and Table 4.6 from the existing data in order to generate a new map for the whole land from a single value of the refractivity gradient represented at sea level. This was done by the use of the elliptic model formula to obtain the individual point values.

In this process the existing data from the SABC have been proved contradictory, as the daytime average value cannot be higher than the nighttime average value. For this reason the land averages have been obtained from the CSIR data set.

It has been demonstrated that it is in principle possible to extend the known values of the refractivity gradient, or the k-factor at certain given points to the area where these values are not yet known, and where they need to be extrapolated without applications of the DTM. However, two problems remain. These are the probability that the accuracy of these predictions is lowest just halfway between the known data points, and that the errors, or inaccuracies of the given data set will themselves propagate in this method.

Otherwise, the two-dimensional map might be a useful device, particularly when a process is altitude independent such as, for example, the modelling of the wet term. In such cases the visualisation remains transparent and very obvious on a flat map.

Chapter 5

THE SEARCH FOR SUITABLE MODELS OF THE K-FACTOR FOR USE IN SOUTHERN AFRICA

5.1 Introduction

This chapter proposes and presents several different approaches to trying to develop an acceptable model for the variation of the k-factor statistics as a function of height for Southern Africa. The refractivity gradient and the k-factor value are linked to the terrain elevation by means of new algorithms. The algorithms are defined in terms of the height of the tropopause and mainly use the well-known exponential refractivity model of the troposphere *Recommendation ITU-R P.453-7*. This results in a set of contours obtained using a suitable digital terrain model (DTM) for South Africa and these results are in turn presented graphically.

In a further development, use has been made of multiple regression analyses of the k-factor in terms of a linear parameter for the height term. Despite the restricted height range, and the limited number of observation stations where radiosonde data were available, this model was found to provide acceptable comparisons between observed and predicted time availability of the k-factor for summer rainfall areas *Baker and Palmer* (2002b), and *Baker and Palmer* (2003). The coefficients resulting from these analyses can be used with appropriate DTM data for Southern Africa to provide predicted contours of the k-factor for specific time availability for the summer rainfall regions of Southern Africa. This was discussed separately in Chapter 3.

5.2 Features of the new model

It is important to distinguish between a general model introduced here as the Elliptic Model of the troposphere, and which is described below in a separate paragraph, and other models, also described here, which use a vertical profile function to spread the refractivity gradient values along terrain elevation.

The defining conditions for the refractivity gradient at the tropopause and at sea level are set in terms of invariants. These remain the same for all models, either linear or non-linear, which are used to obtain the distribution of the refractivity gradient above sea level. In order to compare all

models of the variation of the refractivity gradient, these models must be calibrated to the same value of refractivity at sea level as well as being set to zero at the tropopause surface.

Four models with the same normalised standard value of the refractivity gradient at sea level have been compared at 1km and 2km altitude above sea level. The conclusion is somewhat surprising, namely that they effectively give the same result. It therefore appears that it does not matter which of the models described below are used, the contour values as functions of height will remain similar, and the maps will look much the same.

At this stage, from the point of view of producing maps for telecommunications applications, it may be unnecessary to search further for new models for the vertical distribution of the refractivity gradients, or to investigate the ones described below further. Important considerations for the purpose of mapping relate to basic features such as convenience, friendliness and simplicity in applying the selected model(s).

The basis for the modelling exercise to be described revolves initially around the exponential model of the atmosphere in terms of the scale-height and the height of the tropopause. The tropopause is a region between the troposphere and stratosphere having very specific features. For example, the temperature and pressure of the air remain constant everywhere on this surface, and the water vapour pressure reaches zero. Therefore, the refractivity at the tropopause becomes constant, and that in turn causes its gradient to remain zero on this surface. See for example:

http://radiometrics.com/RS_03.pdf
http://sunspot.nosc.mil/data/ftp/d858/software/ereps/td2648.pdf
http://cgd.best.vwh.net/home/flt/flt03.htm
last visited 14 April 2004.

5.3 Characteristics of the tropopause, scale height and the derivation of the Elliptic Model

The proposed name of the model developed originates from the elliptic curve, which describes the height of the tropopause above sea level. This is used in the model as a reference height in the exponential model of the atmosphere. It may be derived analytically and presented as an algebraic function for description of the model.

The scale-height expression can be easily derived from the empirical formula for the refractivity gradient under the simplifying assumption that the temperature gradient is a known function. In fact this is not the case. One of the recommendations for future work is to investigate the nature and character of the temperature gradient behaviour.

At present in the literature the scale-height and the tropopause height are considered to be two quite different entities and their height similarity is considered to be entirely coincidental. That approach stems from a different physical definitions and designations of both in terms of molecular density, temperature and gravitational considerations. However, to mitigate these two concepts is a challenge committed to the future work.

In order to derive the elliptic curve referred to above it is assumed that the height of the tropopause above the equator is 60, 000 ft (18.3 km) but that above the poles it is only 20, 000 ft (6.1 km) (*Thom,* 1994). In the formulation below the original units of measure are retained.

The shape of the surface described effectively constitutes a squashed spheroid. The "average" internationally accepted height of the tropopause is assumed to be 36, 000 ft (10.98 km). This means that if the tropopause were concentric with the earth, this would be its mean height above mean sea level. A general algebraic expression for the curve may be stated as follows:

$$y = -a * x^{h} + b, \tag{5.1}$$

$$y_{\max} = 60 \ kft \ , \ y_{\min} = 20 \ kft \ . \tag{5.2}$$

$$y_{\min} = -a * 90^{h} + 60 = 20kft, \tag{5.3}$$

$$a * 90^{h} = 40kft, \tag{5.4}$$

Where ***y*** represents the altitude of the tropopause in feet above sea level, ***x*** is the geographic latitude in degrees, ***a*** is an unknown coefficient, and ***h*** is an unknown exponent. Both unknowns are to be determined from the general formulation of the function.

By definition:

$$\frac{\int_{0}^{90}(-a * x^{h} + 60ktf)dx}{(90\,\text{deg} - 0\,\text{deg})} = 36kft, \tag{5.5}$$

The above-mentioned integral is taken over the range of 90 degrees of latitude (90 to 0 degrees from poles to equator) and averaged over the same range in order to obtain the Standard Atmosphere value of 36,000 feet that leads directly to the expression below:

For reasons of convenience, the calculations will be conducted in feet, and later converted to km. Applying the assumptions above, we may write

$$a * \frac{90^{(h+1)}}{(h+1)} = 24kft * 90\,\text{deg}, \tag{5.6}$$

These two equations may be written together as a set, in the form:

$$a * 90^{(h+1)} = 24 * 90 * (h+1) * kft, \tag{5.7}$$

$$a * 90^{h} = 40 * kft, \tag{5.8}$$

Basic algebraic manipulations of these two expressions above lead directly to the determination of the set's solution:

$$h = 2/3, \tag{5.9}$$

$$a = 40kft / 90^{2/3}, \tag{5.10}$$

The final closed form of the Elliptic Curve is as follows:

$$\left(\frac{3}{2} - \frac{y}{40kft}\right)^3 = \left(\frac{x}{90\deg}\right)^2, \tag{5.11}$$

This expression for the elliptic curve must be modified in a manner suitable for the calculation of the reference height for the tropopause altitude in the exponential model of the atmosphere to facilitate calculations on a spreadsheet.

$$y = -40kft * \left(\frac{x}{90\deg}\right)^{\frac{2}{3}} + 60kft, \tag{5.12}$$

It must be pointed out that the average height of the tropopause value given as 36, 000 feet above sea level will not be found at the latitude of 45 degrees from the equator but is calculated from the Elliptic Curve to be at 41.83 degrees of latitude.

The equation above may be expressed in kilometres as:

$$\left(\frac{x}{90\deg}\right)^2 + \left(\frac{y}{12.2km} - \frac{3}{2}\right)^3 = 0, \tag{5.13}$$

5.4 Linear model from the experimental data and an analytic model as an extension to the empirical one.

The Elliptic Model provides a solution such that the value of the refractivity gradient at the tropopause always equals zero. The distance from the sea level, where the value of the refractivity gradient remains constant, to the tropopause becomes a defining parameter of the model adopted for the gradient distribution, and consequently for the distribution of the k-factor along terrain elevation.

Other work supplementary to this thesis involving the analysis of the annual data published by *Nel* (1989) has been done. *Palmer and Baker* (2002), *Baker and Palmer* (2002a and b, 2003) used a multiple regression analysis, which established the important result that a linear height model in fact provides an acceptable fit for communications predictions for observed results in the Southern Africa region.

As a further result, obtained from the Nel's data, a linear model for the refractivity gradient is formulated below for estimating the distribution of the refractivity gradient and the k-factor using a DTM. This produced a variation in the pseudo-tropopause heights, (the height at which the refractivity gradient is conventionally assumed zero) from over 3 km in winter to about 5 km in summer.

These heights are not a true reflection of the tropopause heights during the year. By this it is meant that the linear model obtained does not indicate the real physical heights of tropopause. This linear model, which was derived from the multiple regression results and applied for the purpose of spreading the k-factor over the terrain heights, takes the following form:

$$\frac{dN(h)}{dh} / 50\pi = a * h + b, \tag{5.14}$$

$$a * h_t + b = 0, \tag{5.15}$$

$$a * 0 + b = -\frac{1}{4}, \tag{5.16}$$

$$a = -\frac{1}{4} * \frac{1}{h_t}, \tag{5.17}$$

$$\frac{dN(h)}{dh} / 50\pi = -\frac{1}{4} * \left(1 - \frac{h}{h_t}\right), \tag{5.18}$$

It must be emphasised that the two terms in the model represent respectively the "a*h" the altitude dependent term, and "b" being altitude independent. These two terms can be isolated from the refractivity gradient expression obtained by taking a derivative from the empirical formula for the atmospheric refractivity (*Bem,* 1973).

The terms for the refractive index gradient in the formula (3.23) by *Bem* (1973) are functions of air-pressure, temperature, and water vapour pressure. The formula may be organised for terms, which are altitude dependent ones associated with the temperature gradient, and the altitude independent ones associated with gravitation term.

5.5 Non-linear Model obtained from a theoretical study

A new approach to extract a non-linear model from the known formula (2.1) has been analysed. This shows the scope for more models, or even a class of such models, which could perhaps still be developed. This model uses the framework of the Elliptic Model for its calibration against the tropopause height, and the sea level constant value of its refractivity gradient. It relates in its concept to the linear model mentioned above in the way that altitude dependent and altitude independent terms may be identified in it.

The following steps lead to derivation of the model by splitting the k-factor formula:

$$k = \frac{1}{1 + sh^2\left(sh^{-1}\left(\sqrt{\frac{dN(h)}{dh} / 50\pi}\right)\right)}, \tag{5.19}$$

sh = is hyperbolic sinus, sh^{-1} = is its reverse function,

$$ah + b = sh^{-1}\left(\sqrt{\frac{dN(h)}{dh} / 50\pi}\right), \tag{5.20}$$

$$\frac{dN(h)}{dh} / 50\pi = sh^2(ah + b), \tag{5.21}$$

$$\frac{dN(h_t)}{dh} / 50\pi = 0, \tag{5.22}$$

At the tropopause, by definition, the refractivity gradient equals zero.

Thus

$$sh^2(ah_t + b) = 0 \Rightarrow ah_t + b = 0, \tag{5.23}$$

An average value of the refractivity gradient at sea level normalised to 50π is -1/4

$$\frac{dN(0)}{dh} / 50\pi = -\frac{1}{4}, \tag{5.25}$$

$$sh^2(a * 0 + b) = -\frac{1}{4}, \tag{5.25}$$

$$b = sh^{-1}\left(\frac{j}{2}\right) = j\frac{\pi}{6}, \tag{5.26}$$

$$\frac{dN(h)}{dh} / 50\pi = sh^2\left((1 - \frac{h}{h_t}) j\frac{\pi}{6}\right) = -\sin^2\left((1 - \frac{h}{h_t})\frac{\pi}{6}\right), \tag{5.27}$$

The k-factor may thus be expressed as:

$$k = 1 + tg^2\left((1 - \frac{h}{h_t})\frac{\pi}{6}\right), \tag{5.28}$$

This is an interesting model because it uses the trigonometric functions with periodic properties, meaning that tropopause-like layers are possible above, the actual tropopauses as artefacts. Diurnal and seasonal changes of the refractivity gradient are determined by the height of tropopause. These changes are visible in the linear Nel's model where the difference in tropopause heights during the winter and summer months is apparent. The gradient changes at sea level are determined by finding and assuming its highest and lowest annual values.

The parameters **a**, **b**, and $\mathbf{h_t}$ are defined parameters similar to both other models. They are similarly calculated for the boundary conditions, meaning that the refractivity gradient is zero on the tropopause and –1/4 at the sea level.

5.6 The Exponential Model

This is the best-known non-linear model. It is well documented in (*Recommendation ITU-R P.453-7)* and recommended for use. This non-linear model needs to be mentioned as it is used in the present study for the vertical profile modelling and consequently map production. It may be shown that the Exponential Model profile, which complies with the boundary conditions at the tropopause and at sea level, may be represented by the following expression.

$$\frac{dN(h)}{dh} / 50\pi = a * e^{-\frac{h}{h_t}} + b, \tag{5.29}$$

$$a * e^{-\frac{h_t}{h_t}} + b = 0, \tag{5.30}$$

$$a * e^{-1} + b = 0, \tag{5.31}$$

$$-\frac{1}{4} = a * \left(e^{-\frac{0}{h_t}} - e^{-1} \right), \tag{5.32}$$

A general formulation of the model requires that in the formula the following constant coefficients **a**, **b**, $\mathbf{h_t}$ must be proposed initially, and their values later determined from the boundary conditions.

For consistency too with the other models the lower and upper boundary conditions are applied. These are that the standard value of the refractivity gradient normalised to 50π equals –1/4 at sea level, and is zero at the tropopause height. The final form of the normalised refractivity gradient expression as derived is as follows:

$$\frac{dN(h)}{dh} / 50\pi = -\frac{1}{4 * (e-1)} * \left(e^{-\frac{h}{h_t}+1} - 1 \right), \tag{5.33}$$

At a height of one atmospheric scale height (as opposed to a pseudo scale height for the other two models) the refractivity gradient is zero. In the case of the other models, the refractivity gradient is zero at the tropopause heights as well. Since we have heights up to 1.8 km in the database for South Africa a comparison of these models at 1 km and 2 km heights shows that the differences between them are minimal but that these are expected to be the highest at the 2km above sea level. The values obtained at different latitudes for 1km and 2km heights respectively are illustrated in Table 5.1 and Table 5.2. The use of any of these simple models for the orographic distribution of the refractivity gradient would therefore give very similar results. Effectively any maps produced by these models to show average contours of refractivity gradient or the k-factor will have very similar contour lines with regards to the contour values and placement.

Table 5.1 Comparison of refractivity gradients obtained from different analytic models at 1km height above sea level.

Latitude	Tropopause height	Sin model	Linear model	Exponential Model	Elliptic Model
	18.0	-0.2252	-0.2361	-0.2286	-0.2136
21.75	13.3	-0.2168	-0.2313	-0.2214	-0.2056
22.75	13.2	-0.2165	-0.2311	-0.2212	-0.2052
23.75	13.1	-0.2161	-0.2309	-0.2209	-0.2049
24.75	12.9	-0.2158	-0.2307	-0.2206	-0.2046
25.75	12.8	-0.2154	-0.2305	-0.2203	-0.2043
26.75	12.7	-0.2151	-0.2302	-0.2200	-0.2040
27.75	12.5	-0.2147	-0.2300	-0.2196	-0.2036
28.75	12.4	-0.2143	-0.2298	-0.2193	-0.2033
29.75	12.3	-0.2140	-0.2296	-0.2190	-0.2030
30.75	12.1	-0.2136	-0.2294	-0.2187	-0.2027
31.75	12.0	-0.2132	-0.2292	-0.2184	-0.2023
32.75	11.9	-0.2129	-0.2290	-0.2181	-0.2020
33.75	11.8	-0.2125	-0.2287	-0.2178	-0.2017
34.75	11.6	-0.2121	-0.2285	-0.2174	-0.2013
35.75	11.5	-0.2117	-0.2283	-0.2171	-0.2010

Table 5.2 Comparison of refractivity gradients obtained from different analytic models at 2km height above sea level.

Latitude	Tropopause Height	Sin model	Linear model	Exponential model	Elliptic Model
	18.0	-0.2014	-0.2222	-0.2084	-0.1922
21.75	13.3	-0.1854	-0.2125	-0.1950	-0.1795
22.75	13.2	-0.1847	-0.2121	-0.1944	-0.1790
23.75	13.1	-0.1841	-0.2117	-0.1939	-0.1785
24.75	12.9	-0.1834	-0.2113	-0.1933	-0.1779
25.75	12.8	-0.1828	-0.2109	-0.1927	-0.1774
26.75	12.7	-0.1821	-0.2105	-0.1922	-0.1769
27.75	12.5	-0.1814	-0.2101	-0.1916	-0.1764
28.75	12.4	-0.1807	-0.2097	-0.1911	-0.1759
29.75	12.3	-0.1800	-0.2092	-0.1905	-0.1754
30.75	12.1	-0.1794	-0.2088	-0.1899	-0.1749
31.75	12.0	-0.1787	-0.2084	-0.1893	-0.1743
32.75	11.9	-0.1780	-0.2079	-0.1887	-0.1738
33.75	11.8	-0.1772	-0.2075	-0.1881	-0.1733
34.75	11.6	-0.1765	-0.2070	-0.1875	-0.1727
35.75	11.5	-0.1758	-0.2066	-0.1869	-0.1722

5.7 The Digital Terrain Model and Its Use in the Visualisation of k-factor contours

At present there is a readily available digital terrain model (DTM) for South Africa with a pixel size of 15×15 minutes of arc, or roughly 25×25 km. This pixel size is adequate for telecommunications planning of the sort for which various propagation models can be utilised. By way of comparison, the radio horizon for elevated sites is typically of the order of 50-60 km, which is also typical of the length of radio line-of-sight links. The scale of the DTM can be easily adjusted to a larger pixel size if required, and can be used for evaluating different map configurations with larger pixel sizes.

The particular DTM used in this work, was made available by Dr. K.I. Meiklejohn at the Department of Geography and Geoinformatics at the University of Pretoria.

The estimates of the k-factor values obtained from the refractivity gradient distributions, predicted for various percentage of time for events are verified, either by direct, or indirect measurements. For example, by monitoring the terrestrial microwave-radio link equipment, operating in the area, for outages. Measurements of the field strength in a broadcasting coverage area could be compared with predicted values obtained under some assumed k-factor then. The real value of this approach becomes apparent in this case.

5.8 Distribution of the refractivity gradient on the DTM

In the elliptic model the essential concept is that the distribution of the refractivity gradient, and thus the k-factor obtained from it, may be generated from a single parameter, namely the constant value of the refractivity gradient at sea level. The refractivity gradient then must be assumed to be a constant in the area for a specific time of the day/night, and the season of the year. The values of the refractivity gradient or the k-factor will then be spread along the elevation of the terrain with reference to the height of the tropopause in a profile model of the atmosphere.

In order to visualise the geographic distribution of either the refractivity gradient or the k-factor, a digital terrain model (DTM) for South Africa must be used. This will enable us to generate contours of constant values of the refractivity gradient, or the k-factor.

5.9 Range of the normalised refractivity gradient used for map productions

The average value of the normalised refractivity gradient is –1/4 of 50π [N-units/km] this produces the standard k-factor value of 4/3. This value however does not take into account any diurnal and seasonal changes the refractivity gradient undergoes locally in all parts of the world.

The climatic changes for different regions of the world are known as tropical, moderate, polar, or sometimes, perhaps intermediate ones. These may be peculiar to certain specific regions such as the Persian Gulf, and some are at least partially determined this way, excluding possibly the effects of rainfall.

In the Southern Africa region observed data obtained from the South African Weather Service indicate minimum values of the refractivity gradient of –0.36*50π [N-units/km] and the maximum values of –0.3*50π [N-units/km] over the period of a year. These values, in fact, are used to obtain

the geographical distribution of the gradient and the k-factor according to the altitude and latitude of the terrain. It is thus possible to produce maps with contours of the constant refractivity gradients and the k-factors.

Therefore it is quite apparent that the Southern African region requires, in principle at least, a different approach to the k-index for local use from the standard so-called 4/3rds earth for purposes of radio planning and related processes. The purpose of this study has been to summarise such needs and attempt to fill the gap between the growing requirements of the radio community and the current knowledge of the k-factor in terms of available data. This should allow for more accurate and scientific modelling of the troposphere in terms of telecommunications systems planning using a better understanding of radio propagation.

5.10 Conclusion

It can be seen that the new Elliptic Model, which now generates the above results from a single value of the refractivity gradient by a means of an exponential profile, appears to show the general trends expected in practice. However, it should be noted that temperature and water vapour content are not considered explicitly in this model. The predicted results are obtained and visualised by means of a DTM, as shown in the examples in Figures 5.1 and 5.2, produced using Microsoft Excel ©. A simple philosophy of distributing a value of the gradient along the terrain elevation features from an algorithm of the vertical profile is applied in this case. However, the values of normalised refractivity gradient, namely, the –0.3 and –0.36 have been extracted from Nel's data for 50% of time, which follow a linear model within the altitudes covered as found by a means of multiple regression *Baker and Palmer* (2002). The contours illustrated there, however, are for 0.001 of time of occurrence for inland summer rainfall areas in South Africa. The actual plots are thus different.

The idea of an analytic model revolves around predictable and regular features of the deterministic concepts of the refractivity gradient and the k-factor distribution in space between ground-sea level and tropopause. These distributions oscillate periodically between extremes, according to diurnal and seasonal changes in a deterministic manner. They may be isolated as a predictable invariant from general but frequent-periodic observations, characterised in a probabilistic fashion of occurrence attributed to a changing weather. Long-term meteorological observations gathered in a regular way, by South African Weather Services, need to be converted to the meaningful values, such as refractivity gradients, and examined by comparing them with analytical model values.

These have to be calculated from known terrain features by a means of vertical profiles calibrated from the highs of the tropopause for the same times, in order to determine the differences. It is expected that a regular invariant term could be isolated from the data observed and obtained empirically then the future efforts may be focused on the probabilistic analysis of the remaining difference.

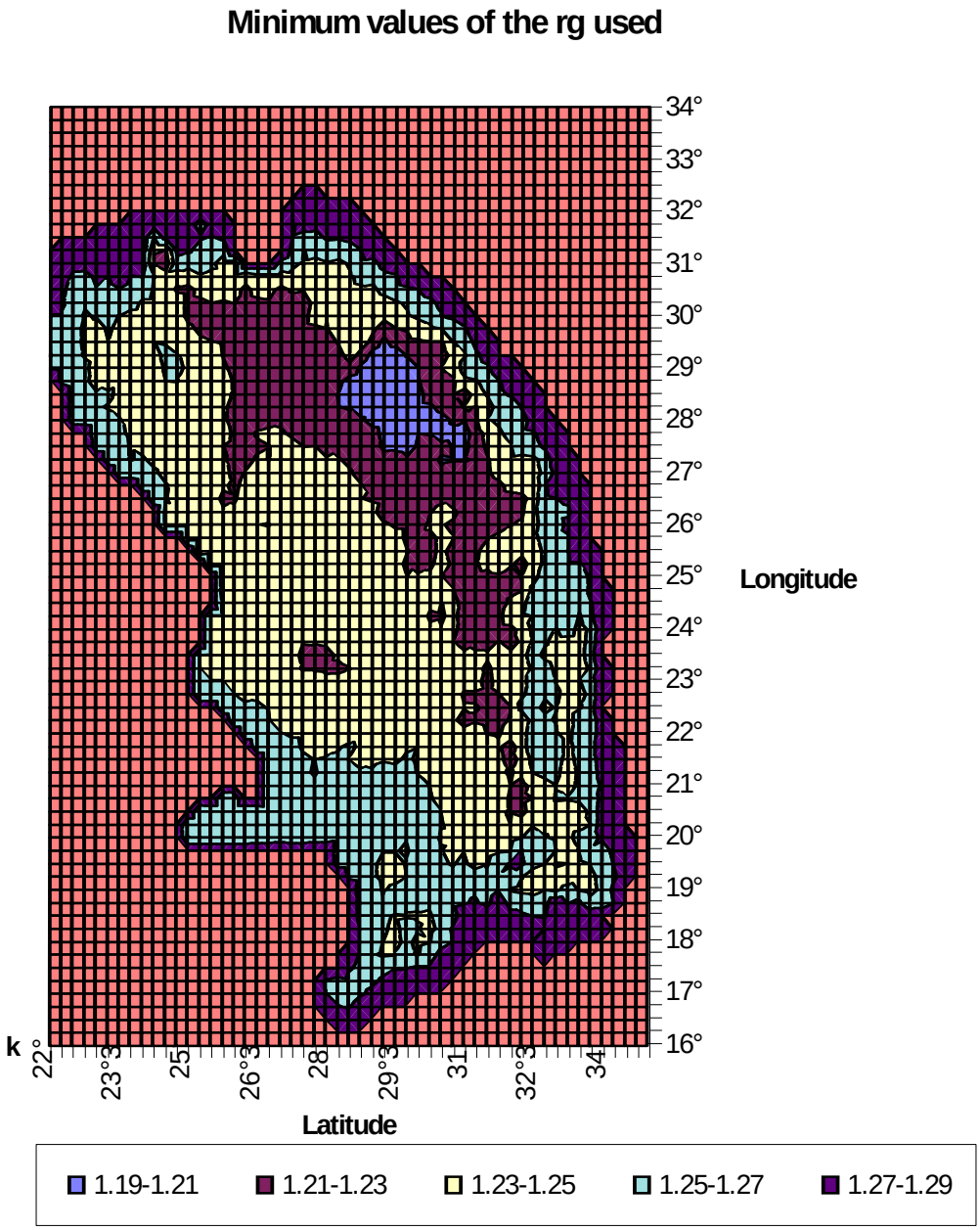

Figure 5.1 The values of the k-factor obtained for the minimum sea level reference value of the refractivity gradient of –0.36 by an exponential model spread on DTM (generated by Microsoft Excel ©).

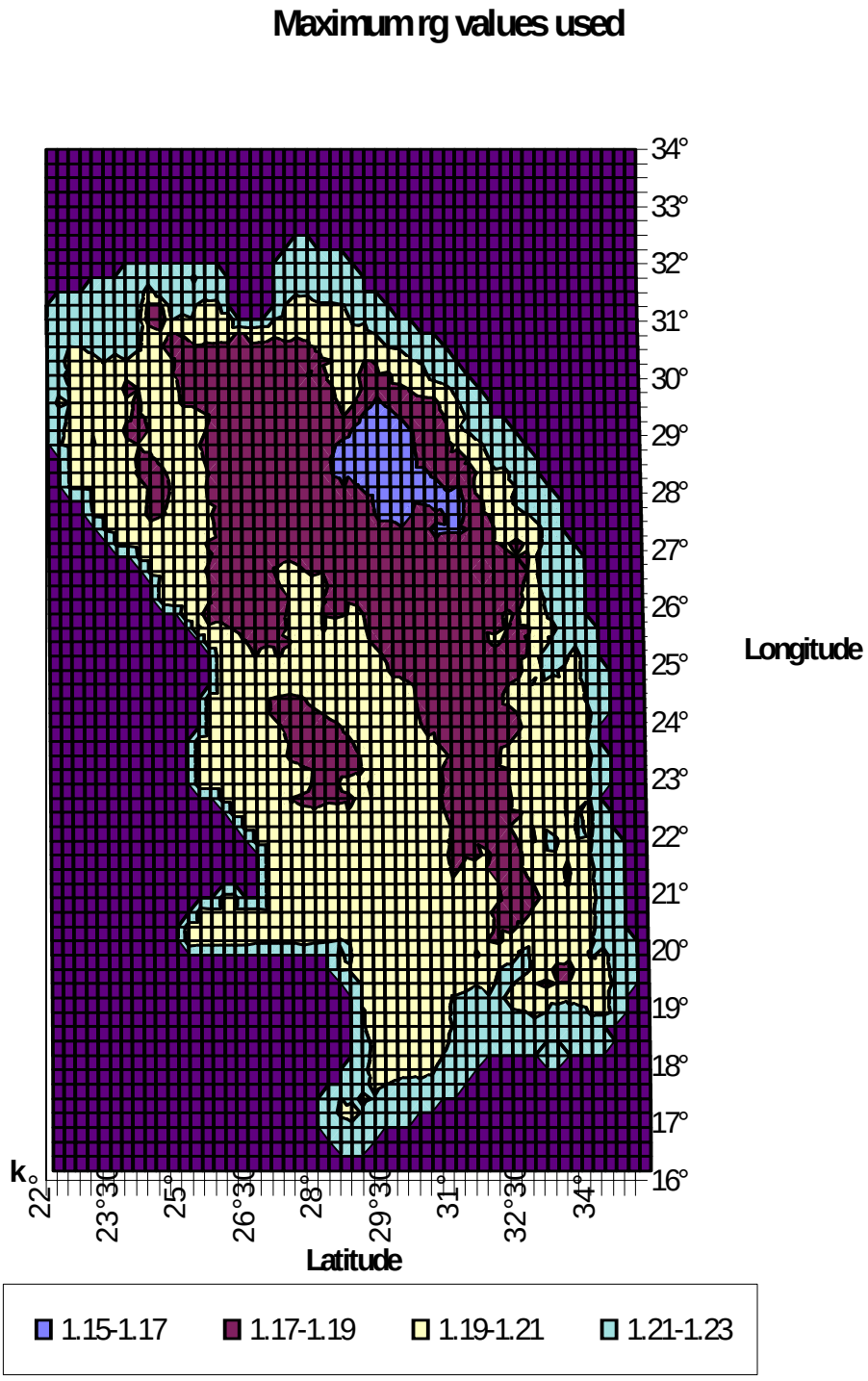

Figure 5.2 The values of the k-factor obtained for the maximum sea level reference value of the refractivity gradient of –0.3 by an exponential model spread on DTM (generated by Microsoft Excel ©).

Chapter 6

GENERAL DISCUSSION AND CONCLUSIONS

6.1 Research Objectives

The basic research objectives, as initially envisaged in the study proposal, were to determine shortcomings in the current approach, as proposed by the CCIR (*Rec. ITU-R P.834-3*), the CSIR (*Pauw,* 1996), the SABC (*Nel and Erasmus*, 1986) and others (*Buljanovic,* 1978), by studying the radio-meteorological data currently available for Southern Africa.

Of particular importance was the requirement to gain sufficient knowledge of the current situation in order to proceed further with modelling the refractivity gradients in the troposphere for radiowave propagation applications by a means of a thorough review of the k-factor data tables supplied by *Nel* (1989).

Finally, in terms of practical applications and use, it was desirable to produce tables and/or maps of the k-factor for visualisation of the results of the modelling process conducted in the studies.

6.2 Research Approach and Methodology

The research approach for the study was initially confined to the existing k-factor data sources, but later extended by using observational meteorological data measured at a number of sites in South Africa, made available by the SA Weather Service.

It was difficult to confine the entire study only to the available k-factor data despite initial successes in processing such data in terms of the hypotheses postulated in this study. The essential reasons were that it was not known with certainty exactly how these results had been obtained, and because it had been possible to compare these results only between data obtained for a limited number of 8 observation stations. The pioneering contributions of Nel and his co-workers *Nel* (1989) to this body of knowledge must, however, be acknowledged. It was therefore decided to establish a new and independent method to reproduce the data by means of an empirical model based on the data from the SA Weather Service as given in Nel's thesis. The models were compared in terms all available data sets. The techniques used were based on available processing technology, namely

what computer software is available nowadays in the form of spreadsheets such as EXCEL ©, digital terrain model data, statistical and regression analysis packages such as MINITAB © and included in EXCEL ©. In particular, the application of new modern algorithms such as GRNN (General Regression Neural Network) and Kriging were explored. It is important to stress that previous researchers in South Africa were not able to take full advantage of these new technological opportunities, as they were simply not available at the time.

6.3 Research Problem Formulation

The original motivation for the work reported here was that a more suitable model of the earth's effective earth radius factor than the popular "4/3rds earth" was necessary. This simplistic approach was insufficient to serve the growing needs for scientific radio planning and for better, more efficient spectrum utilization.

The available k-factor data sources for South Africa served as the starting point in the investigation of a new model. The data were available for 8 sites in Southern Africa, 7 in South Africa and 1 in Namibia. Four of these sites are coastal ones, and the remaining 4 are inland stations at different altitudes.

The main challenge was to find the form of the function, which would predict the distribution of the k-factor as a percentage of time for events at the individual stations, before the height dependence of the refractivity gradients could be determined for these data sets.

6.4 Search for Solutions

It often happens that a search for a solution to a problem depends entirely on the way that the problem is formulated. In other words, a reasonable model, which may finally be obtained, could be found through interaction between the problem formulation and the possible solution for the problem. It could be said that a successful model is the one based on a properly chosen solution to the problem in question.

In the preceding analyses of these solutions care must be taken to avoid those, which do not have physical interpretation, or do not offer any true advantage. A similar situation was encountered in this work for the function for the k-factor as a percentage of time occurrences for events. A second

expression for the k-factor as a function of the refractivity gradient was obtained as an artefact of the solution finally selected.

Analysis of the defining parameters for the k-factor as a function of terrain elevation produced a linear result in terms of height dependence. At this stage the results are satisfactory for the height range considered. It is not yet known whether this is a feature confined to the altitudes available in the observed data for this investigation, or perhaps whether it would behave much differently at greater heights. It could well be that an exponential dependence for the parameters could be more suitable if the observational data spanned a greater range of ground elevation.

6.5 Results, their Configuration, and their Format

Different sets of results were obtained initially from analyses of the existing SABC and CSIR data. These analyses were conducted using the GRNN approach in a spreadsheet format. This led to the fundamental result for expressing the k-factor function for percentage of time of events as a truncated Gaussian function of the refractivity gradient and the k-factor. The resulting formulation was used in turn to conduct a thorough analysis of the most reliable data set published by *Nel* (1989) by means of multiple regression techniques using MINITAB © software. These results have been published elsewhere *Palmer and Baker* (2002), *Baker and Palmer* (2002), *Baker and Palmer* (2003).

A particularly important result found during the analysis of the Nel's thesis annual data indicates that the k-factor distribution is, at least locally, a linear function of altitude. This result was used successfully to produce a distribution of the refractivity k-factor over the summer rainfall area of South Africa assuming a vertical linear model.

Other sets of results have been obtained by devising a method based on the concept of the Eigen-value/Eigen-function to replicate the existing CSIR and SABC data tables with minimum intervention from the new formulas for purposes of comparison.

One of the possibilities to extend a distribution of the k-factor over the Southern African landmass has been developed by adapting the (GRNN) algorithm to a two-dimensional case and extrapolating the values from the given eight observation points to the rest of the landmass.

A number of possible analytic models for the refractivity gradient distribution were proposed and investigated all of these are subject to the same boundary conditions. These models are based on the concept of the Elliptic Curve, which is used to describe the tropopause height assuming that this is an altitude where the refractivity gradient remains constant and equals zero.

Finally additional data obtained from SA Weather Service made it possible to predict the average results at the original eight observation sites where radiosonde data was measured. These investigations were done using a different method from that usually used. The height derivative of the empirical expression for the atmospheric refractivity based on ground measurements was used instead of atmospheric profile data obtained by flying a radiosonde.

The results compare very favourably with the original radiosonde observations except for Alexander Bay. This site warrants further investigation as strong cold ocean effects may influence conditions at this station.

6.6 Body of Knowledge / Literature Survey

Before any research work such as that reported here can commence, it is essential to determine what is known about the subject contemplated for study and research. It was, therefore, imperative to review the authoritative sources on the subject of the k-factor, and to organize this body of knowledge around the main research objectives. This is specialized knowledge, which does not necessarily appear in the textbooks. The knowledge base must be organized in a manner suitable for specialization in the subject, as well as to help to clarify what is already known and what needs to be researched further.

The literature survey for this work was done with this main objective in mind, as well as to determine the originality of the subject for research to ascertain what the potential contribution to the body of knowledge could be.

The literature search was exhaustive, and cover material published over almost the whole of the previous century. For long periods, sometimes decades, almost nothing new was published on radiowave propagation. Therefore, the relevant references were either very old ones or very recent ones.

Out of the extensive bibliography of almost 400 titles built up from scanning about 6000 abstracts, some 70 prime references were selected for the purpose of this thesis. This literature study makes it possible to focus on the subject of tropospheric radio propagation and is essential for the study or research on the k-factor and radio refractivity of the propagating medium.

6.7 Originality of the Problem, and Evaluation of the Solution

Originality of the research problem is essential for it to make a contribution to the body of knowledge in a cognitive sense. This in turn impacts on the originality of the work as a whole. In the present work the originality is believed to lie equally in the concept of the solution, and in the approach of the work.

The initial concept concerns the generalizations of modelling, particularly with regards to finding the function describing the behaviour of the k-factor for percentage of time occurrence for events and for finding the function describing the change in the k-factor with altitude.

The current approach is a new and original one in the sense that for evaluating the behaviour of the refractivity gradient and the k-factor over a large area, the use of Kriging was investigated and the GRNN algorithm was adopted as a possible approach with sparse data.

In addition to the ITU-R exponential model for the behaviour of the k-factor, other analytic models were proposed and reviewed. For the first time, to the best of the author's knowledge of the published literature, the refractivity gradient was also obtained directly from ground based meteorological data whereas all previous results were gathered by flying meteorological radiosondes, or refractometers.

The initial processing of available sets of data of k-factor values was done with the GRNN algorithm using spreadsheets. More detailed analyses were performed using the single and multiple regression options found in the MINITAB © software package.

The resultant coefficients were subjected to further regression analyses in terms of a simple linear height model. This was for inclusion in an extended model for Southern Africa based on the application of a DTM for visualisation, resulting in the production of contour maps of predicted conditions.

This approach appears to be novel when reviewing the available literature. The approach using a DTM makes it possible to assess the predicted results by straightforward inspection of contour displays and thus to detect possible inconsistencies and defects, either in the data or in their presentation.

6.8 Practical Applications of this Research

It was concluded from the extensive literature survey of the existing body of knowledge, on tropospheric radio propagation that the study of the k-factor in particular and atmospheric refractivity in general have been somewhat neglected over time. One of the reasons for this state of affairs may be the fact that radio frequency spectrum acquisition has been almost exclusively a problem for system designers and users but never for equipment suppliers.

Today it is a regrettable fact that frequency congestion, especially in highly populated areas, is reaching the point of saturation. Frequency reuse cannot be planned without an adequate knowledge of the radio meteorological conditions in the area.

The time has come for a reallocation of resources to the research and development of knowledge and proper planning tools. Ideally what is needed is appropriate customized tools and effective software in order to limit congestion of the airwaves.

Furthermore, the time has also come to realize the economic value and importance of the radiowave spectrum, as a natural resource. This must be carefully managed to eliminate misuse and the squandering of the spectrum to the benefit of various services and operations (*Palmer and Baker,* 1999).

Expertise with regards to propagation issues is also crucial for all regulatory matters, whether viewed from a national or an international perspective. This will facilitate proper use of the radio spectrum, and lead to up to date new radio recommendations and regulatory rules, including more suitable radio band allotments.

It is therefore hoped that this work would facilitate a better use of radio communications as referred to above, and that it will make life easier for both the users and planners of radio communications systems.

6.9 Determination of Research Gaps

It is a common occurrence that during the course of research that gaps in the knowledge base are identified without compromising the integrity of the main objective investigated by researchers. Identification of these gaps is a valuable by-product of research work. Such gaps may be identified as possible topics for work that could be pursued at a later stage. This work would supplement, or extend the results initially obtained.

In the current work the lack in South Africa of data for the study of the k-factor for values less than k=1 is a limiting factor. Unfortunately this deficiency in the data cannot be bridged easily because there is no indication as to whether Nel's initial study extended to such extreme cases. The high and low cumulative probabilities are on the distribution tails, which complicates the evaluation of data. Furthermore the paucity of coverage for Southern Africa by means of radiosonde observations is also a limiting factor. Such observations are only available from eight stations, four of these being at the coast and the others inland at heights ranging from roughly 800 to 1800 meters.

Part of the research reported here was undertaken in order to devise a method to extend predictions of the k-factor and/or refractivity gradient to areas well removed from the eight-radiosonde observation sites, and where there are no radiosonde measurements available. It is, however, believed that approximate values may be predicted for these areas far removed from the observation sites, albeit with a greater uncertainty compared to the predictions and /or observations made for the eight observation sites themselves.

One of the objectives in the current work was to propose an analytical model that would accommodate all eight existing observation sites as well as other regions throughout the whole area of the country. A number of such models were conceived, and postulated in addition to the well-known and recommended exponential model, namely ITU-R. The predictions made using these models at various heights do not differ much from each other.

Further analytical work on the formula obtained as the height derivative of the empirical expression for the refractivity of the troposphere indicated that it might be possible to find an appropriate model. Such a model was evaluated for average ground based meteorological data obtained over a period of ten years. The emphasis in the research could now shift to utilizing routine observations made by the SA Weather Service at many more points in South Africa, and spanning a much greater height range. Such derived values of the average gradient, and therefore k-factor, could add significantly to our knowledge of the behaviour of these parameters throughout Southern Africa.

While it is emphasized that these ground-based observations will not give any indication of elevated ducting conditions, it raises the question of investigating the atmosphere's refractive properties as a possible national project, in which technikons and universities could cooperate. Such institution would make observations using radiosondes or radio refractometers flown using tethered balloons, or possibly stationary ultraviolet laser observations (*Segal,* 1985), and (*Hall,* 1996).

6.10 Future Research Directives and Recommendations

The follow up work may well concentrate on improvements and extensions of the present results, meaning a further modelling of the troposphere, but not just limited to a study of measurements from the eight radiosonde sites. The data quality and means of acquisition would need to be improved to support requirements for such data in a segment of the telecommunications industry.

One of the gaps originates from the second expression for the k-factor. However, the cumulative distribution as defined here for $k>1$ indicates that it remains an artefact under this assumption. There may yet exist another distribution function appropriate for $k<1$. At some future stage it might be possible to blend the two into a continuous function with smooth transitions in the region of $k=1$.

It may be possible to commence the future work by first addressing the research gaps as indicated, and then to broaden the scope of this research in a conceptual sense. Perhaps, it would be possible to approach some of the more philosophical questions with regards to radiowave propagation in a cognitive sense. In other words, to investigate the nature of the second expression for the k-factor with a view of how much physical interpretation might be attributed to it.

Further observations and analysis of the shape of the vertical refractivity profiles with regards to modes of propagation such as ducting, sub- and super-refraction and tropospheric propagation

would contribute to a better understanding of the combination of mechanisms that govern radiowave propagation.

Further investigation of the gradient of temperature in the troposphere as a function of height remains an important challenge to effectively incorporate the scale-height and the height of tropopause into the models. These are at present separately defined.

In general there appears to be a great deal of scope to enhance the understanding of the complexities involved in the current view of radiowave propagation.

6.11 Closing Arguments and Final Comments

In closing, it is appropriate to summarize how the objectives, originally set out in the proposal for this study, evolved.

Initially the study aimed at producing an improved model for the k-factor in Southern Africa, and at gaining more understanding of it by analysing all of the existing data in a meaningful way, and synthesizing appropriate means for dealing with such a model. Flowing out of the literature survey, some further ideas were developed to supplement the initial proposal for this work.

By focusing on the subject it was possible to bring about a more uniform and consistent picture of what was known of the k-factor and the refractivity of the troposphere. In addition this also resulted in a better understanding of where the gaps in existing knowledge were.

In many European institutions, a tendency developed to treat these problems as mathematical ones where physical interpretation of the results was a separate matter. That approach has more recently been supported by extensive use of powerful computers and by the fact that the researchers are predominantly trained as mathematicians interested in applications of numerical methods. However, in order for any mathematical model to have relevance for engineering applications, it must provide an acceptable model of real world behaviour.

It is believed that the various models proposed and analysed in this work can be of considerable value to planners of radio communications systems in Southern Africa.

7 References

1. Abdulla, S., Raouf, S. Al-anbari, and A., Kadri, A., Determination of Radar Coverage Diagrams in Complex Environments Using Closed Form Ray Tracing, *Radio-Science, Vol. 26*, pp. 45-50, 1991.
2. Afullo, T. J., Adongo, M. O., Motsoela, and T., Molotsi, D. F. Estimates of Refractivity Gradient and k-factor ranges for Botswana. *The Transactions of the S. A. Institute of Electrical Engineers*, pp. 1-6, March 2001.
3. Allen, K.C., An EHF Telecommunication System Engineering Model, *AGARD-CP-407,* pp. *20A/1-15*, AGARD 20-24 Oct. 1986.
4. Almond, T. Considerations Pertinent to Propagation Prediction Methods Applied to Airborne Microwave Equipment. pp. 28/1-11 (4-7 Oct. 1983) Spatind, Norway.
5. Al-Rizzo, H.M., Al-Hafid, H. T., Vishvakarma, B.R. Effects of Sand and Dust Storm on Terrestrial Microwave Links. *Journal of the Institution of Engineers (India) Electronics and Telecommunication Engineering Division* Vol. 74 pt. ET-! pp. 26-30. 1993.
6. Arnold, J.M., Geometrical theories of wave propagation: a contemporary review, *IEE Proceedings,* Vol. 133, Pt, No. 2, pp. 165-199, April 1986.
7. Baker, T. Y. *Phil. Mag.,* 4, 955, 1927. Title not available.
8. Baker, D.C. and Palmer, A.J. A model for the fraction of time availability of the effective earth radius factor for communications planning in South Africa: Part 2 – Inclusion of the climatic term. *The Transactions of SAIEE*, Vol. 94, No. 3, pp. 129-36, September 2002.
9. Baker, D.C. and Palmer, A.J. A proposed empirical model of the effective earth radius factor for telecommunications use in South Africa. *In Proceedings of IEEE AFRICON'02*, George, South Africa, 2-4 October 2002, pp. 511-516, 2002.
10. Baker, D.C. and Palmer, A.J. A proposed empirical model of the effective earth radius factor for telecommunications use in South Africa. *The Transactions SAIEE*, Vol. 2, pp. 40-45, July 2003.
11. Bashir, S. O. Three Years Statistics of Refractive Index Gradient and Effective Earth Factor for the State of Bahrain. *(ICAP 89) (Conf. Publ. No. 301),* Vol.2, pp. 220-3 Vol.2 (4-7 April 1989)
12. Bean, B.R., Cahoon, B.A., Samson, C.A, and Thayer, G.D. A World Atlas of Atmospheric Radio Refractivity. *U.S. Department of Commerce.*1966.
13. Bem D. J., A*nteny i Rozchodzenie się Fal Radiowych*, Wydawnictwa Naukowo-Techniczne, pp. 365-367, Warszawa, 1973. (no ISBN number given).

14. Bhattacharya, S., Banerjee, P.K. and Reddy, B.M. Estimation of Tropospheric Time Delay at a North Indian Latitude. (*Conference ICAP 89)* pp. 328, 1989.
15. Brooker, H.G. and Walkinshaw, W. The Mode Theory of Tropospheric Refraction and its Relation to Wave-Guides and Diffraction. *Physics and Meteorological Societies,* pp. 80-127, 1945.
16. Budden, K. G. The Wave-Guide Mode Theory of Wave Propagation. *London, England: Logos, 1961.* Title not available.
17. Buljanovic, M. Report on the Propagation Test on the Hekpoort – Thabazimbi Radio Path. *ESKOM* 1978.
18. Burnaby, B.C., Anomalous Propagation-Part 1. *GTE-Lenkurt Demodulator*. Vol. 1, pp. 2-13, July 1975.a
19. Burnaby, B.C., Anomalous Propagation-Part 2. *GTE-Lenkurt Demodulator*. Vol. 2, pp. 14-23, August 1975.b
20. Bye, G.D. and Howell, R.G., Average radio refractive index lapse rate of the lower troposphere for locations in NW Europe. *Conference publication No.301,* Vol. 2, pp. 229-233 (4-7 April 1989).
21. Carr, J.R., Meyers, D.E. and Glass, C.E. Cokriging – a Computer Program. *Computer & Geosciences* Vol. 11, No. 2, pp. 111-127, 1985.
22. Clark, I. Practical Geostatistics. *Applied Science Publishers LTD.* 1979.
23. Clark, I. and Harper, W. Practical Geostatistics 2000. *Eccosse North America Llc, Columbus Ohio.* 2000.
24. Claverie, J. and Dupuis, Ph. Over the sea propagation experiments using a SART transponder. *Conference Publication No. 436 IEE,* pp. 343-346, Edinburgh, 1997.
25. Costa, E. The Effects of Ground-Reflected Rays and Atmospheric Inhomogeneities on Multipath Fading. *IEEE Transactions on Antennas and Propagation,* Vol. 39, No. 6, pp. 740-745, June 1991.
26. Craig, K.H. and Levy, M.F. The Modelling of Anomalous Propagation Conditions. *Fifth International Conference on Antennas and Propagation (ICAP 87) (Conference Publication No. 274),* Vol.2, York, England, pp. 347-350, (30 March-2April 1987).
27. Craig, K.H. Roots of the Mode Equation for Propagation in an Elevated Duct. Fourth *International Conference on Antennas and Propagation (ICAP 85)* (Proceedings No. 248), pp.274-278, (16-19 April 1985).
28. Craig, K.H. Propagation modelling in the troposphere: parabolic equation method. *Electronic letters (UK),* Vol. 24, No 18, pp. 1136-1139, (1 September 1988).

29. Crombie, D. D. Prediction of Multipath Fading on Terrestrial Microwave Links at Frequencies of 11GHz and Greater, *AGARD/NATO Conference Proc,* No. 346, 1983. Title not available.
30. Davies, K. Ionospheric Radio, *IEE Electromagnetic Wave Series 31*, Peter Peregrinus Ltd., 1990.
31. Denny, M. Refracted Propagation Effects for Airborne Radar. *IEEE 2000 International Radar Conference – Proceedings 2000,* pp. 554-559, 2000.
32. Dhein, N.R, Pontes, M.S. and da Silva Mello, L. Statistical behaviour of refractivity gradient in the tropics. *Conference Publication No. 370 IEE,* pp. 340-343, London, 1993.
33. Dobija, M. The Generalised Regression Neural Network (GRNN). Private Communiqué. 1978.
34. Dougherty, H.T. and Hart, B.A. Anomalous Propagation and Interference Fields. *U.S. Department of Commerce.* 1976.
35. Fairbrother, J., Hughes, K.A. and Holden, D.M. Some Measurements of Height Gain at VHF. *Copyright © Controller BMSO,* Vol. 18, pp. 1-16, *London,* 1986.
36. Goldhirsh, J., Dockery, G.D. and Musiani, B.H. Sensing propagation events and fade statistics at C-band for two over-water, line-of-sight propagation paths over a one-year period. *Remote sensing of the Propagation Environment (AGARD-CP-502),* pp. 2/1-12, 30 Sep.-4 Oct. 1991.
37. Greene, J. The Generalised Regression Neural Network (GRNN). *UCT, Workshop-Africon* 1999.
38. Hall, M.P.M. Effects of the troposphere on radio communications. *Peter Peregrinus LTD.* 1979.
39. Hall, M.P.M. and Barclay, L.W. Radiowave Propagation. *Peter Peregrinus LTD.* 1989.
40. Hall, P. S. Editor. Remote Sensing of the Propagation Environment. *Colloquium organised by Professional Group E11 (Antennas and Propagation). Reference Number: 1996/221.* November 1996.
41. Harley, P. Short Distance Attenuation Measurements at 900MHz Using Low Antenna Heights for Microcells. *IEEE Journal on Selected Areas in Communications,* Vol. 7, No.1, pp. 5-11, January 1989.
42. Harvey, R.A., A sub-refractive Fading Model for Microwave Paths Using Surface Synoptic Meteorological Data. *IEEE Transactions on Antennas and Propagation,* Vol. AP-35, No. 7, pp. 832-844, July 1987,

43. Harvey, R.A., Estimation of Sub-refraction Statistics Using Surface Synoptic Meteorological Data. *IEEE Transactions on Antennas and Propagation,* Vol. AP-35, No. 7, pp. 845-851, July 1987.
44. Hata, M. Empirical formula for propagation loss in land mobile radio services. *IEEE Transactions of Vehicular Technology*, Vol. VT-29, pp. 317-325, Aug. 1980. Title not available.
45. Hitney, H. and Vieth, R. Statistical Assessment of Evaporation Duct Propagation. *IEEE Transactions Antennas Propagation (USA),* Vol. 38, No. 6, pp. 794-9, June 1990.
46. Imbeau, R., Lecours, M., Bosse, E. and Dion, D. Ray tracing calculation for wave propagation inside evaporation ducts*. Canadian Crown Copyright, IEEE National Radar Conference,* New York, USA, pp. 223-226, 20-22 April, 1993.
47. Isola, C. and Riccardi, M. Computed-aided VHF/UHF field predictions. *EBU Review Technical, (Belgium),* No. 228, pp. 68-77, April 1988.
48. Jha, K.K., Verma, A.K., and Tevari, R.K., A Structured Review of Propagation Conditions in Troposphere Ducts. *Defence Electronics Applications Laboratory, Dehradun 248 001, India.* Paper No. 78-A by IETE, pp. 476-482, 1989.
49. Jenkinson, G.F. and Van Dijk, M.H. Radio Refractive Index Investigations over Bass Strait, Southern Australia. *IEEE Transactions on Antennas and Propagation,* Vol. AP-17, No. 5, pp. 606-613, Sep. 1969.
50. Kalipada Chatterjee, and Mathur, S. Elevated ducting of radio waves in association with trade wind inversion along the coasts of India. Mausam, Vol. 44, No. 4, pp. 433-8, Oct. 1982.
51. Kheirallah, H.N. and Rizk, M.R.M. Two year refractivity statistics for Mersa Matruh, Egypt. *1988. Electron Letters (UK),* Vol. 24, No. 1, pp. 55-56, 1988.
52. Ko, H. A practical guide to anomalous propagation. *Microwave & RF.* (USA) Vol. 24, No. 4, pp.71-76, April 1985.
53. Ko, H. Don't let ducting clutter system specs. *Microwave & RF.* (USA) Vol. 24, No. 6, pp. 103-108, June 1985.
54. Levy, M.F., "Horizontal Parabolic Equation Solution of Radiowave Propagation Problems on Large Domains," *IEEE Transactions on Antennas and Propagation,* Vol. 43, No. 2, pp. 137-144, February 1995.
55. Levy, M.F. and Craig, K.H., "Case Studies of Transhorizon Propagation: Reliability of Predictions Using Radiosonde Data," *Sixth International Conference on Antennas and Propagation,* (ICAP 89), Vol. 2, No. 301, pp. 456-460, Coventry, UK.

56. Levy, M.F. Instability of the roots of the modal equation for the tropospheric wave-guide. *Radio Science,* Vol. 22, No. 1, pp. 61-68, January-February 1987.

57. Lourens, J.G. and Jury, M.R. Anomalous propagation along the Cape West Coast due to sloping meteorological inversions. *Trans. South Afr. Inst. Electr. Eng.* Vol. 79, No.2, pp. 58-62, December 1988.

58. Millington, G., *Proc. IEE,* Vol. 96III, pp. 53-64. Title not available.

59. Mojoli, L.F. and Mengali, U. Propagation in line of sight radio links. *Telettra Review,*1985.

60. Montgomery, D.C., Runger, G.C. and Hubele, N.H. Engineering Statistics. *John Wiley&Sons, Inc.* 1997.

61. Morita K. Severe Temperature Inversion Layer Regions in the World. *Review of the electrical communication laboratories.* Vol. 28, No. 11-12, pp. 1053-1058, Nov.-Dec. 1980.

62. Mouton, J. How to succeed in your Master's & Doctoral Studies. *Van Schaik,* 2001.

63. Narayana Rao, D. and Kesava Murphy, M.J. Radioclimatology over Southern India. *Indian J. Radio and Space Phys.* Vol. 14, No. 1, pp.7-12, February 1985.

64. Nel, J.W., Erasmus, S.J. and Mare, S. Experience gained and preliminary data obtained in calculation of radio refractivity in Southern Africa. *Elektron,* Vol. 6, No. 1, pp. 11-13, *January* 1989.

65. Nel, J.W., Erasmus, S.J., and Mare, S. The establishment of a radio-refractivity database for Southern Africa. South African Conference on Communications and Signal Processing, Pretoria, South Africa, *IEEE Cat. No. 88TH0219-6, COMSIG 1988,* pp. 144-147, 1988.

66. Nel, J.W. Tyd-ruimtelike variasie in Radiogolf-refraktiwiteit oor Suidelike Afrika (Time-spatial variation in Radiowave Refractivity over Southern Africa) MSc-thesis, *Rand Afrikaans University, Johannesburg,* May 1989. (In Afrikaans).

67. Nel, J.W. and Erasmus, S.J., Die invloed van klimaat op radiogolf-refraktiwiteit (The influence of climate on radio-wave refractivity. *Project report done under guidance of J.T. Harmse, Rand Afrikaans University, Report prepared for the SABC (Johannesburg) Research Department,* Project Report 1986/3 (In Afrikaans).

68. Okumura, Y., Field strength and its variability in VHF and UHF land-mobile radio service. *Review Electronic Communications Laboratory,* Vol. 16, No. 9, Sep.-Oct. 1968. Title not available.

69. Ott, R.H., *1970. Radio Science, Vol. 5,* pp. 767-771. Title not available.

70. Palmer, A.J. and Baker, D.C., Towards a Model of the Radio Refractive Index for Southern Africa – Current Status and Future Perspectives. *AFRICON 99,* Vol.2, pp. 511-516, Cape Town 1999.

71. Palmer, A.J. and Baker, D.C., A model for the fraction of time availability of the effective earth radius factor for communications planning in South Africa: Part 1 – The basic model. The Transactions of SAIEE, Vol. 93. No. 1, pp. 1-7, 2002.

72. Pauw, C.K. Short course on "Radio System Planning" *5-7 November 1996, MIKOMTEK, CSIR, Pretoria.*

73. Pawlowski, W. Recent Results of Radio-meteorological Studies Over the Coastal Region of Poland. *(ICAP 89)* (Conf. Publ. No. 301), Vol.2, pp. 224-8, (4-7 April 1989).

74. Pawlowski, W. Radio climatological studies over the coastal region of Poland. *Nine International Conference on Antennas and Propagation (Conf. Publ. No. 407),* Vol.2, pp. 342-6, 4-7 April 1995.

75. Preston-Whyte, R.A. and Tyson, P.D. The Atmosphere and Weather of Southern Africa. *Oxford University Press,* Cape Town 1993.

76. Rao, D.N., Murthy, M.J.K., Sarkar, S.K., and Pasricha, P.K., Dutta, H.N., Hilly Terrain LOS Fadeouts and Fresnel Zone Considerations from Ray Tracing Techniques. *IEEE Transactions Antennas Propagation (USA)* Vol. AP-35, No. 11, pp.1330-3, November 1987.

77. *Rec. ITU-R P.834-3* Effects of Tropospheric Refraction on Radiowave Propagation.

78. *Rec. ITU-R P.835-3* Reference Standard Atmospheres.

79. Reddy, L.R.G. and Reddy, B.M. Fading Patters and Physical Mechanisms Associated With Deep Power Fading Observed on LOS Microwave Radio Links in Tropics. *IEE Conference Paper*, Vol. 2, No. 370, pp. 660-664, London, UK, 30 March-2 April 1993.

80. Rice, P.L., Longley, A.G., Norton, K.A., and Barsis, A.P. Transmission loss prediction for tropospheric communication circuits, NBS Technical Note 101, Vol. 1 and Vol. 2, Jan. 1967.

81. Robertshaw, G.A. Effective Earth Radius for Refraction of Radio Waves at Altitudes Above 1 km. *IEEE Transactions on Antennas and Propagation,* Vol. AP-34, No. 9, pp. 1101-1105, September 1986.

82. Rotheram, S., Milsom, J.D., Herring, R.N., and Pielou, J.M., Ground-Wave Propagation over Irregular Surfaces, pp. 520-524, *The General Electric Company* 1985.

83. Samir Hussain Abdul-Jauwad, Perez Zahir Khan and Talal Omar Halawani, Prediction of radar coverage under anomalous propagation condition for typical coastal site: A case study. *Radio Science,*Vol. 26, pp. 909-919, July-August 1991.

84. Samson, C.A. Refractivity Gradients in the Northern Hemisphere. *U. S. Department of Commerce,* 1975.

85. Sarkar, S.K., Dutta, H.N. and Reddy, B.M. Recent advances in radio climatological studies over the Indian Subcontinent. *Conference ICAP 87,* pp. 248-252, 1987.

86. Schiavone, J.A. Prediction of Positive Refractivity Gradients for Line-of-Sight Microwave Radio Paths. *The Bell System Technical Journal.* Vol. 60, No. 6, pp. 803-822, July-August 1981.

87. Schiavone, J.A. Microwave radio-meteorology: Diurnal fading distributions. *Radio Science,* Vol. 17, No. 5, pp. 1301-1312, September-October 1982.

88. Segal, B. The Measurement of Tropospheric Refractive Index Relevant to the Study of Anomalous Microwave Propagation-Review and Recommendations. *CRC Report No. 1387, Ottawa,* June 1985.

89. Sharma, R. V. and Subramanian, D. V. Vertical variation of radio refractive index in lower troposphere over Bombay. *Regional Meteorological Centre,* No. 3, pp. 338-339, Bombay July 1982.

90. Shen, X.D. and Vilar, E. Anomalous transhorizon propagation and meteorological processes of a multilink path. *Radio Science,* Vol. 30, No. 5, pp. 1467- 1479, September -October 1995.

91. Slingsby, P.L., "Modelling Tropospheric Ducting Effects on VHF/Uhf Propagation," *IEEE Transactions on Broadcasting,* Vol. 37, No. 2, pp. 25-34, June 1991.

92. Sommerfeld, A.N., *Annals of Physics.* Series 4, Vol. 28, pp. 665, 1909. Title not available.

93. Thom, T. Aviation Law Meteorology. *Air-life Publishing Ltd,* England.1994.

94. Wait J.R. Electromagnetic Waves in Stratified Media. Pergamon Press. 1962.

95. Weiner, M.M. Use of the Longley-Rice and Johnson-Gierhart Tropospheric Radio Propagation Programs: 0.02-20GHz. *IEEE Journal on Selected Areas in Communications*, Vol. SAC-4, No. 2, pp. 297-307, March 1986.

96. Wickerts, S. The refractive-index field in the lowest 2000 meters of the atmosphere. *FOA Reports* Vol. 4, No. 3, pp.1-16, April 1970.

97. Yakovlev, O.I., Matyugov, S.S. and Vilkov, Attenuation and scintillation of radio waves in the Earth's atmosphere from radio occultation experiments on satellite-to-satellite links. *Radio Science, Volume 30, Number 3,* pp. 591-602, May-June 1995.

98. Vardeman, S.B. "Statistics for Engineering Problem Solving," IEEE Press, ISBN0-534 93605-9, 1994.

99. Wait, J. R., Coupled mode analysis for non-uniform tropospheric wave-guide. *Radio Science,* Vol. 15, pp. 275-673, 1980. Title not available.

100. Webster, A. R. Angles-of-Arrival and Delay Times on Terrestrial Line-of-Sight Microwave Links. *IEEE Transactions on Antennas and Propagation,* Vol. AP-31, No. 1, pp. 12-17, January 1983.